

2015-10-08

Boundary Lubricating Ability of Proteoglycan 4 at an Articular Cartilage-Meniscus Biointerface

Dorosz, Samuel

Dorosz, S. (2015). Boundary Lubricating Ability of Proteoglycan 4 at an Articular Cartilage-Meniscus Biointerface (Master's thesis, University of Calgary, Calgary, Canada).

Retrieved from <https://prism.ucalgary.ca>. doi:10.11575/PRISM/25157

<http://hdl.handle.net/11023/2615>

Downloaded from PRISM Repository, University of Calgary

UNIVERSITY OF CALGARY

Boundary Lubricating Ability of Proteoglycan 4 at an
Articular Cartilage-Meniscus Biointerface

by

Samuel Greenlees Dorosz

A THESIS

SUBMITTED TO THE FACULTY OF GRADUATE STUDIES
IN PARTIAL FULFILMENT OF THE REQUIREMENTS FOR THE
DEGREE OF MASTER OF SCIENCE

GRADUATE PROGRAM IN BIOMEDICAL ENGINEERING

CALGARY, ALBERTA

SEPTEMBER, 2015

© Samuel Greenlees Dorosz 2015

Abstract

Proteoglycan 4 (PRG4) is a glycoprotein in synovial fluid (SF) and on the articular cartilage surface, where it acts as a boundary lubricant. Hyaluronan (HA) is another SF constituent that acts as a boundary lubricant at the cartilage-cartilage biointerface and interacts with PRG4 to synergistically lower friction. The meniscus is a fibrocartilaginous pad in the knee, on which PRG4 exists, that is critical for joint health. This thesis aimed to develop an *in vitro* lubrication test to determine the boundary lubricating ability of PRG4 and HA, alone and in combination, at the cartilage-meniscus biointerface, and assess the surface adsorption of recombinant human PRG4 (rhPRG4). A novel cartilage-meniscus test demonstrated that (rh)PRG4 and HA, alone and in combination, act as effective boundary lubricants at this biointerface. rhPRG4 adsorbed to the meniscal surface. This work contributes to the understanding of meniscus lubrication and potential development of osteoarthritis biotherapeutic treatments.

Preface

This thesis is presented in a traditional thesis format. While none of the chapters have been submitted for publication at the time of thesis submission, it is the author's intent to combine the findings of Chapters 2, 3, and 4 and submit for publication in the future.

The author of this thesis work was responsible for the development of the custom articular-cartilage meniscus test set up; planning, sample preparation and execution for all friction tests; all sample preparation, staining and imaging of immunohistochemistry samples; and writing of this thesis. Dr. Tannin Schmidt made important contributions to the planning of this thesis work, review of results, and editing of this thesis.

Acknowledgements

I would like to thank all the organizations that I have been fortunate enough to receive funding from, be it direct scholarships or travel awards. Thank you for allowing me to pursue my scientific interests. NSERC CREATE, USRP Markin, Team OA, the BME Graduate Office, and the Faculty of Graduate Studies have all been very generous during my tenure as a student.

I appreciate the insight, support, and time that have been provided by my committee members, Dr. Shrive and Dr. Herzog, to help direct my project and encourage me to think outside the box. I am also thankful for Dr. Thornton and Dr. Trifkovic taking time from their incredibly busy schedules to read my thesis and ask challenging questions at my defence.

I would be remiss to not acknowledge the time and effort of many program administrators that have advised me on everything from how to write an application to what to do with my life. Ursula, Dr. Lynne, Lorri, and Lisa, thank you for all the assistance you undoubtedly provide to countless students like myself.

This space is far too short and the medium far too impersonal to properly thank all the friends that I have been so lucky as to have met throughout my education. To the high school friends who spend the time to keep in touch and wax nostalgic, the undergraduate engineering buddies who are always willing to watch terrible movies and talk about any possible topic (from theoretical physics to the more nuanced discussions on how to improve beer consumption velocity), the track and field teammates who make self-inflicted pain and circular running seem like a fun use of time, and the numerous labmates who comfort me when the fickle gods of science punish me for not double checking calculations just ONE more time; you have all brought happiness and some semblance of balance to my life.

Special thanks to Taryn for patiently teaching me laboratory techniques, Mike for being all at once incredibly entertaining and impressively educational, and Saleem for always being willing to help with anything; tissue harvesting, abstract editing, and anger management consulting are just some of your many areas of expertise. Thank you all for helping me become a passable scientist.

Thank you to my family for their endless support. Megan, thank you for cooking amazing meals, always giving honest advice, and keeping me humble. Mom and Dad, I am forever grateful for all of your kindness, perspective, and humour. Parental wisdom and home cooking seem to cure any existential crisis that one can have; thank you for everything.

Finally, I would like to thank my supervisor, Tannin Schmidt. You set an amazing example for any and all young scientists. Your dedication to both your research and your students is astounding; the relentless work ethic and scientific curiosity you possess will continue to lead you to success. I appreciate the continuous guidance in technical lab skills, scientific writing, and critical thinking you have given me as well as the patience shown throughout my time in the lab. How you put up with the misadventures of graduate students I do not know, but I have a feeling that you are well prepared to raise young children.

Table of Contents

Abstract	ii
Preface	iii
Acknowledgements	iv
Table of Contents.....	vi
List of Figures and Illustrations	x
List of Symbols, Abbreviations, and Nomenclature.....	xiii
Epigraph.....	xvi
CHAPTER 1: Introduction	1
1.1 Introduction to Thesis	1
1.2 Osteoarthritis	3
1.2.1 Social and Economic Costs	3
1.2.2 Current Treatment Options.....	4
1.3 Articular Cartilage	6
1.3.1 Structure	6
1.3.2 Function.....	10
1.3.3 Articular Cartilage and OA	11
1.4 Meniscus.....	13
1.4.1 Structure	14
1.4.2 Function.....	15
1.4.3 Meniscus and OA	16
1.5 Lubrication Mechanisms	18

1.5.1 Fluid Mediated Lubrication	20
1.5.2 Boundary Lubrication.....	21
1.5.3 Experimental Analysis.....	22
1.6 Proteoglycan 4.....	24
1.6.1 Structure	25
1.6.2 Function.....	25
1.6.3 PRG4 and OA.....	26
1.7 Hyaluronan	28
1.7.1 Structure	28
1.7.2 Function.....	28
1.7.3 HA and OA.....	29
1.8 Thesis Aims	30
 CHAPTER 2: Effect of Sliding Velocity on Lubricating Ability of PRG4 and HA	
at an Articular Cartilage-Meniscus Biointerface	31
2.1 Abstract.....	31
2.2 Introduction	32
2.3 Methods	36
2.3.1 Lubricant Preparation	36
2.3.2 Lubrication Test Tissue Sample Preparation.....	37
2.3.3 Cartilage-Meniscus Boundary Lubrication Test	38
2.3.4 Data Analysis.....	40
2.4 Results	41
2.4.1 Test Sequence 1: PRG4.....	41

2.4.2 Test Sequence 2: HA	42
2.4.3 Test Sequence 3: PRG4 + HA	43
2.5 Discussion.....	45
CHAPTER 3: Synergism of (rh)PRG4 and HA at an Articular Cartilage-Meniscus	
Biointerface	50
3.1 Abstract.....	50
3.2 Introduction	51
3.3 Methods	53
3.3.1 Lubricant Preparation	53
3.3.2 Tissue Sample Preparation	54
3.3.3 Boundary Lubrication Test.....	54
3.3.4 Data Analysis.....	54
3.4 Results	56
3.4.1 Test Sequence 1: PRG4 ± HA	56
3.4.2 Test Sequence 2: HA ± PRG4	57
3.4.3 Test Sequence 3: rhPRG4 ± HA.....	58
3.5 Discussion.....	60
CHAPTER 4: Surface Adsorption of Full-Length Recombinant Human Recombinant	
Proteoglycan 4 on Meniscus	64
4.1 Abstract.....	64
4.2 Introduction	65
4.3 Methods	67
4.3.1 Lubricant Preparation	67

4.3.2 Immunohistochemistry	67
4.4 Results	70
4.4.1 Surface Depletion by PBS Shaking	70
4.4.2 Surface Depletion by PBS Shaking and Salt Extraction	72
4.5 Discussion	75
CHAPTER 5: Conclusions.....	79
6.1 Summary of Findings.....	79
6.2 Discussion.....	82
6.3 Limitations	88
6.4 Future Work	91
Bibliography.....	95
Appendix	105
A.1 Torque and Load Profiles	105

List of Figures and Illustrations

Figure 1-1: Illustrations demonstrating articular cartilage morphology. A, Schematic image demonstrating chondrocyte organization in the three main zones of uncalcified cartilage (i.e., superficial-tangential zone [STZ], middle, deep), the tidemark, and the subchondral bone. B, Sagittal cross-sectional illustration of collagen fiber architecture demonstrating the three salient zones of articular cartilage ³⁵	7
Figure 1-2: Electron micrographs of chondrocytes from the medial femoral condyle of a skeletally mature rabbit. a) superficial zone, b) middle zone, c) deep zone, and d) calcified cartilage zone. N: nucleus, G: glycogen, IF: intermediate filaments, UM: unmineralized matrix, MM: mineralized matrix ³⁴	9
Figure 1-3: Illustration of Knee Joint. Superior view with femur removed ⁴⁵	13
Figure 1-4: The “meniscal pathway” to knee OA due to the negative feedback of tissue damage and loss of function ⁶¹	17
Figure 1-5: Stribeck Curve: Change in lubrication regime with coefficient of friction (red) and fluid-film thickness (blue) on the y-axis and critical lubrication variables, viscosity and velocity, on the x-axis. Adapted from previous work ⁶⁶	19
Figure 1-6: Differing experimental test protocols and interfaces used to assess friction modulating of lubricants. Adapted from previous work ^{65,71,73}	23
Figure 1-7: Surface smoothness affected in PRG4 knockout mice. A and B, Representative photomicrographs of toluidine blue-stained knee joint cartilage sections from 2-week-old PRG4+/- (A) and PRG4-/- (B) mice, demonstrating differences in surface smoothness ⁶⁹	24
Figure 1-8: Schematic of PRG4 molecule ⁸¹	25
Figure 1-9: HA’s chemical structure ⁹⁷	28

Figure 2-1: Cartilage and meniscus sample preparation	38
Figure 2-2: Boundary lubrication test orientation	39
Figure 2-3: Kinetic friction coefficient $\langle \mu_{\text{kinetic,Neq}} \rangle$ for PRG4 at 0.450 mg/mL. Data presented as mean \pm SEM, n=6.....	42
Figure 2-4: Kinetic friction coefficient $\langle \mu_{\text{kinetic,Neq}} \rangle$ for 1.5 MDa HA at 3.33 mg/mL. Data presented as mean \pm SEM, n=6.	43
Figure 2-5: Kinetic friction coefficient $\langle \mu_{\text{kinetic,Neq}} \rangle$ for PRG4+HA with [PRG4] = 0.450 mg/mL, [1.5 MDa HA] = 3.33 mg/mL. Data presented as mean \pm SEM, n=5.....	44
Figure 2-6: Kinetic friction coefficient $\langle \mu_{\text{kinetic,Neq}} \rangle$ for PRG4 at 0.450 mg/mL, 1.5 MDa HA at 3.33 mg/mL and PRG4+HA. Data presented as mean \pm SEM, n=5-17.....	45
Figure 3-1: A) Static friction coefficient $\mu_{\text{static,Neq}}$ and B) kinetic friction coefficient $\langle \mu_{\text{kinetic,Neq}} \rangle$ at $T_{\text{ps}} = 1.2$ s for PRG4 at 0.450 mg/mL \pm 1.5 MDa HA at 3.33 mg/mL. Data presented as mean \pm SEM, n = 4.....	57
Figure 3-2: A) Static friction coefficient $\mu_{\text{static,Neq}}$ and B) kinetic friction coefficient $\langle \mu_{\text{kinetic,Neq}} \rangle$ at $T_{\text{ps}} = 1.2$ s for 1.5 MDa HA at 3.33 mg/mL \pm PRG4 at 0.450 mg/mL. Data presented as mean \pm SEM, n = 4.....	58
Figure 3-3: A) Static friction coefficient $\mu_{\text{static,Neq}}$ and B) kinetic friction coefficient $\langle \mu_{\text{kinetic,Neq}} \rangle$ at $T_{\text{ps}} = 1.2$ s for rhPRG4 at 0.450 mg/mL \pm 1.5 MDa HA at 3.33 mg/mL. Data presented as mean \pm SEM, n = 8.....	59
Figure 4-1: Immunolocalization of PRG4 at meniscal surface. Key: Fresh samples were taken directly from joint and snap-frozen (control). All other samples were shaken overnight in PBS at 4°C, frozen at -80°C, and shaken overnight again in fresh PBS at 4°C. Samples were then incubated in solutions of interest overnight at room temperature. Solutions: PBS (negative control),	

SF (positive control), rhPRG4 and PRG4 both at physiological concentrations of 450 µg/mL.

Negative signifies samples that lacked primary Ab 9G3 but contained secondary gt-anti mouse Ab, positive signifies samples that contained both primary and secondary Abs. Red shows anti-PRG4 mAb 9G3, blue shows DAPI staining on chondrocyte cells. 72

Figure 4-2: Immunolocalization of PRG4 at meniscal surface. Key: Fresh samples were taken directly from joint and snap-frozen (control). All other samples were shaken overnight in PBS with 1.5M NaCl at 4°C, frozen at -80°C, and shaken overnight again in fresh PBS with 1.5M NaCl at 4°C. Samples were then incubated in solutions of interest overnight at room temperature.

Solutions: PBS (negative control), SF (positive control), rhPRG4 and PRG4 both at physiological concentrations of 450 µg/mL. Negative signifies samples that lacked primary Ab 9G3 but contained secondary gt-anti mouse Ab, positive signifies samples that contained both primary and secondary Abs. Red shows anti-PRG4 mAb 9G3, blue shows DAPI staining on chondrocyte cells. 74

Figure 5-1: Immunolocalization of rhPRG4 and HA at meniscal surface. All samples were shaken overnight in PBS at 4°C, frozen over night at -80°C, shaken again in fresh PBS at 4°C and soaked in solutions of interest overnight at room temperature. Solutions: rhodamine-labelled rhPRG4 at 0.450 mg/mL, FITC-labelled 1.5 MDa HA at 3.33 mg/mL, and a combination of rhPRG4 and HA. Blue shows DAPI staining of chondrocyte cells. 94

Figure A-1: Friction data acquired on articular cartilage-meniscus biointerfaces. Torque (τ) profiles obtained during two rotations at three velocities (0.01, 0.3 and 10 mm/s) on PBS (A) and SF (B). Instantaneous axial load (N) profiles acquired simultaneously for PBS (C) and SF (D). 105

List of Symbols, Abbreviations, and Nomenclature

Symbol	Definition
τ	Torque
$ \tau_{\max} $	Maximum axial torque in the first 20° of rotation
$ \tau $	Axial torque averaged over the last 360° of rotation
N	Instantaneous axial load
N_{eq}	Equilibrium axial load
R_{eff}	Effective radius
v_{eff}	Effective sliding velocity
$\langle\mu_{\text{kinetic}}\rangle$	Kinetic coefficient of friction calculated using instantaneous axial load
$\langle\mu_{\text{kinetic,Neq}}\rangle$	Kinetic coefficient of friction calculated using equilibrium axial load
$\mu_{\text{static,Neq}}$	Static coefficient of friction calculated using equilibrium load
μ	Coefficient of friction
ω	Angular velocity
9G3	Anti-PRG4 antibody, mucin domain
4D6	Anti-PRG4 antibody, unknown binding site
Ab	Anti-body
ACL	Anterior cruciate ligament
ANOVA	Analysis of variance
BCA	Bicinchoninic acid assay
C-terminal	Carboxy terminal
CACP	Camptodactyly-arthropathy-coxa vara-pericarditis
CHO	Chinese hamster ovary
CI	Confidence interval
Da	Dalton
DEAE	Diethylaminoethyl
dH ₂ O	Distilled water

EtOH	Ethanol
F	Friction force
FPLC	Fast protein liquid chromatography
GAG	Glycosaminoglycan
HA	Hyaluronan
IHC	Immunohistochemistry
LPN	Anti-PRG4 antibody, C-terminal
LUB:1	Truncated human recombinant lubricin
mAb	Monoclonal anti-body
MS/MS	Tandem mass spectrometry
MSF	Megakaryocyte stimulating factor
MW	Molecular weight
n	One friction testing replicate
N-terminal	Amino terminal
NSAIDs	Non-steroidal anti-inflammatory drugs
OA	Osteoarthritis
PBS	Phosphate buffered saline
PRG4	Proteoglycan 4
R	Radius
R_{inner}/R_i	Inner radius
R_{outer}/R_o	Outer radius
rhPRG4	Recombinant human PRG4
RMS	Root mean square
s	Seconds
SAPL	Surface active phospholipids
SD	Standard deviation
SDS-PAGE	Sodium dodecyl sulfate polyacrylamide gel electrophoresis
SEC	Size exclusion chromatography
SEM	Standard error of the mean
SF	Synovial fluid

SZP

TGF- β 1

T_{ps}

Superficial zone protein

Transforming growth factor β 1

Pre-sliding duration

Epigraph

The truth will set you free. But not until it is finished with you.

David Foster Wallace, *Infinite Jest*

We are here to laugh at the odds and live our lives so well that Death will tremble to take us.

Charles Bukowski

CHAPTER 1: Introduction

1.1 Introduction to Thesis

The meniscus is a fibrocartilaginous pad found in the knee with load-bearing and lubricating properties. It articulates with the articular cartilage of the femoral condyles superiorly and tibial plateau inferiorly. Chronic degradation of cartilage, or osteoarthritis (OA), is an increasingly common condition that lowers quality of life and is costly to treat. OA is a multifactorial disease, but the friction and wear of articulating surfaces in the knee joint may contribute to the onset and progression of this pathology. However, the lubrication at the biointerface formed by articular cartilage and meniscus has not been characterized.

Synovial fluid (SF) provides shock adsorption, lubrication, and nutrition to the surrounding tissues in the knee joint. Two lubricating SF constituents, the mucin-like glycoprotein proteoglycan 4 (PRG4) and the negatively charged polysaccharide hyaluronan (HA), are found on the surfaces of both articular cartilage and the meniscus. Both PRG4 and HA act as effective boundary lubricants at an articular cartilage-cartilage biointerface. In addition, they have been shown to form a complex in solution and interact synergistically to lower friction at this biointerface. The boundary lubricating effects of PRG4 and HA at the articular cartilage-meniscus biointerface have yet to be examined.

Recently, full-length recombinant human PRG4 (rhPRG4) has been produced stably in a mammalian cell line with a high yield and demonstrated the ability to bind to and lubricate cartilage surfaces. While native PRG4 binds to the surface of the meniscus, rhPRG4 has yet to be observed doing so. This is critical, as boundary lubricants must adsorb to the articulating surface to fulfill their role.

The research presented in this thesis addressed these questions and tested the following hypotheses:

1. PRG4 and HA, alone and in combination, lower friction at an articular cartilage-meniscus biointerface at low effective velocities characteristic of boundary lubrication.
2. (rh)PRG4 and HA, alone and in combination, lower friction in a boundary mode of lubrication at an articular cartilage-meniscus biointerface.
3. rhPRG4 is able to adsorb to the surface of the meniscus depleted of PRG4.

This work contributes to the study and understanding of PRG4 and HA's boundary lubricating ability, specifically at the articular cartilage-meniscus biointerface. Furthermore, characterization of rhPRG4's surface adsorption and boundary lubrication properties may indirectly support the development of a biotherapeutic treatment for OA.

The chapters, outlined below, correspond to the three specific hypotheses of the thesis. Chapter 1 provides background information on OA, relevant tissue surfaces in the knee joint, modes of lubrication and the conditions under which they occur, and synovial fluid constituents of interest before outlining the aims of the thesis. Chapter 2 investigates the velocity dependence of kinetic friction for PRG4 and HA, alone and in combination, at the articular cartilage-meniscus biointerface. Chapter 3 examines the boundary lubricating ability of (rh)PRG4, with and without HA, at the articular cartilage- meniscus biointerface. Chapter 4 assesses the adsorption of rhPRG4 to the meniscus following surface depletion by shaking or salt extraction. Chapter 5 summarizes the findings of the thesis, discusses the implications of these results and considers potential future work.

1.2 Osteoarthritis

OA is a chronic disease that affects articular joints throughout the body. Joints that experience high loads and/or very frequent use, such as the hips, knees, or hands, are most often afflicted by OA, which is characterized by degradation of articular cartilage, limited inflammation of synovial tissue and exposure of subchondral bone¹. Symptomatically, OA is associated with function impairment of the affected joint and inflammatory indicators such as pain and stiffness, as well as decreased mobility². Late-stage OA occurs when full thickness lesions in the cartilage surface allows for bone-on-bone contact, leading to debilitating pain and greatly reduced joint function. Primary, or idiopathic, OA is due to aging and general chronic wear, while secondary, or post-traumatic, OA occurs following an acute injury to the joint³⁻⁵.

Finding effective treatments for OA has proven difficult, due in part to the multifactorial nature of the disease. Biomechanical factors, such as abnormal joint loading due to muscle weakness, obesity, or joint laxity, do not account for all the symptoms associated with OA. Risk factors relating to age, ethnicity, and sex such as estrogen levels and bone density play a role in OA progression, as do genetics and dietary intake⁶. However, the articular surface is critical for proper load transfer through the joint, and evidence suggests that increased/altered loading patterns can accelerate both the initiation and progression of OA⁷.

1.2.1 Social and Economic Costs

OA is very prevalent in North America; it the most common form of arthritis in the United States and affects 27.5 million people⁸. Nearly half of all people will experience symptomatic knee OA by the time they are 85, and 50% of all adults over the age of 65 suffer from OA already^{9,10}. Also, it is predicted that 25% of the entire population of the United States

will suffer from OA by 2030, with 25 million of these patients reporting arthritis-related activity limitations¹¹. Costs related to OA treatment total \$US 60 billion annually¹².

Arthritis costs the Canadian economy an estimated \$CAD 33 billion each year¹³. OA is the most common form of arthritis in Canada as well, affecting over 10% of the population and accounting for 90% of knee replacements¹⁴. In the next 30 years it is estimated there will be a diagnoses of OA every 60 seconds, leading 30% of the workforce to experience difficulty working due to their condition¹³.

The lack of proper joint function has been compared to the disability caused by heart disease, and the decreased quality of life associated with OA comparable to that of an advanced cancer patient¹⁵. Furthermore, suffering from OA puts a person at higher risk for a variety of other medical conditions, such as depression, hypertension, and diabetes¹⁶. While OA is often associated with the elderly, it has also been shown to cause lower productivity and increase costs for working aged employees experiencing pain¹⁷. In fact, over a quarter of arthritis sufferers between the ages of 25 and 44 are not working due to their condition¹⁴. Of those who do work, 44% report workplace limitations, and 33% require job modifications¹⁴. This loss of productivity and absenteeism in the working population accounts for a third of the total cost experienced by the health-care system, the rest relating to direct treatment costs. The total cost has been estimated at \$16,146 per annum for OA sufferers, excluding surgery costs¹⁶.

1.2.2 Current Treatment Options

Effectively treating OA could play an important role in reducing health-care costs, but many current treatments focus on reducing patient pain rather than halting or reversing disease progression. Being overweight or obese is a risk factor for OA, and those at risk who lose one

pound experience a four-pound reduction in knee loading each step^{14,18}. As such, the first and cheapest treatment for early stage OA is lifestyle changes, specifically a balanced diet and regular exercise. Non-steroidal anti-inflammatory drugs (NSAIDs) are often used for pain relief but have several negative side effects and do not prevent further tissue degradation¹².

The only option for late-stage OA is total knee replacement, which has a low failure rate and generally positive outcomes^{19,20}. However, this efficacy has led to younger and younger patients receiving total joint replacements²¹. Joint loosening and general wear cause these implants to have lifetimes of 10-15 years, necessitating a revision surgery²². In addition, these replacements can cost \$24,000 and can lead to surgical complications, making earlier intervention attractive^{12,23}.

One type of biotherapeutic treatment aims to restore the function of the SF in the knee by injecting biologically based fluids. HA, a negatively charged polysaccharide found in the knee, is one such injection. HA increases the viscosity of SF in the joint and therefore is called a viscosupplement. The efficacy of these viscosupplements is comparable to or greater than other early stage OA treatments such as improved diet, exercise, and NSAIDs²⁴. However, current viscosupplements begin leaving the joint after only one day, despite lowering pain for up to one month^{25,26}. This suggests that perhaps these treatments only reduce pain rather than offer significant chondro-protective properties²⁷. A commercially available HA supplement, Hylan G-F 20, while showing improved pain scores, produced a higher coefficient of friction in vitro when compared to human SF^{24,28}. These supplements also were shown to decrease an apoptotic marker in chondrocytes compared to a saline control solution, though SF reduced expression of this marker even further²⁸. This suggests that these HA injections do not fully replicate the mechanical functionality of SF, and other constituents of SF are critical for joint health.

1.3 Articular Cartilage

The connective tissue covering the articulating surfaces of synovial joints is hyaline cartilage which, given its role, is called articular cartilage. Despite being only, at most, several millimeters thick, articular cartilage is very resilient under compression and distributes loads to minimize peak stresses on subchondral bone^{29,30}. Articular cartilage is unique among connective tissue in that it is lacking blood vessels, lymphatic vessels, and nerves³¹. Cartilage has low metabolic activity compared to other tissues such as bone or muscle, and as such is less responsive to changes in loading or injury occurrence. Like these other load-bearing tissues however, cartilage has an ordered structure that contributes to its mechanical properties.

1.3.1 Structure

Cartilage is comprised of one cell type, the chondrocyte, and extracellular matrix. This extracellular matrix accounts for the vast majority of the volume of the tissue, as chondrocytes occupy only 1% of the total volume³². Chondrocytes vary in size, shape, and metabolic activity depending on the zone of the cartilage they inhabit, though they all share the necessary organelles for matrix synthesis³³. These cells do not contact one another; rather they are surrounded by extracellular matrix. Chondrocytes synthesize collagen, aggregating proteoglycans, and several noncollagenous proteins that form the molecular framework of the extracellular matrix. The interaction between this frame and tissue fluid provides cartilage with its desirable mechanical properties²⁹.

Water contributes 80% weight to the cartilage. The tissue fluid contains small proteins, metabolites, and a high concentration of cations. The volume and concentration of water within the tissue depends on its interaction with the structural macromolecules within and affect its

behavior. These proteoglycans and other glycoproteins help maintain fluid levels in the matrix and contribute to its mechanical behavior³¹. This framework accounts for 20-40% of the weight of the tissue. 60% of the dry weight of the cartilage is collagen, primarily type-II, 25% is proteoglycans, and the remaining 15% are noncollagenous proteins. These proteins either bind to, or are entrapped in, the collagen framework. This framework is then filled with the aforementioned water.

Grossly, the cartilage is composed of the superficial-tangential zone, transitional or middle zone, deep zone, and calcified cartilage zone that differ morphologically, as shown in Figure 1-1^{31,34}.

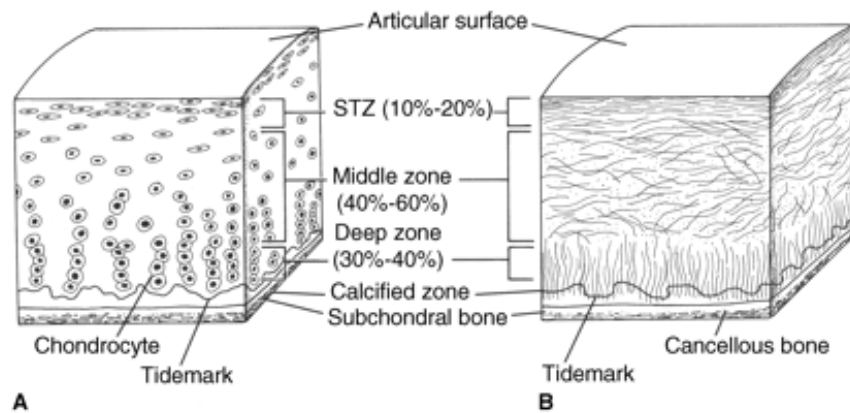


Figure 1-1: Illustrations demonstrating articular cartilage morphology. A, Schematic image demonstrating chondrocyte organization in the three main zones of uncalcified cartilage (i.e., superficial-tangential zone [STZ], middle, deep), the tidemark, and the subchondral bone. B, Sagittal cross-sectional illustration of collagen fiber architecture demonstrating the three salient zones of articular cartilage³⁵.

The superficial zone is the thinnest layer of the cartilage and consists of a clear, acellular

film of fibrils, called the lamina splendens. The rest of this zone is comprised of thin, ellipsoid shaped chondrocytes (see Figure 1-2), whose major axis is parallel to the cartilage surface. These chondrocytes produce a higher concentration of collagen and less proteoglycan relative to the other zones, as well as the most water. The collagen matrix in the superficial zone is very dense and lies parallel to the surface.

The middle, or transitional, zone has spheroidal chondrocytes that produce higher concentrations of proteoglycans and lower concentrations of water and collagen. These collagen fibrils have a greater diameter than those in the superficial zone and have no specific directional alignment.

Below the middle zone, the deep zone has spheroidal chondrocytes that are aligned in pillars, perpendicular to the cartilage surface. Collagen fibers have the thickest diameter in the cartilage here. Collagen and water concentration are low in this layer, but proteoglycan concentration is the highest in the deep zone.

The boundary between subchondral bone and the cartilage itself is a zone of calcified cartilage, where chondrocytes with small volume and few organelles, are encased in calcified cartilage matrix.

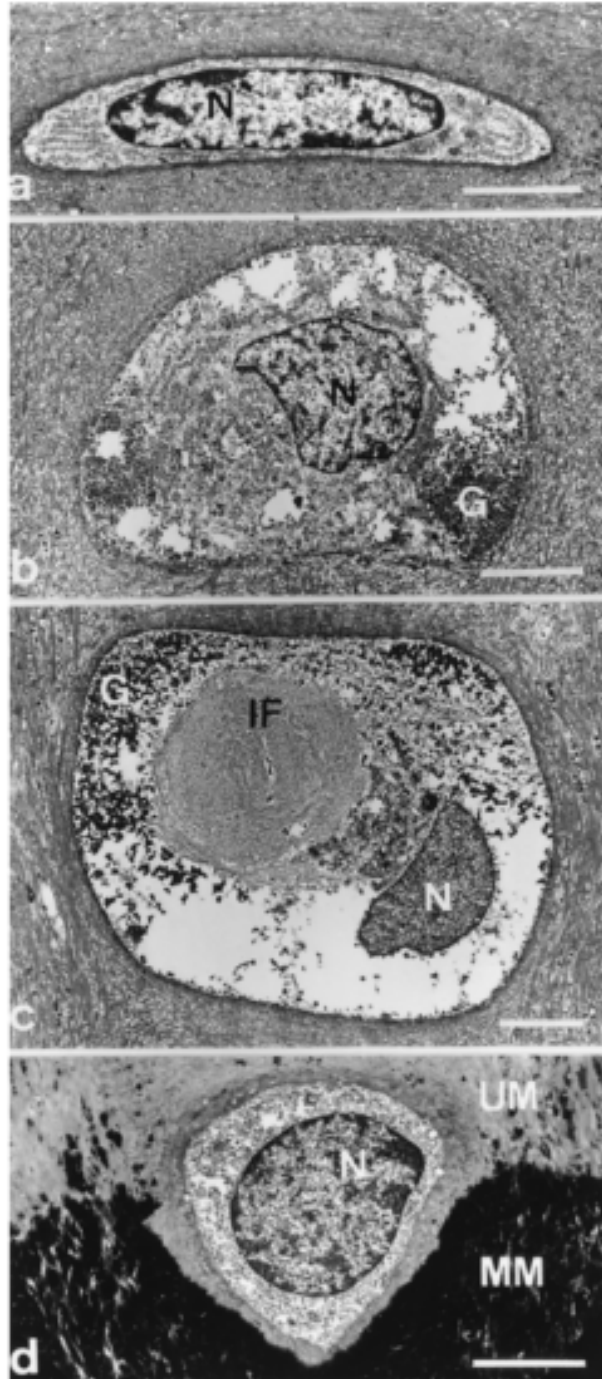


Figure 1-2: Electron micrographs of chondrocytes from the medial femoral condyle of a skeletally mature rabbit. a) superficial zone, b) middle zone, c) deep zone, and d) calcified cartilage zone. N: nucleus, G: glycogen, IF: intermediate filaments, UM: unmineralized matrix, MM: mineralized matrix³⁴.

1.3.2 Function

Cartilage's load-bearing properties are facilitated by the interaction of the positively charged ions in the fluid and the negatively charged proteoglycans in the structural network, which maintains osmotic pressure and provides mechanical stability. This biphasic theory states that the stiffness and resilience of the tissue is due to the osmotic pressure from the macromolecules. These molecules are largely negatively charged due to sulfate or carboxylate groups, repelling similarly charged ions and attracting positively charged ions. This high concentration of inorganic ions causes an osmotic pressure that the collagen meshwork resists^{29,36}.

When the joint is subject to load, the increased interstitial fluid pressure causes fluid to flow out of the tissue, which plays a roll in lubrication (discussed below) and creates drag on the collagen framework³⁷. This drag contributes to the biphasic viscoelastic behavior of the tissue. The collagen framework also has intrinsic viscoelastic properties, thus allowing load to be born by both solid and fluid states^{37,38}.

Cartilage also demonstrates creep and stress-relaxation behavior. Constant compressive loads cause steady deformation, or creep, until an equilibrium value is reached. In a similar fashion, when a constant strain is applied to the tissue, the load experienced increases to a peak before stress relaxing. Both of these mechanisms allow for high stresses or strains to be experienced over periods of time, minimizing sudden failure of the tissue³⁹.

The collagen meshwork in the superficial zone controls permeability in the tissue, which contributes to the biphasic load-bearing mechanism discussed above, but also allows for nutrition and waste to be exchanged between the SF and chondrocytes³¹. In addition, this meshwork resists shear forces at the surface³¹. The randomly aligned collagen meshwork of the middle zone

bears tensile stress, stretching to resist shear stress⁴⁰. Upon being fully stretched, the ultimate tensile strength is determined by the inter- and intramolecular crosslinking of the fibrils³⁹.

1.3.3 Articular Cartilage and OA

Seemingly in spite of these impressive mechanical properties, cartilage can begin to degenerate and lose functionality due to chronic wear or acute injury. OA manifests in several ways throughout the joint, but the primary changes are cartilage loss, subchondral bone remodeling, and the formation of osteophytes⁴¹.

The sign of OA onset is the fraying and fibrillation of the collagen network in the superficial zone, which progress to surface roughness and clefts that reach deeper and deeper into the cartilage. Decreased proteoglycan staining is also observed at an early stage. Eventually these lesions can reach the subchondral bone. This bone becomes increasingly stiff as it remodels which, coupled with enzymatic digestion of the extracellular matrix, only contributes to further cartilage degradation⁴¹.

The progression of the disease in cartilage is characterized by three overlapping stages. The first stage consists of disruptions to the structural framework at the molecular level and increase in water content. Furthermore, the concentration and aggregation of proteoglycans, aggrecan, and glycosaminoglycans decrease. Permeability of the tissue increases as the concentrations of these macromolecules decrease. This causes the stiffness of the cartilage to decrease, allowing for further mechanical damage^{42,43}.

The second stage involves the chondrocytes response in which a variety of cytokines and growth factors are released in an effort to combat the onset of disease. Specifically, the chondrocytes become more metabolically active, as well as increase in number. The now higher number of chondrocytes releases anabolic and catabolic factors and tries to produce more

macromolecules. This can restore the cartilage, but if the chondrocytes cannot keep up with the repair of the tissue, some cytokines, such as interleukin-1, and proteases can cause collagen degradation and weaken the structure of the tissue⁴¹.

If this cellular response in stage two is not effective, the final stage takes place in which there is a progressive loss of cartilage as well as decrease in chondrocyte activity^{42,43}. This is due to the increased damage to the tissue and associated death of chondrocytes as their supportive extracellular matrix degenerates, as well as potential down regulation of anabolic cytokines. This reaction could be facilitated by the increase of molecules that bind to these anabolic factors, preventing their stimulation of the chondrocytes⁴¹.

1.4 Meniscus

The meniscus is a fibrocartilaginous pad in the knee joint with load-bearing and lubricating properties⁴⁴. The menisci are semilunar in shape and insert into the tibial spine, as seen in Figure 1-3, below.

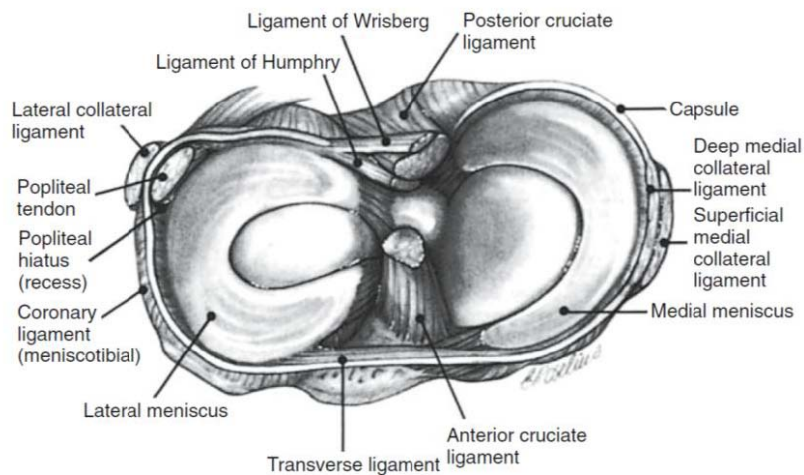


Figure 1-3: Illustration of Knee Joint. Superior view with femur removed⁴⁵

The peripheral part of the menisci are thicker than the inner concave part, resulting in a wedge-like cross-section. This shape allows for congruency in movement between the rounded femoral condyles and comparatively flat tibial plateau during loading. The perimeter of the menisci is attached to the joint capsule through the coronary ligament, limiting movement in the anterior-posterior direction as well as during rotation⁴⁶. The medial meniscus is also attached to the medial collateral ligament (MCL), further reducing its mobility. The lateral meniscus is attached to the femur via the ligament of Humphrey (anterior) and the ligament of Wrisberg (posterior). Finally, the transverse ligament attaches the anterior portion of both menisci. These ligaments serve as stabilizers that prevent the menisci from being extruded during joint

compression^{47,48}. Unlike articular cartilage, the menisci have both vascular and nervous supply, which is crucial for tissue healing⁴⁶.

1.4.1 Structure

The menisci have several structural similarities to articular cartilage. Menisci are composed of 70% water and 30% organic matter. This organic matter is 75% collagen and 8-13% non-collagenous proteins⁴⁹. A notable difference between articular cartilage and the menisci is that, while cartilage contains type-II collagen, the meniscal tissue is comprised mostly of type-I collagen, a structural feature it shares with bone and tendon. However, like the collagen in articular cartilage, this type-I collagen serves as the primary structural framework for the tissue⁵⁰.

These collagen fibers are organized into three layers in the tissue. In the superficial layer, collagen fibers run radially to resist shear stresses and prevent the tissue from splitting. The middle layer has circumferential fibers resisting “hoop” stresses due to load bearing. Running parallel to the periphery of the tissue in woven collagen bundles is the deep layer^{46,50}.

The remainder of the organic matter is composed of proteoglycans and aggrecan, which provide the menisci with mechanical properties similar to articular cartilage via water retention and electrostatic repulsion. Indeed, the tissues’ water exudation due to these molecules not only confers compressive stiffness to the tissue, but also contributes to lubrication when loaded⁴⁶. The greatest concentration of these molecules are in the horns of the meniscus and the inner half of the bulk tissue, corresponding to the major load-bearing areas⁵¹.

The cells that populate the meniscus are several different types of fibrochondrocytes⁵⁰. These fibrochondrocytes have traits of both chondrocytes and fibroblasts; they are round and produce the necessary components of a cartilaginous matrix like chondrocytes, but also produce

type-I collagen like fibroblasts⁴⁶. The cells of the outer periphery are more similar to fibroblasts, producing solely collagen type-I and lacking a pericellular matrix. The inner and middle layers have round cells that produce type-I and -II collagen and possess an extra cellular matrix. The cells of the superficial zone have a fusiform shape and no cytoplasmic projections⁵².

1.4.2 Function

The meniscus is vital for proper joint function and health⁴⁴. The main functions of the menisci are to distribute load during weight bearing, stabilize the joint, nourish and lubricate the articular cartilage, and allow for smooth joint gliding^{47,48,53,54}. It accomplishes these goals through several mechanisms.

The congruent shape of the meniscus allows for an increase in contact area and thus lower contact stresses during motion. As much as 45-70% of the loads in the knee joint are transmitted through the meniscus normally, but if the meniscus is removed this leads to smaller contact areas and a doubling of contact stresses^{46,49,55}.

The menisci accommodate both the posterior translation of the femoral condyles on the tibial plateau, as well as tibial internal rotation. The lateral meniscus experiences more translation movement as compared to rolling, while the medial meniscus is exposed to even amounts of both types of motion⁵⁶. This congruency allows the menisci to stabilize the joint, even when the supporting ligaments are damaged⁵³.

Like articular cartilage, the menisci display viscoelastic properties such as creep, where steady loading causes increasing deformation over time⁴⁶. While this mechanical property, and others such as compressive stiffness, cell nourishment, and lubrication, are provided by the osmotic pressure resulting from proteoglycans and the associated water exudation during loading,

its tensile stiffness is provided by elastin, which comprises only 0.06% of its mass but aids the recovery of shape following loading^{46,50}.

Menisci were believed to function as shock absorbers, and are often described as such⁴⁴. However, recent review of this work suggests that the meniscus does not in fact act to dissipate energy to modify the response of the joint; that is, it does not behave as a shock absorber⁵⁷. This recent work explains that, while shock absorption does occur in the knee joint to attenuate the forces experienced by the rest of the body, it is likely the tissue fluid in which the energy is dissipated, not the menisci^{57,58}. Previous work promoting the meniscus as a shock absorber made several incorrect assumptions, such as assuming that stored elastic energy is a form of shock absorption. In fact, some work shows that meniscectomized knees absorb more shock⁵⁹. Finally, if the meniscus does absorb shock, it is not great enough at physiological loading levels to be significant⁵⁷.

1.4.3 Meniscus and OA

Given that the meniscus functions to maintain joint health, degradation of the menisci and cartilage as seen in OA are interrelated in their progression and contribution to pain and loss of function. Specifically, damage or removal of the menisci can lead to changes in joint loading and subchondral bone structure, which are hallmarks of OA⁶⁰.

Damage to the menisci can occur due to both chronic and acute stimulus. Misaligned joint movement, obesity, and general wear can cause the meniscus tissue to degrade through overloading and changes to the matrix architecture⁶¹. Trauma to the knee joint can cause similar changes that eventually lead to the cycle of OA, as shown in Figure 1-4, where the onset of damage, from whatever source, leads to damage that limits the ability of the tissue to repair itself

and maintain function. This of course leads to further damage and further loss of function. What's more, meniscal lesions are prevalent in the middle-aged and elderly (ranging 19% of women aged 50-59 to 56% of men aged 70-90)⁶².

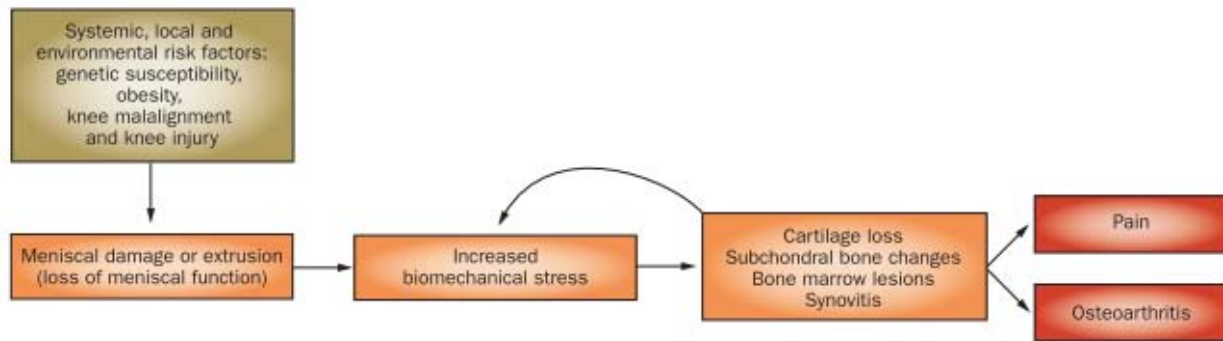


Figure 1-4: The “meniscal pathway” to knee OA due to the negative feedback of tissue damage and loss of function⁶¹.

While damaged menisci can play an important role in the progression of OA, they are not always painful and thus are hard to diagnose, being found often in asymptomatic joints. In fact, 76% of asymptomatic joints showing signs of meniscal damage in the elderly⁶³. Cartilage damage occurs primarily in the regions of meniscal damage⁶⁴, and meniscal damage is correlated to OA⁶⁰. Thus, it is important to identify potential causes of meniscus damage to minimize OA progression in at-risk individuals.

1.5 Lubrication Mechanisms

A biointerface is an interface between a cell, molecule, tissue, or biomaterial with another tissue or biomaterial. Biointerface science contributes to the understanding of interactions between molecules and surfaces; interactions of molecules, and their resulting function, at a surface can be different to those in solution. Biointerfaces are central to many fields of science and engineering, including biotribology. Biotribology is the study of lubrication, friction and wear of sliding biological surfaces that provides insight into the fundamental mechanism of biolubrication.

The biointerface formed by the cartilage and meniscus tissue surfaces is subject to high loads and frequent use, so friction and wear are important variables to consider for proper function. Friction is the resistance to motion between two apposing surfaces. There are two types of friction: surface friction is caused by the adhesion between the apposing surfaces (due to surface roughness or fluid viscosity) and bulk friction, caused by internal energy dissipation (e.g., energy losses of fluid flowing through structural framework in cartilage³⁶). Several types of wear are observed, two of which are fatigue and interfacial. Fatigue wear is a result of repetitive loading, while interfacial wear is due to abrasive surface contact³⁶. Lubrication is the mechanism by which friction is decreased, lowering wear in the process. Friction is quantified by the coefficient of friction and serves as an indicator of lubrication. This coefficient of friction is a ratio of the frictional and inertial forces, shown by the following equation:

$$\mu = \frac{F}{N}$$

Where μ = coefficient of friction (dimensionless), F = frictional force (F), and N = Normal applied load (N)

Lubrication is, generally, defined by two apposing modes: fluid-film and boundary. The active modes taking place depend on forces on the interface, motion between the apposing surfaces, and the time history of loading and motion⁶⁵. The change in lubrication mode is illustrated in the Stribeck Curve in Figure 1-5.

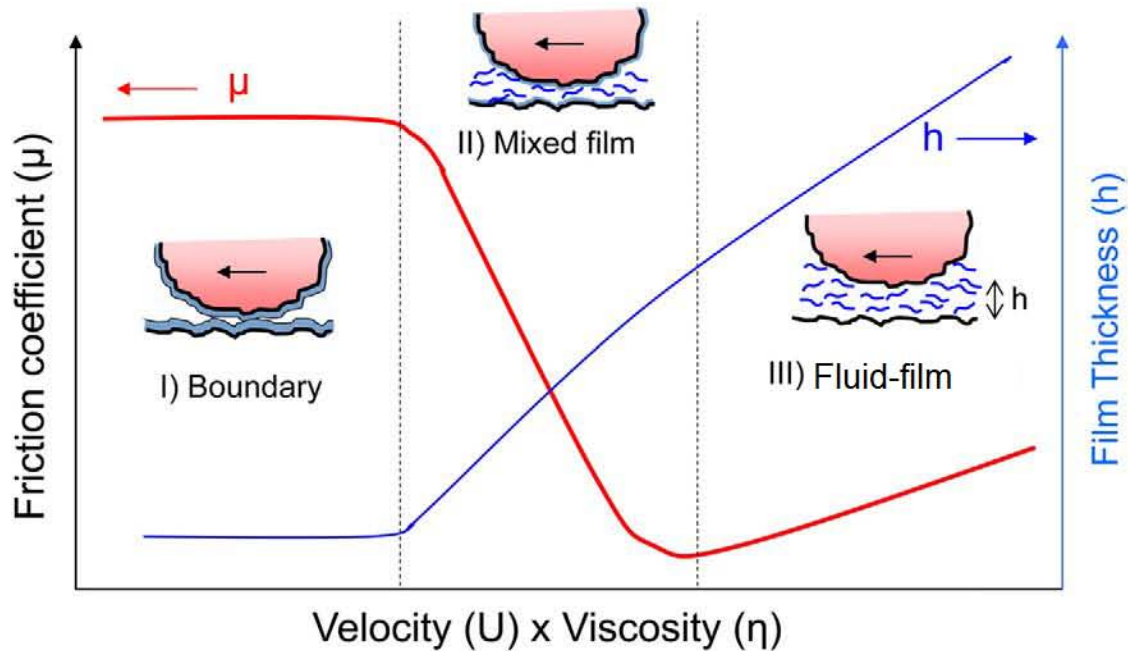


Figure 1-5: Stribeck Curve: Change in lubrication regime with coefficient of friction (red) and fluid-film thickness (blue) on the y-axis and critical lubrication variables, viscosity and velocity, on the x-axis. Adapted from previous work⁶⁶.

The Stribeck curve was developed using a steel-on-steel interface, and thus represents the lubrication between classical engineering materials. Porous, soft, and hydrated tissue surfaces, such as the cartilage and meniscal surfaces, do not directly mimic this behavior⁶⁷, but understanding these mechanisms and which one, or combination of them, takes place in the knee joint can potentially give insight into the wear of cartilage that develops during OA.

1.5.1 Fluid Mediated Lubrication

Fluid-film lubrication is defined by the presence of a layer of fluid completely separating the apposing surfaces. Friction is generally lower during fluid-film lubrication than another type of mode, boundary lubrication. Fluid-film lubrication includes hydrodynamic lubrication, squeeze-film lubrication, hydrostatic lubrication, self-generating lubrication, and boosted lubrication.

Hydrodynamic lubrication involves the fluid pressure generated by surfaces moving relative to one another bearing the load. The motion “drags” fluid between the surfaces, separating them completely. This type of lubrication requires relatively high, continuous speed motion³⁶. The minimum thickness for an effective fluid film, 1.4 μm , is not feasible when considering surface roughness (healthy human talar cartilage has, for example, 0.8 μm on each of the two apposing surfaces for a combined roughness of 1.6 μm . The fluid film must be thick enough to fully separate the surfaces so there is not contact between the asperities of each surface for fluid-mediated lubrication to occur)⁶⁸. Fluid-film lubrication may occur during the swing phase of locomotion, when load is low and motion fast³⁶. When the deformation of the cartilage is considered, elastohydrodynamic lubrication occurs³⁶.

Squeeze-film lubrication occurs when lubricants cannot escape from the space between the surfaces. This pressurizes the fluid and supports the load. This mode depends on the time taken for the fluid thickness to decrease to the minimum sufficient for lubrication, roughly 60 seconds in the synovial joint³⁶. This mode is dependent on fluid viscosity, cartilage permeability, and the ability for the fluid to be replenished over time. This may occur during human motion due to its intermittent loading³⁶.

Hydrostatic lubrication occurs when loading causes the cartilage matrix to exude water to

fill the space between the surfaces, earning it the alternative title “weeping” lubrication. This has been shown to bear significant loads and, as long as the contact area changes fast enough to prevent depressurization, the load can be supported over time⁶⁹. The classical engineering analog for modeling purposes is that of a fluid pump continuously providing flow to the lubrication system³⁶.

Theoretically, when the leading edge of the counterface surface passes over the tissue, fluid will be exuded that facilitates a self-generating mode of lubrication³⁶. This fluid would be reabsorbed in the center of contact and potentially exuded again due to the movement of the trailing edge of the counterface.

A boosted lubrication mechanism is possible when the force of the increasingly close surfaces pushes the water component of SF into the matrix, leaving a gel-layer composed of the SF solutes. This could only be operative for short periods of time, however, as the increasing pressure could eventually cause the surfaces to push through the gel layer³⁶.

During OA, SF viscosity increases as cartilage permeability increases, causing the fluid flow through the cartilage and joint to stagnate, leading to the inability of hydrodynamic and squeeze-film lubrication to bear load^{36,42,43}. Furthermore, modeling suggests that the porosity of cartilage would not allow for long-term fluid film maintenance⁷⁰. Hydrostatic lubrication still plays a role in joint lubrication during OA, but the characteristics of increased friction suggest it is boundary lubrication that accounts for this increase⁷¹.

1.5.2 Boundary Lubrication

In boundary mode lubrication, the articulating surfaces are no longer separated and load is born by surface-to-surface contact. Thus, it is the surface-bound molecules that affect the friction⁶⁵. Unlike fluid-film lubrication, boundary lubrication is associated with high loads and

low speeds. The dynamic nature of the joint means one mode does not alone account for the lubrication of the joint, but when fluid depressurizes it is thought to become the dominant mode operating in the joint³⁶. As depressurization occurs, more surface-to-surface contact is achieved. While this may only amount to 10% of the total area directly bearing load, it is thought that a majority of the friction may be generated here⁷².

Boundary lubrication is indicated when the coefficient of friction is independent of relative sliding velocity and normal load which, as discussed above, normally affect the development and performance of a fluid film layer⁶⁵. In order to study boundary lubrication of articular cartilage independent of other modes of lubrication, experiments must allow for fluid depressurization to occur⁷⁰.

Molecules that are bound to the articulating surfaces can affect friction during boundary lubrication; a variety of molecules found in SF have been investigated³⁶.

1.5.3 Experimental Analysis

Given the importance of understanding the operative mode of lubrication to determine the effectiveness of lubricants, the type of experimental test setup must be considered carefully. The type of lubrication occurring in a test sequence must be understood so that accurate conclusions are reached.

An *in vivo* test would have the most physiologically relevant surface interactions as well as accurate joint kinematics. When an excised joint was used to determine friction through a pendulum motion between the tibia and femoral surfaces, extremely low coefficients of friction were calculated, ~ 0.001 ⁷¹. However, this setup was not able to differentiate between the different modes of lubrication.

In vitro tests allow for more flexibility in experimental design and setup that may help focus on different modes of lubrication. These tests can use a variety of different types of motion, such as reciprocating or rotational. Reciprocating motion is more like joint kinematics and allows for Stribeck analysis, but fluid pressurization at the leading edge of the motion allows for fluid-mediated lubrication to occur. In a rotational setup, the stationary area of contact allows for fluid to depressurize and the boundary mode of lubrication to be dominant⁶⁵.

The materials used in these tests are also important. Synthetic surfaces are easier to manipulate into an appropriate test setup. However, synthetic counterfaces do not accurately replicate the soft, porous tissue surfaces, suggesting that natural tissue surfaces would better represent the physiological environment⁶⁷. To fully replicate the surface interactions found in the joint, two physiological surfaces should be used despite the potential difficulties in test setup. This may effect how naturally occurring lubricants bind to the surface and thus modulate friction.

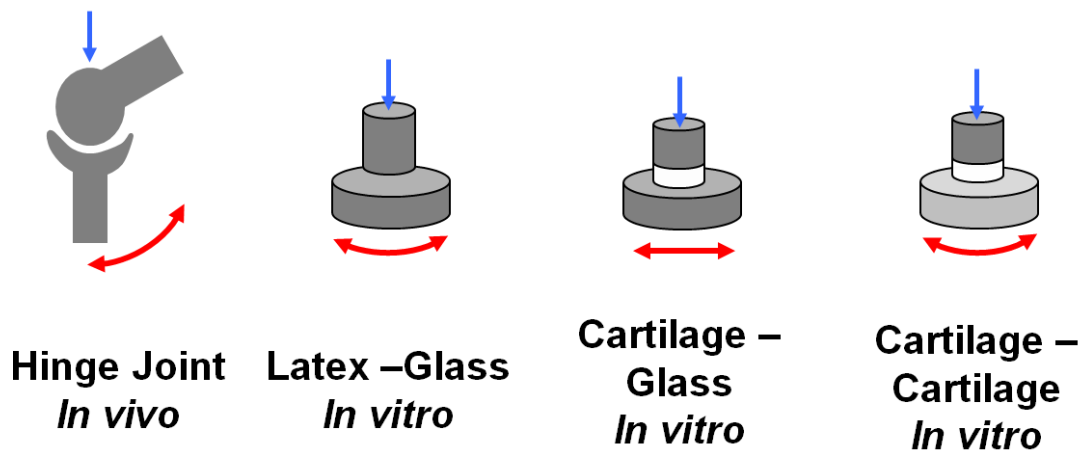


Figure 1-6: Differing experimental test protocols and interfaces used to assess friction modulating of lubricants. Adapted from previous work^{65,71,73}.

1.6 Proteoglycan 4

PRG4 is a glycoprotein found in SF that contributes to, and is necessary for, joint health⁷⁴. In fact, mutations in the PRG4 gene, in the autosomal recessive disorder camptodactylyarthropathy-coxa vara-pericarditis (CACP), result in no PRG4 protein expression and juvenile-onset joint failure⁷⁵. Similarly, animal models have shown increased cartilage wear and high friction, as shown in Figure 1-7⁷¹.

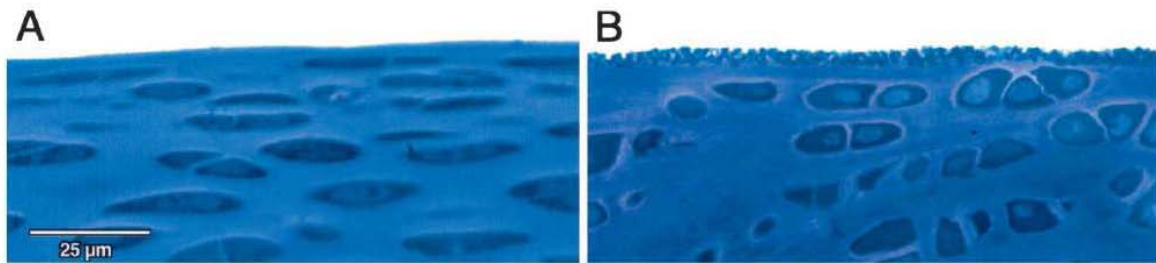


Figure 1-7: Surface smoothness affected in PRG4 knockout mice. A and B, Representative photomicrographs of toluidine blue-stained knee joint cartilage sections from 2-week-old PRG4^{+/-} (A) and PRG4^{-/-} (B) mice, demonstrating differences in surface smoothness⁶⁹.

PRG4 is synthesized and secreted by cells near the surfaces of both articular cartilage and the meniscus, and is found on the articulating surfaces of these tissues^{74,76,77}. It is also found throughout the body wherever sliding is common, such as in the eye⁷⁸, in tendons⁷⁹, and the intervertebral disc⁸⁰. The PRG4 gene codes for the production of megakaryocyte-stimulating factor (MSF), superficial zone protein (SZP) or lubricin⁷⁴, which are all different names of the same protein that for the extent of this work will be referred to collectively as PRG4.

1.6.1 Structure

PRG4 is a 12-exon glycoprotein with a central mucin-like domain. This domain has a carboxyl (C) terminal and an amino (N) terminal on either side of it, which play a role in bonding to other PRG4 molecules and the extracellular matrix⁷⁴.

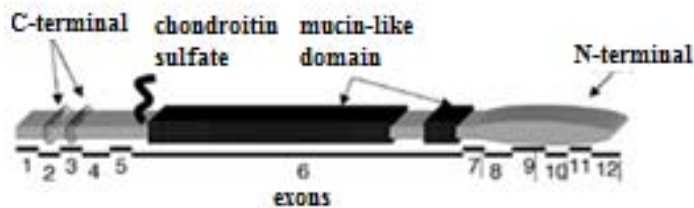


Figure 1-8: Schematic of PRG4 molecule⁸¹.

This mucin domain is glycosylated with negatively charged O-linked oligosaccharides, many of which have sialic acid caps⁸². Generally, mucins can form into multimers via disulfide bonds, first dimerizing in the endoplasmic reticulum after protein translation before further multimerization in the golgi apparatus⁸². Structural changes in mucins tend to produce functional changes, and it appears PRG4 is similar to mucins in this manner^{82,83}.

1.6.2 Function

PRG4 is an effective boundary lubricant at a variety of interfaces^{73,84-86}. At an *in vitro* cartilage-cartilage biointerface it appears to also interact with HA synergistically to lower friction further, while another SF constituent, surface active phospholipids, did not contribute to lubrication^{65,84}. PRG4 has also been shown to have anti-adhesive properties, preventing nonspecific adhesion of globular proteins⁸⁷.

There are several theories as to how PRG4 provides these remarkable low-friction properties. PRG4 may form a sacrificial layer on the surface of the tissue that is sheared off during motion due to the speed at which this layer is replenished by SF following depletion⁸⁸. The mucin domain of the PRG4 is known to facilitate lubrication through electrostatic repulsion and osmotic pressure⁷⁴. Specifically, the negatively charged glycosylations repel other surfaces with similar charges, such as an opposing layer of PRG4. Osmotic pressure occurs due to the binding of the cysteine rich C and N terminals to the surfaces via disulfide bonding. When anchored to the surface in the presence of other molecules, this causes the molecules to rearrange themselves to minimize steric forces. This causes the molecules, given enough density, to form a brush-like layer on the surface^{87,89,90}. This brush layer repulses similar brush layers to prevent further increase in molecular density. It has also been proposed that the hydrophilicity of the glycosylations attracts water that forms a hydration layer. This layer can not only bear load, but still behaves as a fluid at small scales and thus has little resistance to shear⁸⁶.

1.6.3 PRG4 and OA

Levels of PRG4 in SF can drop precipitously following acute knee injuries, which are highly associated with subsequent progressive cartilage degeneration leading to OA^{4,91}. A year following major joint injury, PRG4 levels return to their previous levels⁹². An ovine model, however, suggests that PRG4 levels rise quickly in the first weeks after an injury before returning to normal, though this SF did not lubricate effectively⁹³. As such, this measured value may not be indicative of full-length functional protein.

PRG4 molecule interactions within the joint remain to be clarified, but preclinical studies show that local administration of PRG4 is therapeutically effective in preventing cartilage

degeneration^{27,94}.

1.7 Hyaluronan

HA is a glycosaminoglycan found in SF that has been shown to be an effective boundary lubricant at a cartilage-cartilage biointerface^{84,95}. It is currently used in viscosupplementation and is considered quite effective¹². However, the residency time in the joint is fairly low for HA, with higher molecular weight (MW) forms decreasing in concentration over time²⁴. This is a problem, because HA's MW affects its boundary lubricating ability⁹⁶.

1.7.1 Structure

HA's negatively charged, polymeric structure is constructed from alternating glucuronic acid and N-acetylglucosamine. This repeating structure causes a wide range of physiologically observable MWs, up to 4 MDa.

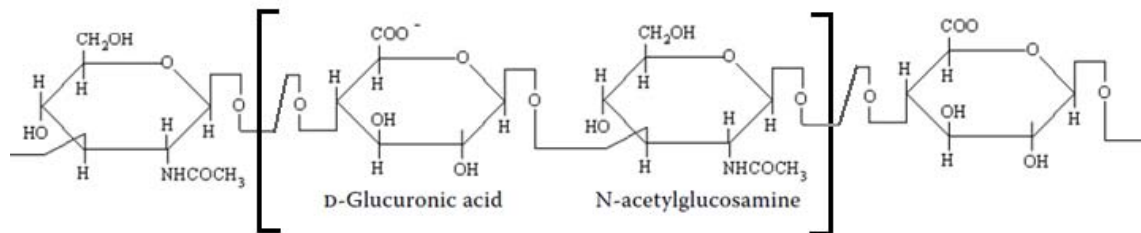


Figure 1-9: HA's chemical structure⁹⁷.

1.7.2 Function

HA provides SF with its viscoelastic properties, hydrates the tissue surface, and enables assembly of glycoproteins⁹⁷. Mechanically, it is a dose-dependent boundary lubricant at the cartilage-cartilage biointerface, being slightly more effective as its MW increases^{84,96}.

While PRG4 and HA have been shown to reduce friction more effectively when

combined, the mechanism by which this is accomplished is not yet understood⁸⁴. Electron microscopy suggests that the interaction was a physical one due to hydrophobic attraction, rather than a chemical bond⁹⁸. Particle tracking research suggested that PRG4 helps organize HA molecules; specifically decreasing the intramolecular interactions of the rigid HA polymer and allowing it to align with the direction of the flow⁷¹. Recent work demonstrates that, in solution, PRG4 and HA bind together to create a large complex that may provide this lubricating function⁹⁶.

HA also exhibits a surface-dependent function. While both latex-glass and mica-mica interfaces have shown PRG4 to be an effective boundary lubricant, HA results haven't been in agreement^{86,98,99}. At a cartilage-cartilage biointerface however, where appropriate physiological interactions occur, HA does effectively lower friction in a boundary mode^{84,96}. It is important to consider the type of surfaces when assessing HA's lubricating function.

1.7.3 HA and OA

With OA, HA's concentration in SF can remain the same, but more low MW species of HA have been found to be present^{93,94}. What's more, the lubricating ability of this SF is diminished, though this can be counteracted with a PRG4 dose^{93,94}. This is beneficial because, while HA's MW affects its lubricating ability alone, when combined with PRG4, MW does not affect its ability to lower friction⁹⁶.

1.8 Thesis Aims

The three hypotheses stated in section 1.1 will be tested with the following specific aims:

Aim 1: Determine the velocity dependence of the kinetic coefficient of friction at an articular cartilage-meniscus biointerface with SF constituents.

Aim 2: Measure the boundary lubricating ability of (rh)PRG4 \pm HA at an articular cartilage-meniscus biointerface.

Aim 3: Assess the surface adsorption of rhPRG4 to the meniscus following depletion of endogenous PRG4.

CHAPTER 2: Effect of Sliding Velocity on Lubricating Ability of PRG4 and HA at an Articular Cartilage-Meniscus Biointerface

2.1 Abstract

Objective: Determine the velocity dependence of the kinetic coefficient of friction at an articular cartilage-meniscus biointerface with SF constituents.

Methods: The friction-reducing ability of PRG4 and HA was tested using a novel *in vitro* articular cartilage-meniscus test by modifying a previously described boundary lubrication experimental setup with rotational geometry and stationary area of contact. Samples were harvested from mature bovine stifle joints. Articular cartilage annuli were cut from the patellofemoral groove while the meniscus cores were cut from the tibial facing surface of the meniscus. Following vigorous shaking to remove residual surface-bound molecules, samples were tested in phosphate buffered saline (PBS) (negative control), the lubricant of interest (PRG4, HA, or PRG4+HA), and SF (positive control). The articular surfaces of bovine cartilage and meniscus samples were articulated against one another over a wide log scale range of effective velocities (v_{eff}): 10, 3, 1, 0.3, 0.1, and 0.01 mm/s. A kinetic coefficient of friction was calculated and used to compare the effectiveness of the lubricants.

Results: PRG4 lowered friction compared to PBS at low and intermediate v_{eff} , but was not an effective lubricant at higher v_{eff} . HA lowered friction at all v_{eff} compared to PBS. When PRG4 and HA were used in combination, friction was lowered, approaching the level of whole SF.

Conclusions: These results suggest that effective velocity affects PRG4's friction-reducing capability and must be considered to properly evaluate its boundary lubricating ability.

2.2 Introduction

The knee is one of the most heavily loaded joints in the body, and the specialized tissues that compromise it are critical for proper function and long-term health. One such tissue is articular cartilage, which covers the ends of long bones. In the knee, it covers the posterior surface of the patella, the femoral condyles and groove, and the tibial plateau. It is a soft, porous, and hydrated tissue³¹ that provides several key biomechanical properties; it is load bearing, wear-resistant, and low friction^{29,30}. These properties are provided by the interaction of the fluid, the ions contained therein, and the collagen framework within the cartilage^{31,37}. However, due to either wear and tear over time or traumatic joint injury, the cartilage can begin to degrade, leading to pain and loss of function^{1,3,4}. This chronic breakdown of cartilage, OA, lowers quality of life and increases medical bills for the afflicted patients¹². While OA is a multifactorial condition, one of the contributing mechanisms is the breakdown of proper lubrication *in vivo*¹⁰⁰.

Another tissue within the knee joint that contributes to proper function is the meniscus. This fibrocartilaginous pad articulates with the femoral condyles superiorly and the tibial plateau inferiorly. Menisci are semi-lunar shaped wedges that facilitate congruent movement between the rounded femoral condyles and the relatively flat tibial plateau⁴⁵. This shape contributes to the menisci's function as a load-bearing and lubricating tissue⁴⁶⁻⁴⁸. Like articular cartilage, these mechanical properties are provided by the interaction between the fluid and solid phases within the tissue⁵⁰. Unfortunately, the menisci also share cartilage's potential for degradation. The menisci can break down due to overloading and the accompanying changes in overall joint mechanics, which also effects the cartilage and subchondral bone^{60,61}. What's more, once the menisci start to degrade, they become more susceptible to further damage and their surgical removal only worsens the OA symptoms in the joint^{60,64}. Thus, it is very important that the tissue

remains healthy and does not begin this negative cycle.

These tissues provide effective lubrication for the knee joint, contributing to the maintenance of overall joint health. Lubrication is generally divided into two opposing modes: fluid-mediated lubrication and boundary lubrication⁶⁵. Fluid-mediated lubrication occurs when the fluid both between and within the tissue surfaces bear significant portions of the load with little shear resistance³⁶. This mode of lubrication is affected by fluid properties such as viscosity and film thickness³⁶. Conversely, when the tissues are in surface-to-surface contact and the load is borne by direct contact, it is the surface-bound biomolecules that modulate friction⁶⁵. Given the biphasic properties of both cartilage and the menisci, as well as the wide range of loading conditions that occur in the knee joint during different activities (e.g., walking, running, jumping, or standing), it is no surprise that both of these types of lubrication, and indeed, a mixture of both, occur³⁶. However, while boundary lubrication only occurs over a small part of the joint surface, it is thought that these locations are also where the majority of the friction is generated⁷² as this mode of lubrication is classically associated with increased levels of friction (and wear). As such, it is important to consider boundary lubrication in the joint.

Boundary lubrication occurs when there is direct surface-to-surface contact between the apposing tissue surfaces. This situation arises when the fluid in the relevant joint tissue has depressurized, significantly decreasing the load from being borne by a fluid film³⁶. Similarly, when the load is high and the velocity is low, a viscous fluid film of sufficient thickness to fully separate the apposing surfaces is not consistently formed, causing boundary lubrication to be dominant at the biointerface⁶⁵. As such, these conditions must be in place to specifically investigate boundary lubrication *in vitro*⁷⁰. Once testing conditions are such that boundary lubrication can be facilitated, the friction-reducing effect of surface-bound molecules can be

studied. These boundary lubricants mediate friction during this critical mode of lubrication and elucidating their comparative boundary lubricating ability contributes to the understanding of a fundamental joint lubrication mechanism, and potentially could contribute to future development of injectable biotherapeutics for treatment of OA.

Perhaps unsurprisingly, the best boundary lubricants are likely naturally occurring constituents of SF. PRG4 is one such molecule. The mucin-like glycoprotein is found on the surface of articular cartilage and meniscus, as well as in the SF^{74,76,77} and has been shown to be an effective boundary lubricant at a variety of different surfaces and in different test setups. Between synthetic surfaces such as latex-glass⁹⁸ or mica-mica^{86,99}, physiological surfaces like cartilage-cartilage^{84,85}, or a combination such as cartilage-glass⁷³, PRG4 lowers friction effectively. In addition, it has been demonstrated so for both reciprocating and rotational motion. This is a critical point, as rotational test geometry allows for a boundary mode of lubrication to be operative and a reciprocating test is more similar to joint kinematics with a mixed lubrication regime^{65,70}. When investigating boundary lubrication of articulating tissues in the knee joint, using physiological surfaces (i.e., tissues) could facilitate molecular and surface interactions seen *in vivo* compared to synthetic surfaces. Furthermore, a stationary contact area with rotational motion will allow for fluid depressurization and prevent a fluid film from forming due to exudation^{36,70}. This test setup will allow PRG4's boundary lubricating ability to be investigated specifically.

Another SF constituent of interest is HA, a negatively charged polysaccharide found in the joint. HA has been shown to operate as a dose-dependent boundary lubricant at a cartilage-cartilage biointerface^{84,96}, though at synthetic interfaces it does not behave like a boundary lubricant⁹⁸. HA's cartilage boundary lubricating ability has also been linked with its MW,

specifically that the higher MW HA is a more effective lubricant⁹⁶. This is important as during OA, while HA concentration remains the same in the joint, the molecules' MW decrease⁹⁴.

HA also has been shown to interact synergistically with PRG4 to lower friction in an *in vitro* cartilage-cartilage boundary lubrication test, further than either molecule alone⁸⁴. In solutions these two molecules form a larger complex, but the specifics of this interaction are unknown⁹⁶. HA is currently used as a viscosupplement to treat OA¹², so learning how these molecules interact could benefit future injectable treatments.

While PRG4 and HA are shown to be effective boundary lubricants at a cartilage-cartilage biointerface, they not been investigated at the cartilage-meniscus biointerface. The meniscus is critical for joint health, with a majority of loads experienced by the knee transmitting through it⁵⁵. Furthermore, the meniscus helps provide lubrication to the knee joint⁴⁶⁻⁴⁸, suggesting that the boundary lubricating ability of SF constituents PRG4 and HA should be determined at this important biointerface.

As such, the objective of this study is to determine the velocity dependence of the kinetic coefficient of friction at an articular cartilage-meniscus biointerface with PRG4 and HA, alone and in combination. This will provide insight into the lubrication mode that takes place at this biointerface and how naturally occurring SF constituents affect it.

2.3 Methods

An *in vitro* boundary lubrication test was modified to accommodate an articular cartilage-meniscus biointerface and used to test the ability of a variety of lubricants to affect the kinetic coefficient of friction over a wide range of velocities. Fluid depressurization and stationary contact geometry facilitated an operative boundary mode of lubrication. The lubricants PRG4, HA, and PRG4+HA are tested in comparison with a negative control, PBS, and positive control, SF.

2.3.1 Lubricant Preparation

Skeletally mature bovine stifle joints were obtained from a local abattoir (Calgary, AB, Canada). Fresh bovine SF was aspirated from synovial joints within 15 minutes of slaughter and visually inspected for signs of blood before purchase, at which point it was aliquoted, and stored at -80°C for several months before use⁸⁴.

PRG4. PRG4 was purified from media conditioned by bovine articular cartilage explants, as described previously^{84,96}. Briefly, cartilage discs with a 6 mm diameter were cut from the patellofemoral groove of these bovine joints and cultured in Dulbecco's Modified Eagle's Medium (Life Technologies, Carlsbad, CA) with 0.01% bovine serum albumin. This media had 25 µg/mL of ascorbic acid and 10 ng/mL of recombinant human transforming growth factor-β added to enhance PRG4 secretion¹⁰¹. The media were purified using gravity flow-through diethylaminoethanol anion exchange (DEAE) chromatography (GE Healthcare Life Sciences, Baie d'Urfe, QC, Canada) and step elutions of increased salt concentration^{101,102}. The 0.615 M NaCl batch elution was collected and filtered through a 100 kDa spin filter. The retentate was collected and pooled with filter rinse before being stored at -80°C. A bicinchoninic acid (BCA)

assay (Sigma-Aldrich, St. Louis, MO) was used to determine the total concentration of protein in the final solution. The purity of this solution was confirmed using 3-8% Tris-Acetate sodium dodecyl sulfate polyacrylamide gel electrophoresis (SDS-PAGE). These gels were subject either to western blot, where they probed with PRG4-specific antibody LPN (Life Technologies, Carlsbad, CA), or stained with Simply Blue protein stain (Life Technologies, Carlsbad, CA) and analyzed with densitometry software (Image J, Bethesda, MD)⁸³. PRG4 was prepared in PBS at physiological concentration, 450 $\mu\text{g}/\text{mL}$, from this concentrated and filtered solution¹⁰³.

HA. 1.5 MDa HA was acquired commercially (Lifecore Biomedical, Chaska, MN) and prepared in PBS at a physiological concentration of 3.33 mg/mL ⁹⁵.

2.3.2 Lubrication Test Tissue Sample Preparation

Cartilage annuli ($R_{\text{outer}} = 3.2 \text{ mm}$ and $R_{\text{inner}} = 1.5 \text{ mm}$) were cut from osteochondral blocks harvested from the patellofemoral groove of mature bovine stifle joints^{65,84}, acquired as described above. Meniscal cores ($R = 6 \text{ mm}$) were cut from menisci taken from these same joints. Cores were harvested from these menisci from the femoral to tibial facing surfaces. The femoral facing surface was cut away to leave a flat surface, on which a coring punch was then used. A custom cutting-jig was then used to cut this cored tissue sample into $\sim 2.5 \text{ mm}$ thick discs with the tibial facing surface of the menisci intact. Samples were shaken vigorously overnight in PBS at 4°C to remove residual SF from the surface^{65,84} before the first test in PBS. The meniscal discs were then adhered to a wooden plug of the same radius with Crazy Glue (Westerville, OH) prior to lubrication testing, as shown below in Figure 2-1.

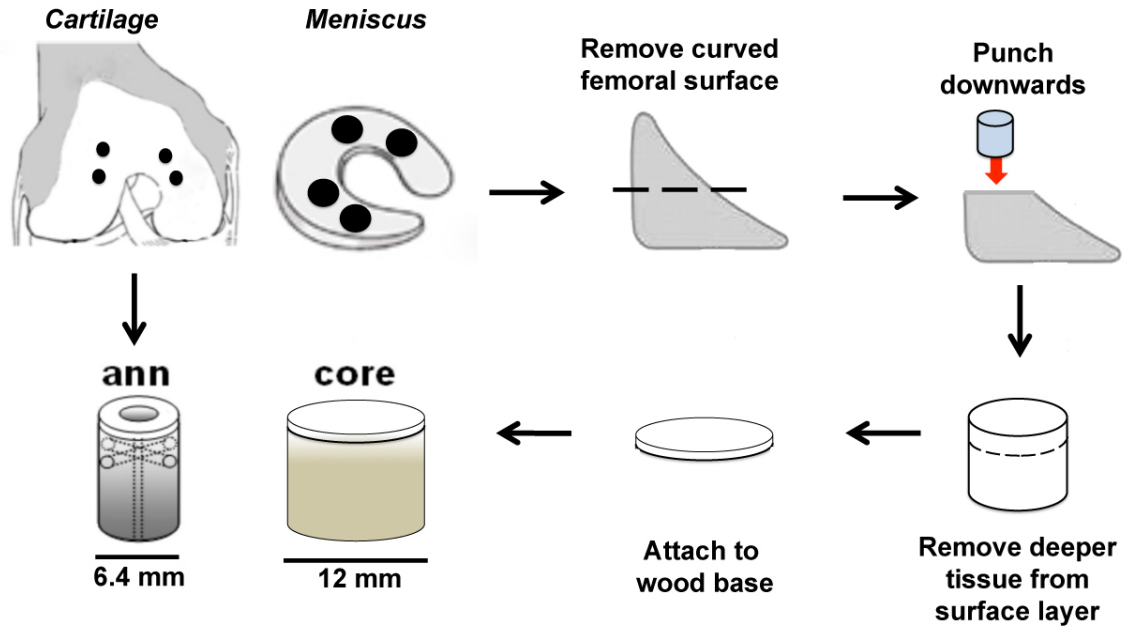


Figure 2-1: Cartilage and meniscus sample preparation

2.3.3 Cartilage-Meniscus Boundary Lubrication Test

The lubrication testing was conducted on a Bose ELF 3200 biomechanical testing device (Bose ElectroForce Systems Group, Eden Prairie, MN) equipped with sensors for axial displacement ($\pm 6,250$ mm range), axial load (N, ± 45.0 N range), and torque (τ , ± 70.0 N mm range). Test protocol was modified from previous studies^{84,94,96} to determine velocity dependence to friction in each lubricant at the articular cartilage-meniscus biointerface. Custom fixtures were used to attach the samples to the testing device, oriented concentrically and articulating surfaces in apposition. The cartilage annulus was fixed to the sensors and axial actuator superiorly while the meniscal core was secured to the rotational actuator inferiorly. The core was had inert silicon tubing circumferentially attached to serve as a lubricant bath in which ~ 0.3 ml lubricant was placed to completely immerse both surfaces, as shown below in Figure 2-2.

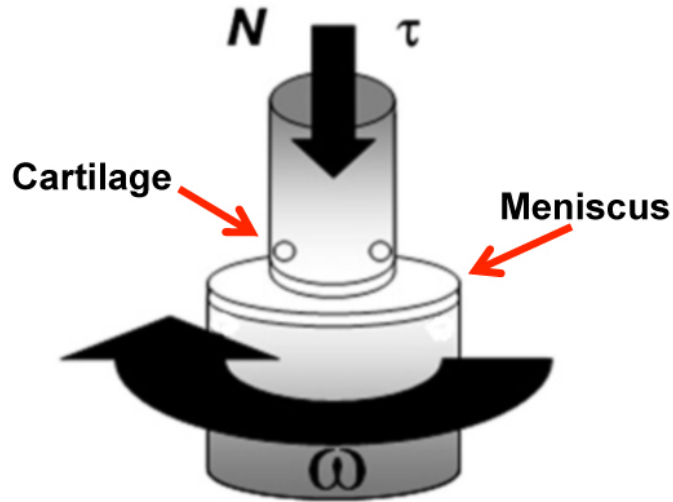


Figure 2-2: Boundary lubrication test orientation

Each sample is compressed to 18% of total cartilage thickness (shown to be sufficient for boundary lubrication and a cartilage-cartilage biointerface and similar to compression experienced in the joint during squatting^{65,104}) before stress relaxing for 40 minutes to allow for fluid depressurization interstitially. Samples were then rotated two revolutions in both directions at varying effective sliding velocities ($v_{\text{eff}} = \omega \times R_{\text{eff}}$, where R_{eff} is effective radius (= 2.4 mm) and ω is angular velocity^{65,84}). These v_{eff} were varied along a log scale through several orders of magnitude, such that lubricants that have different viscosities may be compared. First there was a 10 mm/s pre-conditioning spin before beginning the data collection with $v_{\text{eff}} = 10, 3, 1, 0.3, 0.1, 0.01$ mm/s with a pre-sliding duration (T_{ps}) of 120 seconds before each new velocity. This test protocol was used for three sequential test sequences to compare different lubricants:

- 1) PBS, PRG4, SF; n = 6.
- 2) PBS, HA, SF; n = 6.
- 3) PBS, PRG4+HA, SF; n = 5.

Following each test, the samples were bathed in the next test lubricant. Annuli were

bathed in 0.1 mL of fluid, the core 0.2 mL. This allowed the articulating surface to be completely submerged while the samples were stored in 4°C overnight.

2.3.4 Data Analysis

The kinetic coefficient of friction, which is the resistance to continuous motion, was calculated from torque (τ) values measured during the second revolution of each test and axial load (N). To calculate the coefficient of kinetic friction, the equilibrium load, N_{eq} , was used, given by the formula $\langle \mu_{kinetic, N_{eq}} \rangle = \tau / (R_{eff} \cdot N_{eq})$ ⁶⁵. This equilibrium load, N_{eq} , is measured after the initial 18% compression and 40-minute stress relaxation of the apposing tissue surfaces, but before the rotational testing begins. As such, it neglects the viscoelastic and hydrodynamic forces within the cartilage tissue that may cause variations in the instantaneously measured load, N, during the revolutions.

Data are presented as mean \pm SEM. ANOVA was used to determine the effect of lubricant and V_{eff} as a repeated factor on the kinetic coefficient of friction. One-way ANOVA test was then run, followed by Tukey post-hoc test, to compare lubricants at velocities of interest, specifically the highest (10 mm/s), lowest (0.01 mm/s), and an intermediary velocity that was shown to be sufficient for boundary lubrication at an articular cartilage-cartilage biointerface (0.3 mm/s)⁶⁵. Statistical analysis was implemented with Systat12 (Systat Software, Inc., Richmond, CA).

2.4 Results

A novel *in vitro* articular cartilage-meniscus lubrication test was developed, enabling repeatable measurements to be made to compare different lubricants in terms of ability to lower kinetic coefficient of friction at a previously uninvestigated, and physiologically important, biointerface. PRG4, HA, and PRG4+HA were tested in separate sequences, compared to PBS and SF. The velocity dependence of the kinetic coefficient of friction was observed for each lubricant of interest.

2.4.1 Test Sequence 1: PRG4

PRG4 lowered kinetic coefficient of friction at intermediate velocities compared to PBS, while at both high and low velocities PRG4 had higher friction than PBS, though they were similar. $\langle \mu_{\text{kinetic,Neq}} \rangle$ values varied with test lubricant and velocity ($p < 0.05$), with an interaction ($p = 0.011$). For all intermediary velocities (0.1-3 mm/s), $\langle \mu_{\text{kinetic,Neq}} \rangle$ values were highest in PBS and lowest in SF, while PRG4 was intermediary. $\langle \mu_{\text{kinetic,Neq}} \rangle$ values appeared to increase as the effective velocity increased.

At the velocity of interest, $v_{\text{eff}} = 0.3$ mm/s, PBS values were highest (0.132 ± 0.027), SF lowest (0.047 ± 0.018), and PRG4 intermediate (0.105 ± 0.004). PBS was significantly different from SF ($p < 0.05$), though there was not significant difference between PRG4 and either PBS ($p = 0.579$) or SF ($p = 0.107$).

At low speed, $v_{\text{eff}} = 0.01$ mm/s, PRG4 values were highest (0.093 ± 0.017), PBS slightly lower (0.085 ± 0.018) and not significantly different ($p = 0.909$). SF had the lowest value, (0.053 ± 0.004), but was not significantly different from either PRG4 or PBS ($p = 0.153, 0.295$ respectively). At high speed, $v_{\text{eff}} = 10$ mm/s, PRG4 was again the highest (0.237 ± 0.053), with PBS slightly lower (0.229 ± 0.054) and statistically similar ($p = 0.991$). SF had the lowest

coefficient of friction, 0.096 ± 0.013 , and was not significantly different from either PBS or PRG4 ($p = 0.120, 0.096$ respectively) (Figure 2-3).

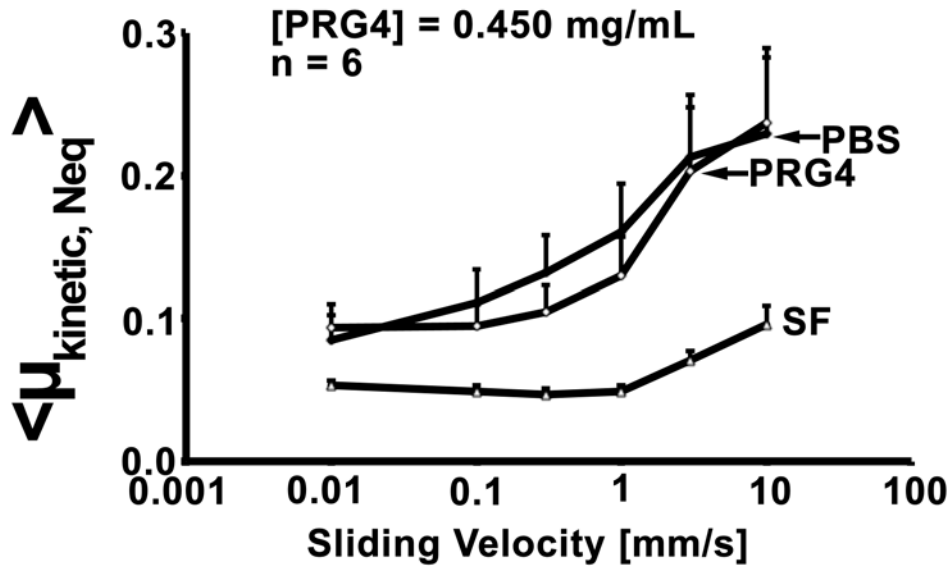


Figure 2-3: Kinetic friction coefficient $\langle \mu_{kinetic, Neq} \rangle$ for PRG4 at 0.450 mg/mL. Data presented as mean \pm SEM, $n=6$.

2.4.2 Test Sequence 2: HA

1.5 MDa HA lowered friction compared to PBS at all velocities. $\langle \mu_{kinetic, Neq} \rangle$ varied with both lubricant and velocity ($p < 0.001$), with an interaction between the two ($p < 0.05$). At all velocities, $\langle \mu_{kinetic, Neq} \rangle$ values were highest in PBS, lowest in SF, and intermediate in HA.

At $v_{eff} = 0.3$ mm/s, PBS (0.147 ± 0.016) was statistically different ($p < 0.005$) from both HA (0.083 ± 0.009) and SF (0.046 ± 0.007), although HA and SF were not quite significantly different ($p = 0.080$).

Similarly, at low speeds, PBS (0.103 ± 0.014) and SF (0.072 ± 0.006) were significantly different ($p < 0.005$). HA (0.047 ± 0.006) was not significantly different from either, however ($p =$

0.085, 0.170). At high speeds, PBS (0.201±0.037) was statistically different ($p < 0.05$) from both HA (0.099±0.017) and SF (0.093±0.008). HA and SF were no different, however ($p = 0.984$) (Figure 2-4).

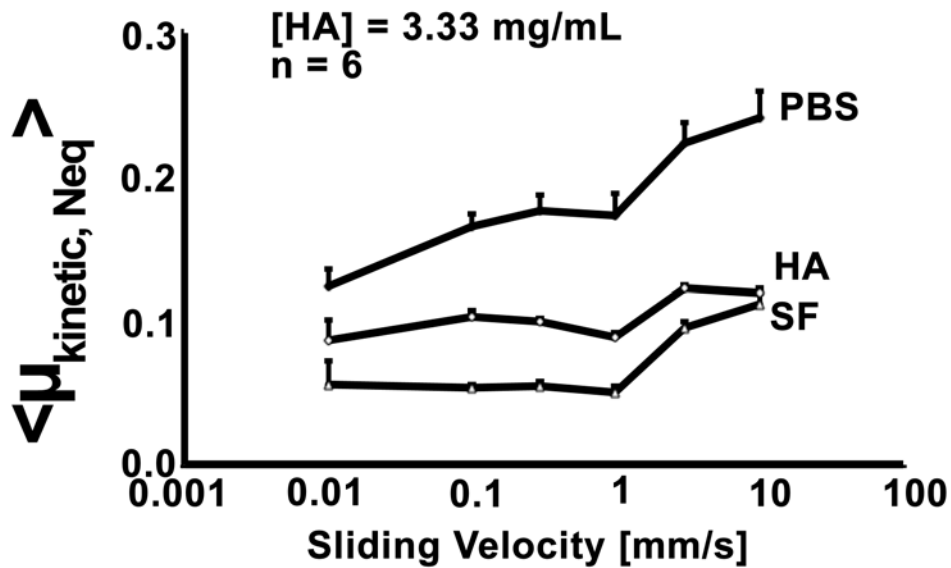


Figure 2-4: Kinetic friction coefficient $\langle \mu_{kinetic, Neq} \rangle$ for 1.5 MDa HA at 3.33 mg/mL. Data presented as mean±SEM, n=6.

2.4.3 Test Sequence 3: PRG4 + HA

PRG4+HA lowered friction compared to PBS at all velocities and was not significantly different from SF. Both lubricant and velocity affected $\langle \mu_{kinetic, Neq} \rangle$ ($p < 0.01$), and an interaction was observed ($p < 0.005$). PBS had the highest values of $\langle \mu_{kinetic, Neq} \rangle$, SF the lowest, and PRG4+HA was intermediate for all tested velocities.

All speeds displayed the same trends, with PBS (0.105±0.015 to 0.238±0.049) being significantly different ($p < 0.05$) from both PRG4+HA (0.062±0.005 to 0.109±0.022) and SF (0.046±0.006 to 0.080±0.009), except at $v_{eff} = 0.3$ mm/s, where PBS and PRG4+HA were almost

significantly different ($p = 0.052$). PRG4+HA and SF, however, were not significantly different ($p = 0.522$ to 0.793) (Figure 2-5).

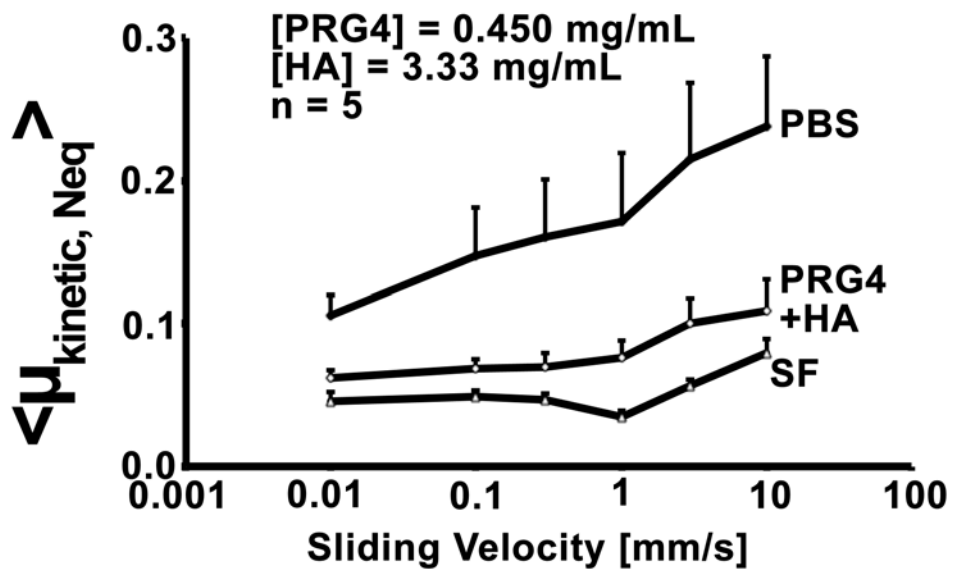


Figure 2-5: Kinetic friction coefficient $\langle \mu_{kinetic, Neq} \rangle$ for PRG4+HA with [PRG4] = 0.450 mg/mL, [1.5 MDa HA] = 3.33 mg/mL. Data presented as mean \pm SEM, n=5.

2.5 Discussion

The results from this study support the hypothesis, showing that velocity does affect the lubricating abilities of SF and its constituents such as PRG4 and HA, both alone and in combination, at an articular cartilage-meniscus biointerface. What's more, this effect is similar for all lubricants tested here, with the kinetic coefficient of friction remaining the same or increasing slightly from $v_{\text{eff}} = 0.01 - 1.0$ mm/s, before increasing more sharply to 10 mm/s. PRG4 appeared to lower friction at low and intermediate velocities, but did not reduce friction compared to PBS at higher velocities. HA and PRG4+HA were effective lubricants across a wide range of velocities, approaching the level of SF. Summarized data shown below in Figure 2-6 for comparison.

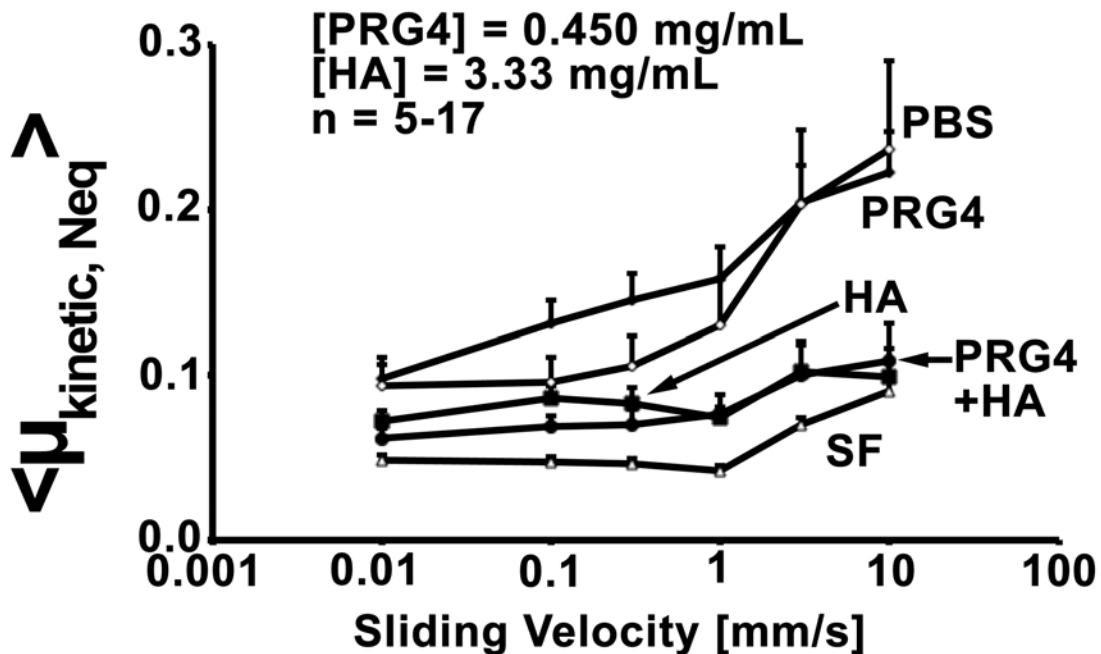


Figure 2-6: Kinetic friction coefficient $\langle \mu_{\text{kinetic, Neq}} \rangle$ for PRG4 at 0.450 mg/mL, 1.5 MDa HA at 3.33 mg/mL and PRG4+HA. Data presented as mean \pm SEM, n=5-17.

Using an *in vitro* articular cartilage-meniscus lubrication test with rotational motion has both advantages and disadvantages. While an *ex vivo* test can more closely resemble the physiological kinematics of a knee joint⁸⁵, in which different modes of lubrication will be operative, this *in vitro* setup allows for a boundary lubrication to be examined through specific test parameters that could not be controlled in an *ex vivo* situation⁷¹. Similarly, a reciprocating pendulum test may provide more accurate kinematics⁷³, but the transition between fluid and boundary mediated lubrication would make it difficult to draw conclusions on either mode of lubrication. The rotational geometry used in this test minimizes fluid exudation, while the 40-minute stress relaxation allows for fluid depressurization. Together this prevents a fluid film from developing and allows a boundary mode of lubrication to be dominant⁶⁵. Synthetic surfaces would allow for even more careful control of test parameters (surface roughness, charge, etc.)^{86,98,99}, but would not retain the physiological interactions present at an articular cartilage-cartilage^{65,84} or cartilage-meniscus biointerface. The novel articular cartilage-meniscus test that was developed does not accurately simulate the joint motion of the knee or the same stress distribution experienced therein (i.e., hoop stresses in the meniscus). It does, however, replicate the physiological surfaces present in the joint and create the conditions in which boundary mode lubrication, where the majority of wear occurs *in vivo*, is operative.

It is worth noting the tissue variability seen in these tests. For example, the average PBS values from all 17 tests for $v_{\text{eff}} = 0.3$ mm/s, (0.145 ± 0.015) were different than those seen in the PRG4 trials (0.132 ± 0.027). Given the range between the negative and positive controls PBS and SF, this tissue variability may explain, in part, the lack of significant differences between PBS and PRG4 seen in those tests, despite consistent trends being observed.

PRG4 has been shown to be an effective lubricant at a variety of interfaces, both

synthetic^{73,98} and physiological tissue^{84,85}. The results of this study are consistent with these findings and in general show PRG4 lowers friction at intermediary speeds when compared to the negative control PBS, but does not reduce friction at high velocities. This supports its role as a boundary lubricant; that is, when speeds are slow enough for boundary lubrication to occur it effectively reduces friction. When speed increases however, fluid-mediated lubrication may play a more important role in reducing the measured friction³⁶ and thus PRG4, with a viscosity equivalent to that of saline and significantly less than SF, does not lubricate.

At an articular cartilage-cartilage biointerface, HA has been shown to be an effective, dose-dependent lubricant^{84,96}, which is also supported by the findings of this study at the cartilage-meniscus biointerface. Indeed, here HA reduces friction compared to PBS, approaching the level of whole SF. Furthermore, when combined with PRG4, friction was again reduced. In fact, PRG4+HA was not significantly different from SF across a range of velocities. This showcases HA's lubrication both at slow speeds where boundary mode is operative, but also at higher velocities where fluid properties, such as viscosity, mediate friction. It also appeared at intermediate speeds that the combination of PRG4 and HA lower friction further than either molecule alone, suggesting they do interact synergistically to reduce friction through formation of a complex in solution⁹⁶ and/or at the biointerface tested here.

It is unknown how specifically PRG4 and HA provide their boundary lubricating properties in the joint. A boundary lubricant must bind to the surface by definition^{74,105}, but the specific mechanism by which these lubricants reduce friction is less clear. One possibility is the formation of hydration layers around hydrophilic domains of boundary lubricants⁸⁶. The water molecules are strongly attracted to these domains, supporting high pressures, while retaining their fluidity. This fluidity allows for low friction shearing at the slip plane between the apposing

surfaces. It has also been suggested that boundary lubricants function as a sacrificial layer, protecting the surface from wear by shearing away during surface-to-surface movement⁸⁸. Indeed, SF was shown to replenish the layer of boundary lubricants faster than they were depleted; however, isolated PRG4 solution did not replenish as quickly⁸⁸, suggesting PRG4 alone may not be able to lubricate in this fashion. Similarly, Greene et al.¹⁰⁵ suggest that the PRG4+HA complex operates “adaptively”. Under low loads, PRG4 binds to the surface and becomes entangled with HA, acting as lubricating complex. As load increases, HA is compressed and entraps PRG4, which is redistributed to places of higher shear due to its weaker surface attachment, much like the sacrificial layer^{88,105}.

This sacrificial or adaptive theory has been challenged for relying on replenishment from hydrostatically exuded fluid, which is argued does not affect the friction¹⁰⁶. Recently, atomic force microscopy (AFM) showed that layers of PRG4 had steric or entropic repulsion when bound to a series of differently charged surfaces⁸⁹. While PRG4 did rearrange under shear as suggested in the adaptive mode, preventing damage at higher pressures, the repulsive forces of the surfaces point to PRG4 acting as a polymer brush^{89,105}. It is believed that the C and N terminals bind to the surface, allowing the negatively charged hydrophilic mucin domain to be exposed. As the density of surface adsorbed PRG4 increases, these domains reform into tall, brush-like structures to lower entropy. That is, the similarly charged domains want to be in the lowest possible concentration while adhered to the surface. In the eye, where PRG4 is also found⁷⁸, it has been suggested that very low friction in boundary mode of lubrication may be attributed to these brush-like formations of PRG4 repelling one another due to the aforementioned steric repulsion, as well as electrostatic repulsion⁹⁰. In fact, in blinking lubrication, friction is actually lowest in boundary mode due to this behavior, rising slightly as

speed increases due to the tear film's shear thinning property⁹⁰. SF is also shear thinning¹⁰⁶, and together with this polymer-like lubrication would explain the low friction values at low speeds rising at higher speeds, as shown in this study.

The performance of SF constituents PRG4 and HA at the cartilage-meniscus biointerface is very similar to that seen in previous studies at the cartilage-cartilage biointerface^{65,84,96}. Indeed, in a boundary mode of lubrication, facilitated in these studies by a rotational test geometry and fluid depressurization, at physiological surfaces both PRG4 and HA operate as boundary lubricants. Surface characteristics are important considerations for boundary lubrication. The similarities between these surfaces could be due to the analogous structure-function relationships present in these tissues. Cartilage and meniscus are both composed of a collagen framework (with adhering macromolecules) bathed in a fluid containing charged ions^{44,107}. The structure in these tissues leads to the biphasic interaction between these components that provides, in part, the tissues mechanical properties^{29,50}.

In conclusion, a novel *in vitro* articular cartilage-meniscus lubrication test was developed that showed, for the first time, that SF constituents PRG4 and HA lubricate at this important biointerface. The data obtained in this study suggest that at an articular cartilage-meniscus biointerface, velocity does affect the kinetic coefficient of friction, as do SF constituents PRG4 and HA, alone and in combination. At slower speeds, PRG4 appears to lower friction, and does so further when combined with HA, approaching the level of whole SF. At higher speeds, PRG4 seems to be less effective, suggesting that a mixed lubrication regime may be approaching at 3-10 mm/s. This study suggests that a velocity of 0.3 mm/s is sufficient for boundary mode lubrication at the articular cartilage-meniscus biointerface, as it was at the cartilage-cartilage biointerface.

CHAPTER 3: Synergism of (rh)PRG4 and HA at Articular Cartilage-Meniscus Biointerface

3.1 Abstract

Objective: Measure the boundary lubricating ability of (rh)PRG4 \pm HA at an articular cartilage-meniscus biointerface..

Methods: An *in vitro* articular cartilage-meniscus boundary lubrication test, using 18% compression, 40-minute stress relaxation and 0.3 mm/s velocity, was used to calculate both static and kinetic coefficients of friction for PRG4 and HA, alone and in combination. rhPRG4 was also tested with and without HA at this biointerface.

Results: (rh)PRG4 lowered friction significantly alone compared to PBS, and appeared to lower friction further when combined with HA, approaching the level of SF. HA lowered friction as well compared to PBS alone.

Conclusions: This study suggests that PRG4 and HA's synergistic boundary lubricating ability at the articular cartilage-cartilage biointerface is retained at the cartilage-meniscus biointerface. In addition, rhPRG4 lubricates effectively at this biointerface as well, while still appearing to interact with HA to further lower friction. These results could potentially contribute to the development of injectable rhPRG4 \pm HA biotherapeutics for treatment of OA.

3.2 Introduction

In Chapter 2, PRG4 was shown to be an effective boundary lubricant at an articular cartilage-meniscus biointerface for the first time. PRG4 has been shown previously to lower friction at a cartilage-cartilage biointerface, further supporting its role as a boundary lubricant at physiological biointerfaces found in the joint^{84,85}. HA has now been shown to operate as a boundary lubricant at both the cartilage-cartilage^{84,96} and cartilage-meniscus biointerfaces, as seen in the previous chapter. The *in vitro* lubrication test used in Chapter 2 utilized stationary contact geometry and fluid depressurization, which appeared to facilitate an operative boundary mode of lubrication at lower velocities. A velocity of 0.3 mm/s was shown to be sufficient for boundary lubrication at both the cartilage-cartilage⁶⁵, and now at the cartilage-meniscus, biointerfaces.

A majority of friction and wear are generated during boundary lubrication in the knee⁷², suggesting that effective boundary lubricants, such as PRG4 and HA, could contribute to joint health. Indeed, when PRG4 is absent, be it from the genetic disorder camptodactylarthropathy-coxa vara-pericarditis (CACP) or observed in PRG4 knockout mice, joint degradation occurs^{69,75}. Furthermore, PRG4 supplementation has chondroprotective effects^{71,85,94}. Similarly, HA has also been used in an effort to restore this joint function. These viscosupplements are currently used to treat OA^{12,24}; treatments have been shown to reduce pain but have a very short residency time in the knee, raising questions about their efficacy^{12,28}. As such, PRG4 and HA individually contribute to joint health.

These two molecules have also been found to synergistically interact to lower friction at a cartilage-cartilage biointerface^{84,96}. Furthermore, combining with PRG4 allows for HA to contribute to effective lubrication at synthetic surfaces⁹⁹. The work in Chapter 2 showed that

combining PRG4 with HA appeared to decrease kinetic friction further than either molecule alone at the cartilage-meniscus biointerface at a variety of rotational velocities. This synergistic interaction makes PRG4 and HA excellent candidates for biotherapeutic treatments for OA^{84,94,96}.

To this end, several different forms of recombinant human PRG4 (rhPRG4) have been investigated. A truncated form of rhPRG4, called LUB1, was developed and shown to have chondroprotective effects and stayed in joints for 28 days¹⁰⁸. However, this shortened structure may have other effects on the molecules' function, as the glycosylated domain of PRG4 that was shortened for production of LUB1 is thought to contribute to lubrication^{81,83}. Other work has shown that structural changes of a different version of rhPRG4 prevent proper binding to a cartilage surface¹⁰⁹.

However, recently a full-length version of rhPRG4 was produced stably and in large amounts by Lubris, LLC. This rhPRG4 has been shown to have the ability to dimerize as well as the appropriate glycosylations¹¹⁰. Furthermore, it has shown the ability to lubricate effectively, both with and without HA, at an ocular biointerface and an *in vitro* cartilage-cartilage biointerface^{110,111}. This rhPRG4 has never been tested at the physiologically relevant articular cartilage-meniscus biointerface, either alone or in combination with HA.

As such, the objective of this study is to measure the boundary lubricating ability of (rh)PRG4 and HA, alone and in combination, at the articular cartilage-meniscus biointerface.

3.3 Methods

The modified *in vitro* boundary lubrication test used in Chapter 2 to investigate friction at the articular cartilage-meniscus biointerface was again utilized to test the ability of a variety of lubricants to affect friction, in this case both kinetic and static coefficients of friction. Fluid depressurization, stationary contact geometry and, based on the findings of Chapter 2, an effective velocity of 0.3 mm/s facilitated an operative boundary mode of lubrication. The lubricants PRG4, HA, and rhPRG4 were tested alone in comparison with a negative control, PBS, and positive control, SF. A combination of (rh)PRG4 and HA was also tested in each sequence.

3.3.1 Lubricant Preparation

Lubricants SF, PRG4, and HA were prepared as outlined in section 2.3.1.

rhPRG4 was prepared as described previously¹¹⁰. Lubris LLC (Framingham, MA), in collaboration with Selexis SA (Geneva, Switzerland), transfected a Chinese hamster ovary (CHO) line with the PRG4 gene, which was then used to condition culture media. The gene encoding the full-length 1404 amino acid human PRG4 was inserted into commercially available plasmid vectors at Selexis SA. This provides enhanced gene expression in mammalian CHO cells. Shake flask culture with fed-batch cultivation (SFM4CHO medium [Hyclone, Logan, UT]) was supplemented with 8 mM L-Glutamine, hypoxanthine, and thymidine (1x HT, Life Technologies, Carlsbad, CA) and the rhPRG4 media collected from the high expressing rhPRG4 clonal cell lines.

Enriched rhPRG4 was prepared by concentrating the raw rhPRG4 media using a 100 kDa MW cutoff centrifugal filter. As with native PRG4, BCA assay (Sigma-Aldrich, St. Louis, MO)

was used to determine concentration and 3-8% Tris-Acetate SDS-PAGE gel was used to confirm purity. rhPRG4 was diluted in PBS to a physiological concentration, 450 $\mu\text{g}/\text{mL}$ ¹⁰³.

3.3.2 Tissue Sample Preparation

Tissue samples were prepared as outlined in section 2.3.2.

3.3.3 Boundary Lubrication Test

Boundary lubrication test equipment, sample orientation, and test parameters were the same as outlined in section 2.3.3.

Following 18% compression and 40-minute stress relaxation, samples then were held stationary for a pre-sliding duration (T_{ps}) of 1200, 120, 12, and 1.2 seconds (s). Following each of these waiting periods, samples were rotated at $v_{eff} = 0.3$ mm/s for +/- 2 revolutions. Then the test repeats itself in the opposite direction of rotation, +/- 2 revolutions. This test protocol was used for three test sequences to test synergism between (rh)PRG4 and HA:

- 1) PBS, PRG4, PRG4+HA, SF; n = 4.
- 2) PBS, HA, PRG4+HA, SF; n = 4.
- 3) PBS, rhPRG4, rhPRG4+HA, SF; n = 8.

3.3.4 Data Analysis

Both the static coefficient of friction, which is the resistance to the onset of motion, and the kinetic coefficient of friction, representing the resistance to continuous motion, were calculated. The static coefficient of friction, $\mu_{static,Neq}$, was calculated from the τ values measured during the first 10 degrees of rotation and N_{eq} using the formula $\mu_{static,Neq} = \tau / (R_{eff} \square N_{eq})$ ⁶⁵. The

kinetic coefficient of friction, $\langle \mu_{\text{kinetic,Neq}} \rangle$, was calculated using the same formula, but using the τ values measured during the entire second test revolution. Data are presented as mean \pm SEM. Repeated measures ANOVA was used to determine the effect of both lubricant and T_{ps} on the coefficients of friction discussed above. This was followed by a one-way ANOVA at $T_{\text{ps}} = 1.2$ s and a Fisher LSD post-hoc test to compare PBS, (rh)PRG4 or HA, and (rh)PRG4+HA. Statistical analysis was implemented with Systat12 (Systat Software, Inc., Richmond, CA).

3.4 Results

A boundary lubrication test showed that (rh)PRG4 and HA appeared to reduce both static and kinetic coefficients of friction at an *in vitro* articular cartilage-meniscus biointerface compared to PBS. When combined, friction was lowered even further, approaching the level of SF. Static friction increased with T_{ps} , while kinetic friction was relatively invariant. As such, kinetic coefficients of friction are presented at $T_{ps} = 1.2$ s for clarity and brevity, as done previously^{84,96,112}.

3.4.1 Test Sequence 1: PRG4 ± HA

PRG4 lowered friction at an articular cartilage-meniscus biointerface, and when combined with HA lowered friction to a level that was not statistically different from SF. $\mu_{static,Neq}$ varied with T_{ps} and test lubricant (both $p < 0.001$), with an interaction ($p < 0.001$). Values appeared to increase with T_{ps} . PBS consistently had the highest values, while PRG4 was intermediate and PRG4+HA and SF were similar and lowest (Figure 3-1A).

$\langle \mu_{kinetic,Neq} \rangle$ values exhibited similar trends, varying with lubricant and T_{ps} (both $p < 0.001$) increasing only slightly with T_{ps} (0.168 ± 0.005 to 0.204 ± 0.009 in PBS), with an interaction ($p < 0.001$). T_{ps} has minimal affect on kinetic friction coefficients because the time the tissue surfaces have had to interact does not affect frictional forces once steady motion has been achieved. $\langle \mu_{kinetic,Neq} \rangle$ values at $T_{ps} = 1.2$ s were greatest in PBS (0.168 ± 0.005) and lowest in SF (0.032 ± 0.005). Values in PRG4 (0.090 ± 0.021) and PRG4+HA (0.039 ± 0.002) were significantly different from each other ($p < 0.05$), as well as PBS ($p < 0.01$) (Figure 3-1B).

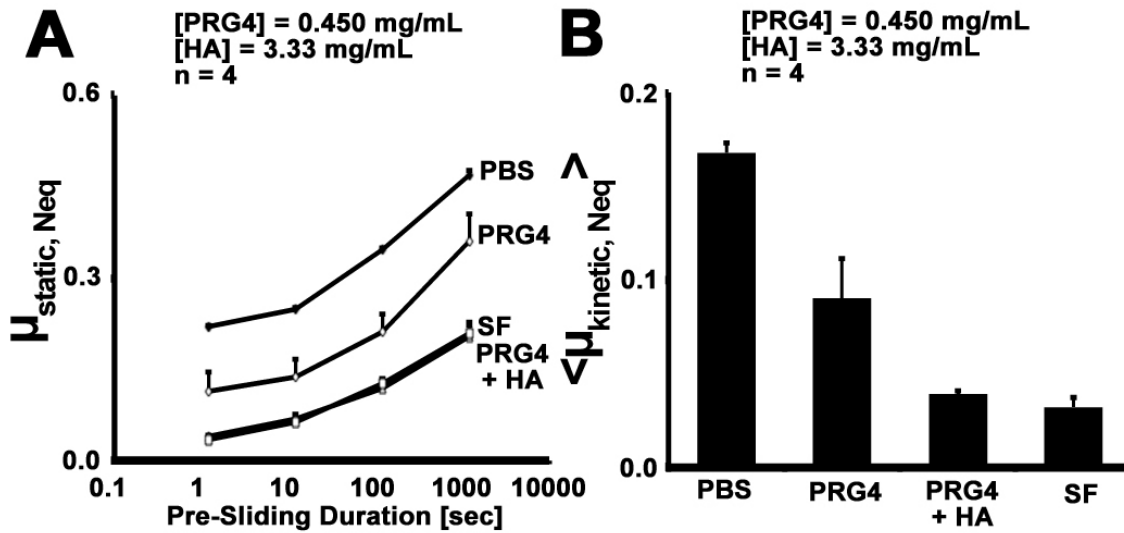


Figure 3-1: A) Static friction coefficient $\mu_{static, Neq}$ and B) kinetic friction coefficient $\langle \mu_{kinetic, Neq} \rangle$ at $T_{ps} = 1.2$ s for PRG4 at 0.450 mg/mL \pm 1.5 MDa HA at 3.33 mg/mL. Data presented as mean \pm -SEM, n = 4.

3.4.2 Test Sequence 2: HA \pm PRG4

HA appeared to lower friction compared to PBS, and further reduced friction when combined with PRG4. $\mu_{static, Neq}$ varied with both T_{ps} and test lubricant (both $p < 0.001$), with an interaction present ($p < 0.05$). Friction values increased with T_{ps} . PBS had the highest values at all T_{ps} , while HA values were intermediate. PRG4+HA and SF values were lowest (Figure 3-2A).

Values of $\langle \mu_{kinetic, Neq} \rangle$ also varied with T_{ps} and test lubricant ($p < 0.001$) with an interaction ($p < 0.001$). At $T_{ps} = 1.2$ s, $\langle \mu_{kinetic, Neq} \rangle$ values were greatest in PBS (0.166 ± 0.009) and lowest in SF (0.034 ± 0.006). Values in HA (0.083 ± 0.013) were significantly lower than those in PBS, as were values in PRG4+HA (0.040 ± 0.004) ($p < 0.001$). HA and PRG4+HA were also significantly different ($p < 0.05$) (Figure 3-2B).

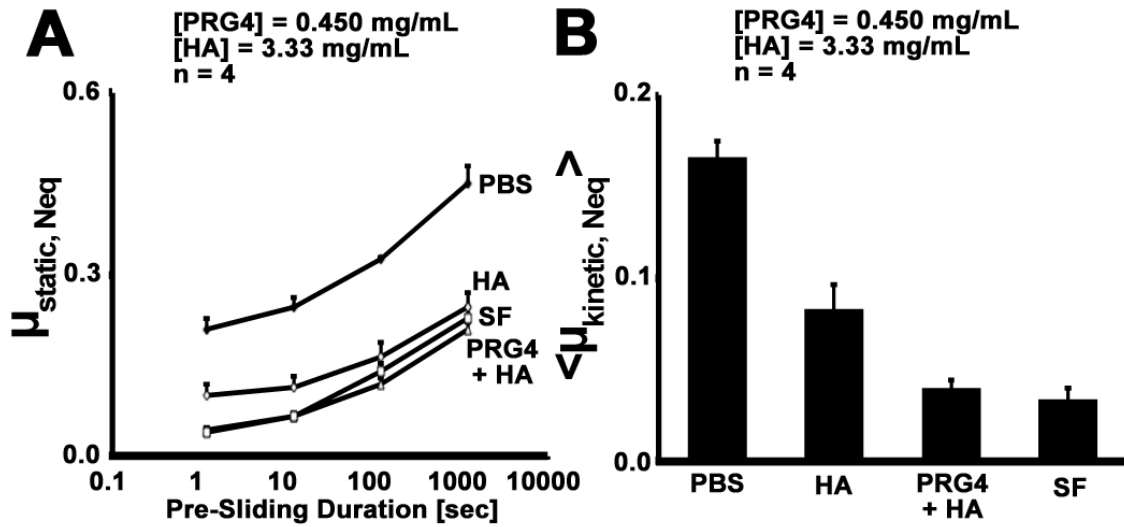


Figure 3-2: A) Static friction coefficient $\mu_{static,Neq}$ and B) kinetic friction coefficient $\langle \mu_{kinetic,Neq} \rangle$ at $T_{ps} = 1.2$ s for 1.5 MDa HA at 3.33 mg/mL \pm PRG4 at 0.450 mg/mL. Data presented as mean \pm -SEM, n = 4.

3.4.3 Test Sequence 3: rhPRG4 \pm HA

rhPRG4 lowers friction alone and in combination with HA, approaching the level of SF. $\mu_{static,Neq}$ values varied with T_{ps} and test lubricant (both $p < 0.001$), with an interaction ($p < 0.001$). Values appeared to increase with T_{ps} . PBS consistently had the highest values, while those in rhPRG4 were intermediate, and those in rhPRG4+HA and SF being the lowest (Figure 3-3A).

$\langle \mu_{kinetic,Neq} \rangle$ values also varied with lubricant and T_{ps} (both $p < 0.001$) increasing only slightly with T_{ps} , with an interaction ($p < 0.01$). $\langle \mu_{kinetic,Neq} \rangle$ for the lowest T_{ps} value showed PBS values (0.129 ± 0.033) to be highest and significantly different from rhPRG4 and rhPRG4+HA values ($p < 0.05$). SF values (0.032 ± 0.004) were lowest. rhPRG4 (0.057 ± 0.009) and rhPRG4+HA (0.038 ± 0.004) values were not significantly different ($p = 0.512$), though the addition of HA appeared to lower friction (Figure 3-3B).

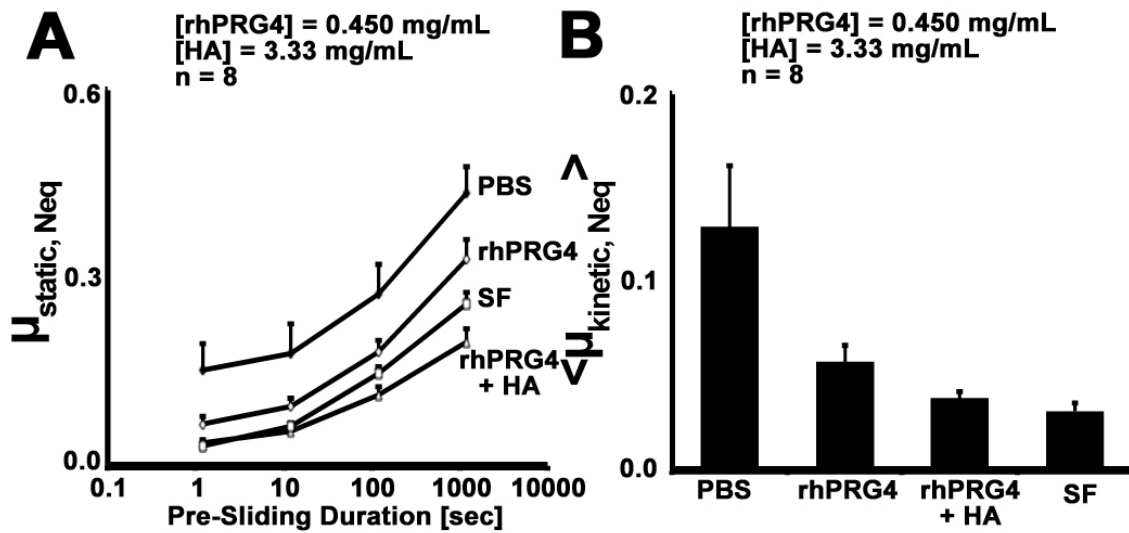


Figure 3-3: A) Static friction coefficient $\mu_{\text{static, Neq}}$ and B) kinetic friction coefficient $\langle \mu_{\text{kinetic, Neq}} \rangle$ at $T_{\text{ps}} = 1.2$ s for rhPRG4 at 0.450 mg/mL \pm 1.5 MDa HA at 3.33 mg/mL. Data presented as mean \pm -SEM, n = 8.

3.5 Discussion

The aim of this study was to investigate the synergistic boundary lubricating ability of (rh)PRG4 and HA at the articular cartilage-meniscus biointerface. It was hypothesized that (rh)PRG4 and HA would lower friction in a boundary mode of lubrication at the critical articular cartilage-meniscus biointerface. This hypothesis was correct as it was shown that with varied sequences and both native and recombinant PRG4, the ability of a (rh)PRG4 + HA complex to synergistically lower friction at physiological surfaces, in this case the cartilage-meniscus biointerface, is retained. Each sequence showed the improvement from a SF constituent alone to the combination, which was similar to SF in all cases.

The synergistic ability of PRG4 and HA to improve boundary lubrication has been observed at both synthetic and physiological interfaces^{84,96,98,99}, and now has been observed at a new physiologically relevant biointerface, articular cartilage-meniscus. It was shown in test sequences 1 and 2, as in other studies, that HA and PRG4 lubricate physiological surfaces effectively alone but reduce friction even further when combined. Despite the frequent observation of this relationship, the specific mechanism by which they interact remains unknown. PRG4 and HA are known to form a complex in solution, but how this complex reduces friction is debated⁹⁶. It has been suggested that HA and PRG4 become entangled within one another and form an adaptive surface layer that shears off during loading, redistributing across the surface, before being replenished by SF^{88,105}. Conversely, others believe that PRG4 binds to the surface and acts as a negatively charged polymer brush⁸⁹. Such systems rely on the steric and electrostatic repulsion generated by these brush layers. The addition of HA, a large, negatively charged polymer, would only increase the osmotic pressure to keep apposing surfaces, possibly covered in the same layer, separated⁹⁰.

However these two SF biomolecules interact, they are effective lubricants at physiological biointerfaces. While PRG4 reduces friction at a range of surfaces, HA is effective alone only at physiological surfaces⁸⁴. At synthetic surfaces such as latex, glass, and mica, HA does not operate as a boundary lubricant^{86,98,99}. This suggests its lubricating ability alone relies on specific surface interactions. In fact, it has been postulated that PRG4 improves HA's lubricating ability at man-made surfaces simply by acting as link protein⁸⁶. While this theory may explain HA's improvement, it does not account for PRG4's lubricating ability alone. These potential surface interactions are critical for boundary lubricants, however. The similar trends observed at the articular cartilage-meniscus biointerface may be explained by the analogous structure-function relationship of these tissues. Both tissues are comprised of collagen frameworks and fluid filled with ions and macromolecules^{41,44}; and both gain their mechanical function from the interplay between the solid and liquid states of this structure^{37,50,113}. Indeed, at the boundary layer film scale of biomolecules adhered to the surface during direct surface-to-surface contact, the articular cartilage-meniscus biointerface is hard to distinguish from the cartilage-cartilage one structurally. Perhaps it is not surprising then that the differences functionally, at least in an *in vitro* boundary lubrication test, are minimal.

Test sequence 3 showed the lubricating ability of rhPRG4, alone and combined with HA. While rhPRG4 has been shown to be effective in animal studies previously¹⁰⁸, the importance of binding sites and glycosylations to PRG4's function suggested a full-length version was needed^{83,109}. A new, full-length rhPRG4 was shown to have the ability to multimerize and have glycosylations like that in native protein¹¹⁰ and reduce friction at ocular and cartilage surfaces^{110,111}. Given the similar morphologies and functional mechanisms of articular cartilage and meniscal tissue, it is not shocking that rhPRG4 reduced friction alone, as well as appearing

lower friction further when combined with HA. It is important, however, that rhPRG4 functions similarly at a cartilage-meniscus biointerface as native protein. When compared to native protein directly at a cartilage-cartilage biointerface, rhPRG4 did in fact lower friction similarly to PRG4¹¹¹. The potential for PRG4 to improve the lubricating ability of the current viscosupplement HA^{12,24}, potentially by increasing its viscosity¹¹⁴ or residency time¹⁰⁸, points to rhPRG4 as a viable candidate for use in biotherapeutic injections for treatment of OA.

This study used a test that was previously characterized in Chapter 2 to operate in boundary mode lubrication at a velocity of 0.3 mm/s. Using this test at the identified velocity required for boundary lubrication, the lubricating ability of (rh)PRG4 and HA was effectively demonstrated. However, there is, like the previous study presented in Chapter 2, variable presence of significant differences between the SF constituents, particularly when alone, and the negative control, PBS. PBS friction values appear to be lower than in cartilage-cartilage biointerfaces, where $\langle \mu_{kinetic,Neq} \rangle$ values of ~ 0.2 are measured compared to ~ 0.15 at the cartilage-meniscus biointerface, but are still consistently the highest value. This more effective negative control (though still the least effective lubricant) may make it more difficult to find differences within a group of reasonably effective lubricants. However, the reliably similar trends present in all sequences suggest that the SF constituents of interest tested in this study do in fact reduce friction as compared to a negative control.

This observed reduction of friction at relatively high loads and slow velocities is critical for a boundary lubricant, as is the ability to adsorb to the articulating surface⁶⁵. PRG4 is found on both the cartilage and meniscal surfaces^{76,77}, and rhPRG4 was recently shown to adsorb successfully to a cartilage surface¹¹¹. However, rhPRG4 has not yet been shown to adsorb to the

meniscal surface. Given the importance of the meniscus to knee joint health in general and lubrication specifically, this surface adsorption warrants further study.

To conclude, PRG4 and HA, while effective boundary lubricants at the articular cartilage-meniscus biointerface, are even more effective when combined, retaining their synergistic interaction seen at other surfaces. In addition, full-length rhPRG4 lowers friction, alone and in combination with HA, at this physiologically important tissue biointerface.

CHAPTER 4: Surface Adsorption of Full-Length Recombinant Human Recombinant Proteoglycan 4 on Meniscus

4.1 Abstract

Objective: Assess the surface adsorption of rhPRG4 to the meniscus following depletion of endogenous PRG4.

Methods: Immunohistochemistry (IHC) with anti-PRG4 mAb 9G3, and secondary antibody Alexa Fluor-594 rhodamine-conjugated goat-anti mouse IgG, was employed to visualize the adsorption of PRG4 preparations to the surface of meniscal explants. Bovine meniscal samples were either fresh, or depleted of PRG4 by shaking in PBS or PBS with 1.5M NaCl. Meniscal samples were then incubated in lubricants of interest including PBS, PRG4, rhPRG4, or SF, prior to processing for IHC.

Results: rhPRG4-soaked meniscal samples showed protein immunolocalized to the surface similar to that observed for samples soaked in native PRG4 and SF, both at the articulating and cut surfaces of the tissue. Shaking in PBS depleted endogenous PRG4 from the surface, as indicated by decreased fluorescence. Salt extraction did not appear to further deplete PRG4 from the surface; however, it did appear to limit repletion of PRG4 at the articular surface.

Conclusions: These results demonstrate rhPRG4 is able to adsorb to the meniscal surface, which is a requirement for boundary lubrication function, in a manner consistent with that observed for native PRG4 and whole SF. This finding, combined with rhPRG4's boundary lubrication synergism with HA at a cartilage-meniscus biointerface, make it an attractive candidate for future development and evaluation as an OA biotherapeutic.

4.2 Introduction

PRG4, the mucinous glycoprotein found in the SF of the knee joint, has been shown to be an effective *in vitro* boundary lubricant at several physiological biointerfaces: cornea-eyelid¹¹⁰, articular cartilage-cartilage^{84,96,112}, and now, as shown in chapters 2 and 3, articular cartilage-meniscus. Furthermore, the recently available full-length rhPRG4 was also demonstrated to function as a boundary lubricant at the cartilage-meniscus biointerface. As normal PRG4 expression is necessary for knee-joint health and its main function is to provide boundary lubrication, proper boundary lubrication of joint tissues may be an important and contributing factor in prevention of tissue degradation and eventual development of OA^{28,71,74,85}.

Boundary lubrication occurs during surface-to-surface contact, often due to high loading, fluid depressurization, and low sliding speeds^{36,65}. The testing protocol used in the previous chapters demonstrated (rh)PRG4's efficacy in this lubrication regime through specific parameters that facilitated boundary lubrication: 18% tissue compression, 40-minute stress relaxation time, and stationary contact geometry⁶⁵. In this lubrication paradigm, it is molecules adhered to the surface of the articulating surfaces that mediate friction. While other types of lubrication occur in the knee joint, the nature of boundary lubrication occurring during surface-to-surface contact and high loads means a majority of friction experienced by the joint occurs in the boundary mode⁷².

To act as a boundary lubricant properly, a molecule must, by definition, be able to bind to the articulating surface⁶⁵. PRG4 is found at both the meniscus and articular cartilage surfaces in joints, supporting the case it is a boundary lubricant^{74,76,77}. Assessing this surface adsorption of proteins can be accomplished by IHC. IHC is a method by which protein can be visualized in tissue sections through binding of specific antibodies to the protein of interest. Detection of this

antibody may be done directly or with a secondary antibody via chemiluminescent, fluorescent, or enzymatic detection.

Recently it was shown with IHC that rhPRG4 does adsorb to the surface of articular cartilage following surface depletion, comparable to the level of native protein¹¹¹. The cartilage surface was repleted with protein following surface depletion by vigorous shaking in PBS; enzymatic, ionic, and other mechanical methods of surface depletion may alter the surface properties of the tissue and as such were avoided^{103,109,115}. Indeed, salt extraction has been shown to deplete the surface of PRG4 in skeletally immature bovine calf cartilage^{109,115}.

It is unknown if rhPRG4 is able to adsorb to the surface of the meniscus. Indeed, if rhPRG4 molecule is to be operative effectively as a boundary lubricant *in vivo* at the articular cartilage-meniscus biointerface, it must be able to localize to the surface of the meniscus. As such, the objective of this study is to assess the surface adsorbing ability of rhPRG4 on the meniscal surface.

4.3 Methods

To assess the surface adsorption of rhPRG4, meniscus tissue discs were shaken in either PBS alone or PBS with 1.5M NaCl to deplete the surface of endogenous PRG4 before soaking in PBS, PRG4, rhPRG4, or SF to assess repletion. These meniscal samples were then snap-frozen, cryosectioned, and processed for PRG4 immunolocalization with an anti-PRG4 mAb. A fluorescent secondary antibody was then used for PRG4 localization on the meniscal tissue using confocal microscopy.

4.3.1 Lubricant Preparation

SF was prepared as described in section 2.3.1; rhPRG4 was prepared as described in section 3.3.1.

4.3.2 Immunohistochemistry

Meniscal samples were cut from the articular surface of a mature bovine stifle joints meniscus, obtained from a local abattoir. First, meniscal explants were harvested from the tibial facing articular surface of the meniscus (thickness = 2.5 mm, diameter = 6mm). “Fresh” samples were taken from the joint, submerged in media (Tissue Tek OCT, Sakura, Torrance, CA) and snap-frozen in isopropanol cooled by dry ice. These samples served as positive controls for PRG4 that is on the tissue surface *in vivo*.

Other samples were shaken vigorously overnight in either in PBS or PBS containing 1.5M NaCl at 4°C to deplete the surface of residual/endogenous PRG4. The samples were then frozen at -80°C to prevent further PRG4 production from viable chondrocytes. These samples were then thawed and again shaken overnight at 4°C in fresh PBS ± 1.5M NaCl before being

incubated for 24 hours at room temperature in the test lubricants. These lubricants were placed in a 48-well plate (VWR Scientific Products, Radnor, PA) completely covering the samples. The test lubricants were PBS as a negative control, native PRG4, rhPRG4 and bovine SF. Both native PRG4 and rhPRG4 were at a physiological concentration of 450 $\mu\text{g/mL}$ ¹⁰³. After incubation, samples were snap-frozen in OCT medium and stored at -80°C.

A cryostat microtome (Microm HM550, Thermo Scientific, Waltham, MA) was used to cut 5-micron thick sections of each sample, which were then placed on positively charged glass slides (Superfrost Plus Adhesion Slides, Thermo Scientific, Waltham, MA). Sections were quickly washed in PBS to remove OCT before being fixed with 4% paraformaldehyde in PBS¹⁰³. Another PBS wash followed before blocking with 10% hydrogen peroxide in methanol. After PBS wash, serum blocking with 10% normal goat serum with 1% BSA in PBS occurred at room temperature in a humidity chamber. Half of the samples were then incubated in anti-PRG4 mAb 9G3 in 1.5% normal goat serum at 1:200 concentration¹¹⁶ to serve as positive controls, while the remaining half were incubated in 1.5% normal goat serum alone. These samples served as negative controls for the primary Ab. Following a PBS wash, all samples were incubated in secondary antibody Alexa Fluor-594 (a rhodamine conjugated goat anti-mouse IgG [Life Technologies, Carlsbad, CA]) in 1.5% normal goat serum at 1:1000 concentration¹¹⁵. After a final PBS wash, samples were mounted with mounting medium containing nuclear counterstain DAPI (Vectashield, Vector Laboratories Inc., Burlingame, CA) and sealed with microscope over slips (VWR Scientific Products, Radnor, PA).

Results were imaged using Zeiss LSM 780 microscope (Carl Zeiss, Oberkochen, Germany) with a 20x magnification lens (water, 0.8 NA). Fluorescence images were obtained for red (Alexa Fluor-594 rhodamine detected PRG4; excitation/emission spectrum maximum of

594/617 nm) and blue (DAPI detected cell staining; excitation/emission spectrum maximum of 358/461 nm) fluorescence.

4.4 Results

rhPRG4 soaked meniscal samples showed protein immunolocalized to the surface similar to that observed for samples soaked in native PRG4 and SF, both at the articulating and cut surfaces of the tissue. Shaking in PBS depleted endogenous PRG4 from the surface compared to fresh explants, as indicated by decreased fluorescence. Salt extraction did not appear to further deplete PRG4 from the surface; however, it did appear to limit repletion of PRG4 at the articular surface.

4.4.1 Surface Depletion by PBS Shaking

IHC of meniscus discs showed a discrete 9G3-immunoreactive layer of PRG4 at the articulating surface of fresh explants, the majority of which could be removed with vigorous shaking in PBS. This fluorescence was localized to the surface of fresh, unshaken samples. None was observed on the cut side and was specific; no non-specific signal was observed in the negative control.

Shaking appears to have slightly reduced the layer of PRG4 present at the articular surface as evidenced by decreased red fluorescence on the surface of PBS soaked samples. PRG4 and rhPRG4 both had thicker, brighter immunoreactivity at the surface, suggesting increased protein adsorption, comparable to SF. Interestingly, the cut edge of the PRG4, rhPRG4, and SF soaked samples also displayed immunoreactive bands on the surface, though they were fainter.

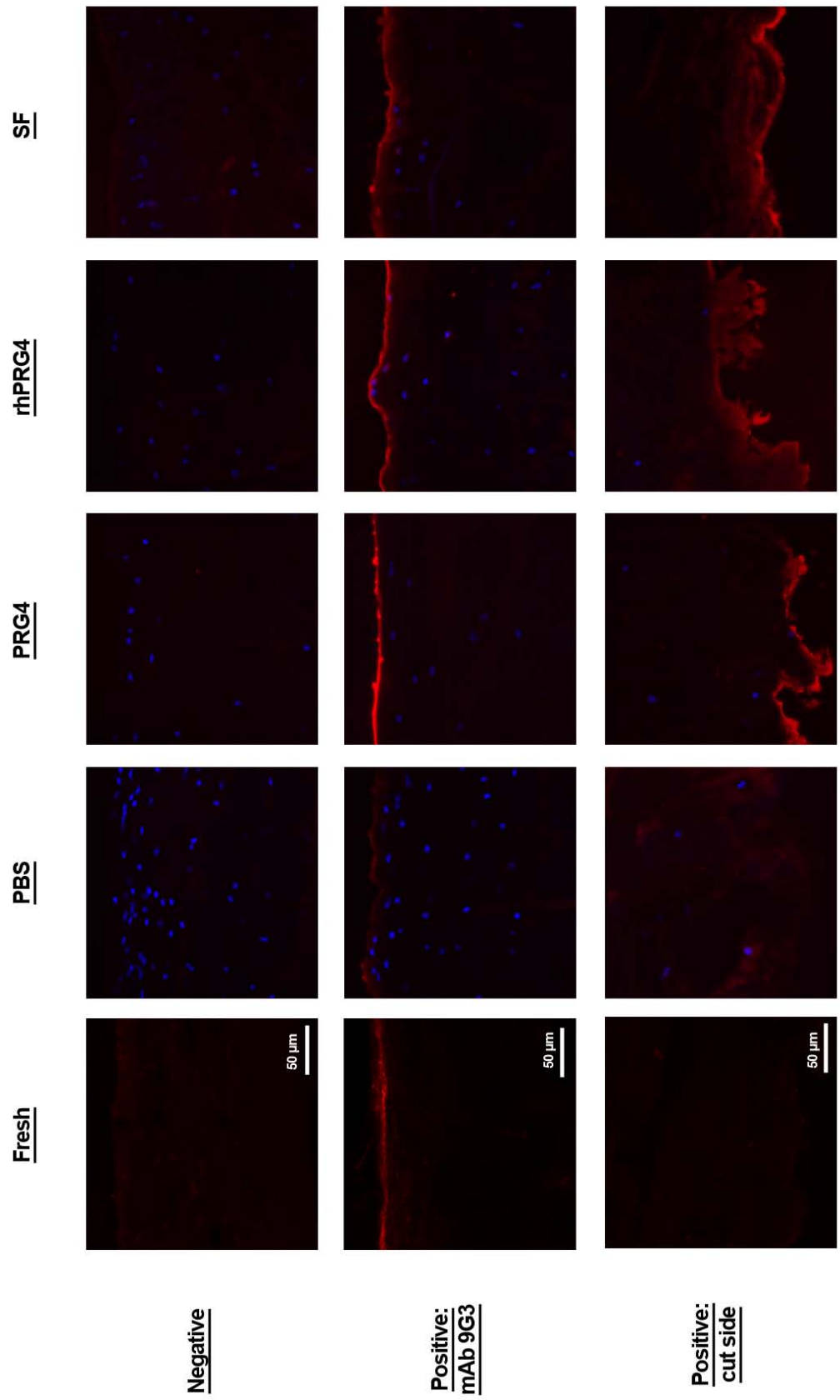
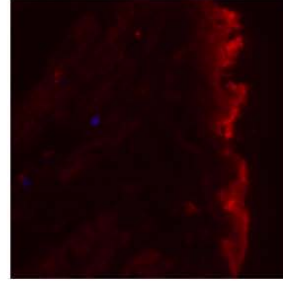
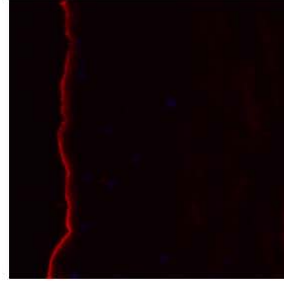
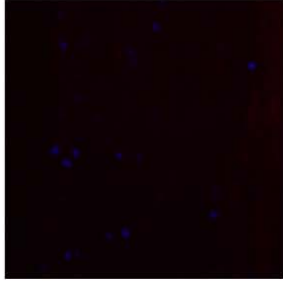


Figure 4-1: Immunolocalization of PRG4 at meniscal surface. Key: Fresh samples were taken directly from joint and snap-frozen (control). All other samples were shaken overnight in PBS at 4°C, frozen at -80°C, and shaken overnight again in fresh PBS at 4°C. Samples were then incubated in solutions of interest overnight at room temperature. Solutions: PBS (negative control), SF (positive control), rhPRG4 and PRG4 both at physiological concentrations of 450 µg/mL. Negative signifies samples that lacked primary Ab 9G3 but contained secondary gt-anti mouse Ab, positive signifies samples that contained both primary and secondary Abs. Red shows anti-PRG4 mAb 9G3, blue shows DAPI staining on chondrocyte cells.

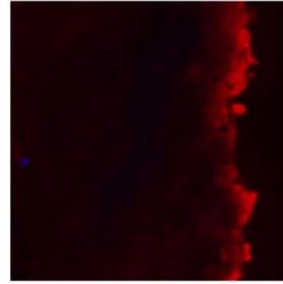
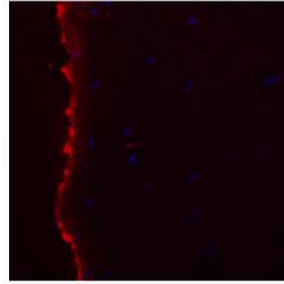
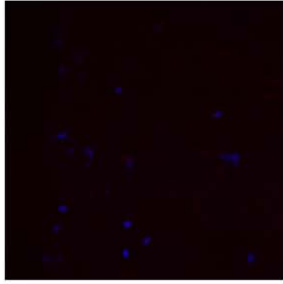
4.4.2 Surface Depletion by PBS Shaking and Salt Extraction

Following salt extraction by shaking in PBS with 1.5M NaCl, immunoreactivity was still faint but present at the meniscal surface of samples soaked in PBS. Contrary to the depletion by PBS shaking, following salt extraction native PRG4 samples demonstrated a discontinuous immunoreactive layer at the surface. rhPRG4 and SF again had a distinct, solid immunolocalized band on the surface. Cut surfaces of PRG4, rhPRG4 and SF samples were stained similarly to the articulating surface, though the surface appeared more roughened and the observed fluorescent signal being more diffuse into the tissue.

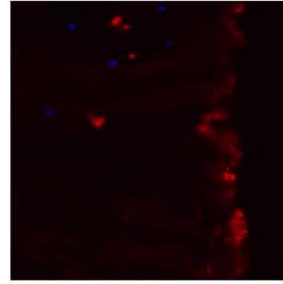
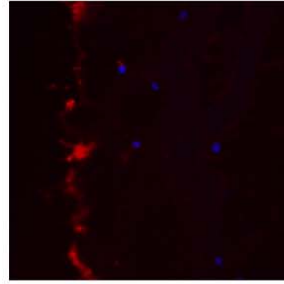
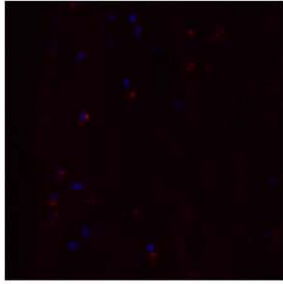
SF



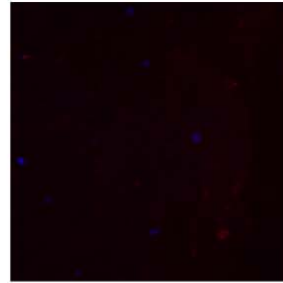
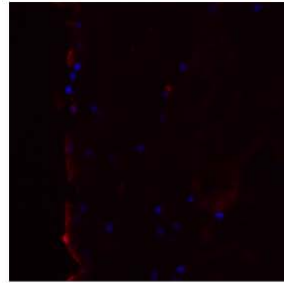
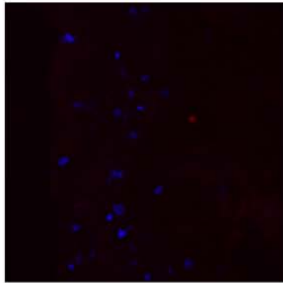
rhPRG4



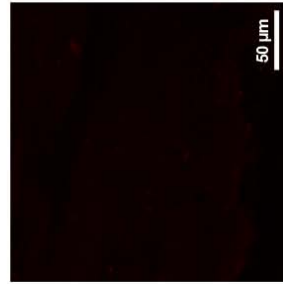
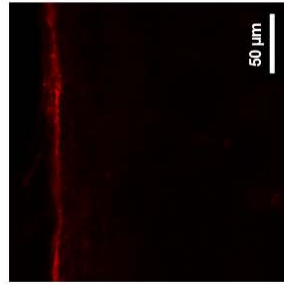
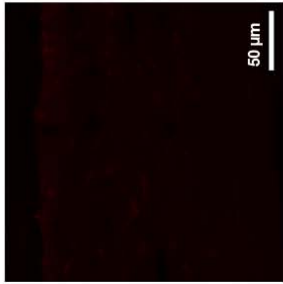
PRG4



PBS



Fresh



Negative

Positive:
mAb 9G3

Positive:
cut side

Figure 4-2: Immunolocalization of PRG4 at meniscal surface. Key: Fresh samples were taken directly from joint and snap-frozen (control). All other samples were shaken overnight in PBS with 1.5M NaCl at 4°C, frozen at -80°C, and shaken overnight again in fresh PBS with 1.5M NaCl at 4°C. Samples were then incubated in solutions of interest overnight at room temperature. Solutions: PBS (negative control), SF (positive control), rhPRG4 and PRG4 both at physiological concentrations of 450 µg/mL. Negative signifies samples that lacked primary Ab 9G3 but contained secondary gt-anti mouse Ab, positive signifies samples that contained both primary and secondary Abs. Red shows anti-PRG4 mAb 9G3, blue shows DAPI staining on chondrocyte cells.

4.5 Discussion

The goal of this study was to assess the ability of full-length rhPRG4 to adsorb to the surface of the meniscus following depletion of the surface layer by shaking and/or salt extraction. The hypothesis was that the rhPRG4 would successfully adsorb to the meniscal surface, and indeed it did. The rhPRG4 demonstrated the ability to adsorb to the surface of the meniscus effectively following both shaking and salt extraction in levels comparable, qualitatively, to SF. PRG4 also bound to the surface of the meniscus in both situations, though it appeared that salt extraction may limit its ability to replete the surface. For PRG4-, rhPRG4-, and SF-soaked samples, the cut edge of the explants showed immunoreactivity consistent with staining for PRG4 on the articulating surface.

Shaking was shown to reduce the fluorescence observed at the surface of the meniscal tissue, indicative of endogenous PRG4, though not completely remove it. This method was chosen over more invasive enzymatic digestion of the tissue to prevent any potential damage to the articulating surface^{103,109,115}. While these images suggest not all of the surface-bound PRG4 is removed, similarly shaken surfaces have worse lubricating ability at the cartilage-meniscus biointerface, as shown in chapters 2 and 3. Similarly, poor lubricating ability was seen in PBS shaken samples at the cartilage-cartilage biointerface^{65,84}. Indeed, PRG4 seems to be firmly attached to the surface, as incubation in PBS does not remove it with or without agitation^{103,111}. Further enzymatic treatments have unknown effects on the tissue despite removing the protein, though there may be other ways of reducing the surface layer of PRG4¹¹⁷.

Salt extraction has been shown to remove protein from the surface of the cartilage while still allowing for repletion of the boundary layer¹⁰⁹. Further salt extraction with shaking at the meniscal surface in this study did not remove all residual PRG4, nor did it prevent repletion of

the protein layer. While this contradicts previous studies showing salt extraction removing PRG4^{109,115}, those studies used immature bovine cartilage, while this study used mature bovine meniscus. However, it did appear to limit the ability of native PRG4 to adsorb to the tissue. This may be due to the removal of naturally occurring glycosaminoglycans that could contribute to PRG4's binding¹⁰⁹.

Following soaking in PRG4, rhPRG4 and SF, immunoreactivity was observed at the articulating surface of the meniscus for both shaken and salt extracted samples. This supports rhPRG4's role as a boundary lubricant at physiologically relevant biointerfaces^{110,111} and that it appears to retain the appropriate structural features of native PRG4 to bind to the tissue, as seen with native protein on both articular cartilage and meniscal surfaces^{74,76,77}. Recently, rhPRG4 was shown to adsorb to cartilage surfaces as well¹¹¹, further supporting the idea that rhPRG4 could be an effective injectable tribosupplement^{108,118}.

Interestingly, the cut surface of the meniscus demonstrated immunolocalization via fluorescence similar to the articulating surfaces. In cartilage, the cut surface's ability to facilitate binding is still unknown as studies have produced conflicting results^{109,111}. However, this may be due simply to methodology, as the study with different results than this one with respect to cut surface binding was mounted on a glass slide prior to incubation, perhaps limiting exposure of the surface to the lubricant bath. Conversely, in both this study and a previous cartilage study, the whole explant was exposed to the lubricant solution and as such, the cut surface was repleted with protein¹¹¹.

While protein layers can be visualized on the surface of the meniscus with this IHC technique, precise comparisons of protein concentrations at the surface cannot be made due to the qualitative nature of IHC¹¹⁹. Indeed, the specific levels of PRG4 found on the surface cannot

be determined. However, the presence of an immunoreactive surface layer clearly exhibits the ability of rhPRG4 to replete the surface as compared to PBS-soaked samples. Surface depletion was not fully achieved prior to this repletion through either vigorous PBS shaking or salt extraction; residual protein was localized to the surface of samples following these procedures. Despite this, the increased fluorescence present at the meniscal surface in samples soaked in PRG4, rhPRG4, and SF compared to PBS-soaked samples suggests increased protein at the surface.

To quantify the surface adsorption in the future, rhPRG4 molecules could be radio-labelled prior to the IHC procedure. Following fixation, tissue sections could be scanned in a gamma counter to determine a quantitative value of the rhPRG4 that binds to the meniscal surface. Another potential avenue of study is the investigation of how specifically PRG4 binds to the meniscal surface and how, if at all, other SF constituents such as HA help facilitate this.

In conclusion, these results demonstrate rhPRG4 is able to adsorb to the meniscal surface, which is a requirement for boundary lubrication function⁶⁵, in a manner consistent with that observed for native PRG4 and whole SF. This finding, combined with rhPRG4's boundary lubrication synergism with HA at a meniscus-cartilage biointerface shown in previous chapters, make it an attractive candidate for future development and evaluation as an OA biotherapeutic.

4.6 Acknowledgements

The authors would like to thank Dragana Ponjevic for guidance with immunohistochemistry, Dr. John Matyas and Umberto Banderali for their expertise with confocal microscopy, and Saleem Abubacker for the methodology used herein.

CHAPTER 5: Conclusions

6.1 Summary of Findings

There were three goals for the work described in this thesis. First, an *in vitro* articular cartilage-meniscus boundary lubrication test was to be developed and then used to determine the velocity dependence of the kinetic coefficient of friction at this physiologically relevant biointerface. Next, the boundary lubricating ability of native and recombinant human PRG4, as well as HA, was tested alone and in combination at the cartilage-meniscus biointerface. Finally, the surface adsorption of rhPRG4 to meniscus tissue would be assessed by IHC following surface depletion and then repletion. The major findings of this work are as follows:

1. A novel *in vitro* boundary lubrication test was developed for the articular cartilage-meniscus biointerface. A boundary mode of lubrication was dominant due to the tissues being depressurized (facilitated by an 18% compression of total tissue thickness and 40-minute stress relaxation) and a stationary contact geometry, thus allowing for surface-to-surface contact.
2. The kinetic coefficient of friction increased with velocity. PBS had the highest friction values for all v_{eff} , while SF had the lowest. At slow and intermediate speeds, PRG4 lowered friction compared to PBS, but at higher v_{eff} PRG4 did not lower friction effectively. HA lowered friction effectively at all velocities. For both of these SF constituents, kinetic friction was invariant at low velocities, suggestive of their role at the cartilage-meniscus biointerface as boundary lubricants.
3. At $v_{\text{eff}} = 0.3$ mm/s, PRG4 and HA both reduced static and kinetic coefficients of friction compared to PBS at an articular cartilage-meniscus biointerface, functioning

effectively as boundary lubricants alone. Furthermore, when combined, they lowered friction even further, approaching the lubricating ability of whole SF.

4. rhPRG4 lowered both static and kinetic coefficients of friction at the articular cartilage-meniscus biointerface. rhPRG4 also appeared to interact synergistically with HA to lower friction further, behaving similarly to native PRG4 as a boundary lubricant at this biointerface.
5. rhPRG4 demonstrated the ability to adsorb to the surface of the meniscus effectively, replenishing the surface layer similarly to native PRG4 following surface depletion by shaking or salt extraction.

Collectively the work described in this thesis work demonstrates the lubricating function of naturally occurring SF constituents at a physiologically relevant articular cartilage-meniscus biointerface. A novel *in vitro* lubrication test for the articular cartilage-meniscus biointerface demonstrates that this biointerface can operate in the boundary mode of lubrication, which is critical for understanding the role this tissue plays in the joint. In addition, this test highlights the lubricating ability of PRG4 and HA to lower friction at low and intermediate velocities, indicating that these molecules function as boundary lubricants at this biointerface. The synergistic interaction to lower friction of these two molecules further, previously observed at a cartilage-cartilage biointerface, is retained at the articular cartilage-meniscus one. Given HA's current use as a viscosupplement for treatment of OA and PRG4's effective use in animal models, this finding is potentially important support for the future development of a new biotherapeutic injection. To this end, rhPRG4 is shown to lower friction similarly to native PRG4, as well as adsorb to the meniscal surface following surface depletion, indicating its role as a boundary lubricant. These findings cumulatively demonstrate the importance of PRG4 at this

physiologically relevant, and previously uninvestigated, biointerface and potentially contribute to the development of a recombinant biotherapeutic injection that could benefit those suffering from OA.

6.2 Discussion

The meniscus is an important part of healthy knee-joint function given its load bearing and lubricating function^{44,47,48}. While this lubricating function is often described as one of its key roles, studies looking specifically how the meniscus tissue affects friction are few. While an intact whole joint friction test showed that the presence of a meniscus prevented cartilage wear, it did not investigate one mode of lubrication specifically, nor did it vary lubricants¹²⁰. As such, this thesis work was both novel and significant. It is important to consider meniscal lubrication as it pertains to knee-joint mechanics as both rolling and sliding motion occurs due to the femoral condyle motion and tibial internal rotation⁵⁶. Furthermore, up to 70% of loads in the knee joint are transmitted through the meniscus⁵⁵. This highly loaded environment provides the conditions for boundary lubrication; indeed, boundary lubrication is thought to generate most of the friction and wear in the knee⁷².

In the knee joint, the menisci slide against the articular cartilage surface, which has been shown to similarly have load-bearing and lubricating properties^{29,30}. For both articular cartilage and meniscus, these mechanical properties are due, at least in part, to the specific structure of the tissue. Both tissues are comprised of a solid collagen meshwork with negatively charged proteoglycans and a fluid phase consisting of an interstitial fluid and positively charged ions in said fluid^{29,49,50}. The electrostatic attraction between the macromolecules and the ions keep the tissue hydrated, but the repulsive interaction between the macromolecules themselves creates osmotic pressure that provides mechanical strength^{29,36}. In both tissues, the proteoglycans responsible for this stiffness are in greater concentrations in areas of high loading^{34,51}. Also, collagen fibril orientation at the articulating surfaces of both tissues are similarly arranged to resist shear forces on the surface^{34,46}. Given these structural similarities, it is unsurprising that

articular cartilage-cartilage tests and the cartilage-meniscus tests conducted in this thesis show the same friction reduction due to SF constituents^{84,96}.

There are, however, some differences between articular cartilage and meniscus tissue. The main structural difference is that while articular cartilage is composed primarily of type-II collagen, meniscus' solid phase is mainly comprised of type-I collagen, like bone and tendon^{34,50}. While type-II collagen is found in the meniscus, it is localized deeper in the meniscus, not at the surface layer; this surface is dominantly type-I collagen^{52,121}. Type-I collagen has a larger diameter and, due to this, has higher tensile strength¹²². Furthermore, meniscus tissue was found to have a stiffer surface than apposing articular cartilage surface in compressive tests, though it can vary greatly deeper in the tissue¹²³. This difference in surface stiffness and compressive modulus could cause the equilibrium loading to be slightly higher and lead to lower friction coefficients in PBS tests compared to PBS values observed in cartilage-cartilage tests⁹⁶. When PRG4 or HA are the lubricants however, the slight changes in equilibrium load are minimal compared to the greatly reduced frictional force from improved lubrication.

Test parameters were specifically set to facilitate an operative boundary mode of lubrication. Tissues were compressed 18% of total thickness, first shown at an articular cartilage-cartilage biointerface, and now at the cartilage-meniscus biointerface, to be sufficient for boundary lubrication⁶⁵. This sufficiency was determined at the cartilage-cartilage biointerface by the invariance of friction at a higher 24% compression. Just as 0.3 mm/s was shown to be slow enough for boundary lubrication to be operative, 18% compression was found to be a high enough load. A 40-minute stress relaxation period and fluid depressurization holes cut in the subchondral bone (leaving the articular surface undisturbed) allowed for the interstitial fluid to depressurize, preventing said fluid from bearing significant portions of the load and facilitating

fluid-mediated lubrication^{65,70}. Finally, a stationary contact geometry was used to contribute to limit fluid exudation and repressurization that can occur in reciprocating test protocols involving hydrated tissues⁶⁵. Boundary lubrication generally occurs at low velocities and high loads⁶⁵, and in Chapter 2 velocity was investigated by assessing the velocity dependence of kinetic friction at the articular cartilage-meniscus biointerface (at the cartilage-cartilage biointerface 18% compression was sufficient for boundary lubrication, as were low velocities of 0.1, 0.3 and 1.0 mm/s⁶⁵). At low and intermediate velocities, PRG4 lubricated effectively compared to PBS, but at $v_{\text{eff}} = 1$ mm/s and higher, PRG4 decreased in lubricating function, suggesting that it only contributes to boundary lubrication, and when fluid-mediated lubrication occurs at higher velocities, where fluid properties such as viscosity contribute to lubrication³⁶, PRG4 does not help reduce friction. The invariant friction values found for PRG4 at low velocities show that a sufficiently low velocity has been reached for an operative boundary mode of lubrication.

HA lowered friction effectively at lower and intermediate velocities as well, showing that it lowers friction in a cartilage-meniscus boundary lubrication test. HA has been shown to be an effective boundary lubricant alone at physiological biointerfaces and Chapter 2 supports this conclusion^{84,96}. However, it also reduced friction at high velocities, suggesting it improves lubrication in a fluid-mediated lubrication paradigm as well; this improvement then could be a result of HA's viscosity. Stribeck analysis compares friction to viscosity, velocity and load. Stribeck analysis is not valid for soft, porous, hydrated tissue surfaces, and it requires a reciprocating test protocol, so may not be an appropriate model for this test setup. However, it is a worthwhile tool for comparing the relative effects of viscosity, velocity, and load in lubrication. For this test, compression and velocities were controlled. If HA's viscosity was estimated to be an order of magnitude higher than that of PBS or PRG4, the curve would shift to the right, where

the friction is still low, and invariant, at low velocities. This further supports HA's role as a boundary lubricant at physiological biointerfaces.

HA's lubricating ability is important as it is currently used as a viscosupplement, though the residency time in the joint has called into question its efficacy^{12,24}. PRG4 injections however have been shown to have a residency time of 28 days in animal models¹⁰⁸, dramatically longer than the 24-48 hours observed for HA-based viscosupplements^{25,26}. In addition, PRG4 and HA have been shown to interact synergistically to lower friction at synthetic^{86,98,99} and physiological^{84,96} interfaces. As such, Chapter 3 investigated their synergism in a lubrication test (now using $v_{\text{eff}} = 0.3$ mm/s to ensure boundary mode lubrication) at the articular cartilage-meniscus biointerface. Indeed, combining PRG4 and HA further lowered both kinetic and static coefficients of friction, approaching the level of SF.

While it is known that PRG4 and HA form a larger complex in solution, the specific mechanism by which this complex reduces friction is unknown and subject to debate⁹⁶. It has been suggested that PRG4 forms a sacrificial layer on the surface of the tissue, so when an apposing surface moves across the tissue the PRG4 is sheared off, protecting the tissue⁸⁸. When HA is added, an "adaptive" mode of lubrication occurs where HA and PRG4 become entangled and PRG4 that is sheared off under high loads is entrapped by the HA¹⁰⁵. This mechanism relies on replenishment of the surface layer by the lubricating fluid⁸⁸. Conversely, if the exuded fluid is not sufficient for this to occur¹⁰⁶, PRG4's lubricating ability may be due to a polymer brush-like behavior where its end terminals are bound to the surface and its negatively charged mucin domain is exposed, resulting in steric and electrostatic repulsion^{89,90}. HA's negatively charged polymer chains could contribute to this repulsion and further reduce friction as the apposing surfaces repel one another. This is the lubricating mechanism thought to work in ocular

lubrication during blinking⁹⁰, with the brush-like layer causes very low friction due to steric repulsion, before increasing slightly into fluid-mediated lubrication with a shear thinning fluid film. While velocity dependence shown in Chapter 2 closely follows this trend, the forces present in the knee are much greater than the eye; in fact, high forces were shown to damage the PRG4 brush-like layer, despite protecting the surface⁸⁹.

These different potential mechanisms of lubrication and synergism are important to understand, but the test used in these studies likely cannot distinguish between them. Rather, this macro scale *in vitro* lubrication test is designed for testing physiologically relevant tissue surfaces with specific parameters to ensure a dominant boundary mode of lubrication. Other test parameters are able to manipulate the surface properties of synthetic materials to better understand how PRG4 might function there, but these hard materials do not have the same surface interactions as *in vivo* tissue^{86,89,98,99}. Testing motion could also reciprocate to better emulate joint kinematics, but this would lead to fluid exudation and mixed mode of lubrication, preventing boundary lubrication from being studied and understood specifically⁷⁰. Specific characteristics of boundary lubrication must be considered, as well as the interface, when studying putative boundary lubrication of physiological tissues.

Another important characteristic of a boundary lubricant is the ability to bind to the articulating surface⁶⁵. PRG4 also fulfills this criteria, as it is found naturally on both articular cartilage and meniscus^{76,77}. rhPRG4 has been previously shown to do the same for articular cartilage in levels comparable to native PRG4¹¹¹. In Chapter 4 it was shown that rhPRG4 is also able to replete the surface layer at the meniscus following depletion by either shaking or shaking and salt extraction. While IHC is qualitative, the levels of rhPRG4 adsorbed to the surface were noticeably greater than residual protein remaining on the surface following soaking in just PBS

and comparable to native PRG4, SF, and fresh samples. Furthermore, the cut surface was also adsorbed to, as seen in cartilage previously¹¹¹. rhPRG4's ability to adsorb to the cartilage¹¹¹, and now meniscal, surfaces is indicative of its role as a boundary lubricant at the cartilage-meniscus biointerface.

This surface layer on articular cartilage has been shown previously to vary in thickness between monomer-enriched and multimer-enriched PRG4 preparations¹²⁴. PRG4's ability to disulfide bind to other PRG4 monomers, forming multimers, is a critical function of its N terminal, while the C terminal is thought to account for surface binding¹⁰⁹. Multimer-enriched PRG4 preparations reduce friction more than primarily monomeric PRG4 solutions at a cartilage-cartilage biointerface, suggesting, potentially, that a thicker surface layer could improve lubricating function¹²⁴. This would seem to support the sacrificial layer model of lubrication, as there is more PRG4 at the surface to be sheared away, which has been shown to be effectively replenished in PRG4 solutions¹¹¹. Furthermore, this model involves the C terminal binding to the surface while the N contributes to multimerization, unlike the polymer brush theory in which both terminals bind to the surface of the cartilage^{89,90,109}.

Cumulatively this work, through the development of a novel *in vitro* articular cartilage-meniscus lubrication test, determined the velocities at which boundary lubrication was dominant, demonstrated the lubricating ability of (rh)PRG4 and HA, alone and synergistically in combination, at this biointerface, and observed the surface adsorbing ability of rhPRG4 to the meniscus. All told, this contributes to the understanding of tribology in the knee joint at the infrequently studied, yet important, meniscal surface, and may aid in the future development of a biotherapeutic injection making use of both HA and rhPRG4.

6.3 Limitations

This thesis work has several limitations that, while they do not invalidate the conclusions of the work, are worth recognizing and considering their effects. Foremost among these is the *in vitro* nature of the methodology. The lubrication occurring in the joint takes place at a complex surface geometry whose resulting kinematics are more complex than those tested in the proceeding studies. Furthermore, this motion leads to a mixed lubrication mechanism in which different types of lubrication occur over different times, velocities, and loads. The test setup employed here was certainly not a knee-motion simulator, but did, however, allow for a specific type of lubrication that accounts for much of the wear in the knee⁷², to be tested at a physiologically relevant biointerface.

The test setup did not accurately represent the specific anatomical interactions that occur. The meniscal surface harvested for use in the samples was taken from the tibial facing surface, while the cartilage used was cut from the patellofemoral groove. These surfaces do not directly articulate against one another, of course, though in both tissues the surface morphology is largely the same throughout the tissue^{35,46}. As such, the surface of the tissue that is exposed to shearing force during motion would be similar for purposes of boundary mode lubrication. Another mechanical difference in the whole tissue that would not likely play a role in this test protocol are hoop stresses in the circumferential fibers of the meniscus^{46,50}. These stresses may alter the mechanical strength of the tissue in tension, but given that lubricants are the changed factor while the tissue conditions remain the same, the comparisons are still valid.

The developed test methodology also presented some factors to consider. The range of friction coefficient values between the positive and negative controls, SF and PBS, was not as large as in cartilage-cartilage tests. Previous studies using a rotational test geometry at the

cartilage-cartilage biointerface had a range of $\langle \mu_{\text{kinetic,Neq}} \rangle$ values $\sim 0.02-0.2$ between SF and PBS^{65,84,96,112}. The articular cartilage-meniscus lubrication tests however have a range 0.025-0.18. This smaller range of values makes it more difficult for statistically significant differences to be found at lower values of n. The studies contained in this thesis had n values between 4 and 8 for boundary lubrication tests and while the trends were consistent, significant differences were not. The PBS values were quite variant, possibly due to tissue variability, between these studies as well. $\langle \mu_{\text{kinetic,Neq}} \rangle$ values for PBS ranged from 0.129 ± 0.033 to 0.168 ± 0.005 at the cartilage-meniscus biointerface. However, such issues can be overcome with higher sample numbers.

Sample preparation presented some challenges. The meniscal samples, when cut from the surrounding tissue, often swelled, making it difficult to achieve appropriate flat articulating surface necessary for the boundary lubrication test. As such, a maximum difference between the first and last point of contact of the tissue surfaces of 0.1 mm was observed. This swelling may also result in the collagen framework being stressed relative to the *in vivo* tissue, as well as altering the osmotic pressure within the framework. Furthermore, as shown in Chapter 4, shaking the meniscal samples did not fully remove residual protein, though boundary lubricating ability is greatly decreased. The tissue used should also be considered; it was taken from bovine joints. While cartilage-cartilage testing has achieved similar results using human and bovine tissue^{94,96,112}, no human menisci have been tested to be compared to bovine tissue as of yet. These challenges must be considered, but do not affect the comparative testing of different lubricants as the tissue flatness is controlled, residual protein greatly reduced, and bovine tissue used consistently.

While the IHC imaging provided high quality, comparative images, no quantitative data were generated. As such, the conclusions drawn from these images have to be considered as a

conceptual insight into the surface adsorption of rhPRG4, not a direct, numerical comparison. Regardless, IHC does allow for visual comparisons in immunoreactivity to be made that can indicate relative levels of protein.

Consideration of different modes of lubrication tends to involve the use of Stribeck analysis. Indeed, boundary mode is often defined by the characteristics of it seen in the Stribeck curve. However, somewhat paradoxically, this methodology is not valid for a stationary geometry or rotational motion test, nor a soft, porous, and hydrated tissue surface like cartilage or meniscus⁶⁷. It can, however, be used to examine the effects of velocity on a lubricating interface and provide insight into the type of lubrication at play in a specific situation.

Despite these limitations, this thesis work was successful in investigating the biotribology of the articular cartilage-meniscus biointerface. In fact, many of these limitations are due to specific decisions made in test and study design. The *in vitro* boundary lubrication test setup used herein may not be a knee-joint simulator, but allowed for an important mode of lubrication to be specifically investigated at a physiologically important biointerface. Specific mechanisms may not be directly observed, but the comparisons between naturally occurring lubricants at this physiological biointerface allows for physiological interactions between the molecules and tissues and may contribute to the development of treatments for OA.

6.4 Future Work

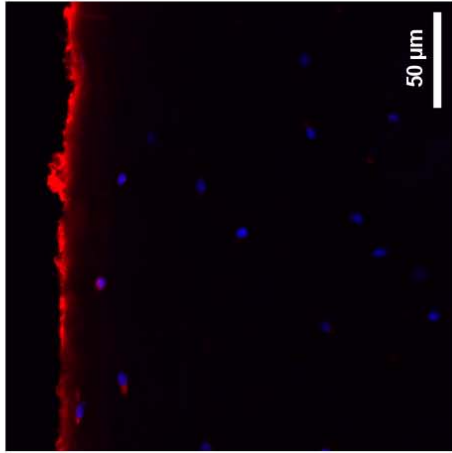
Moving forward, there are several potential areas for further study for these specific topics. For *in vitro* boundary lubrication testing, replicating the test with human cartilage and meniscus tissue would be a worthwhile endeavour to confirm that bovine tissue is an appropriate model of human tissues in this biotribological context. Human cartilage has been used previously in tests for SF and showed the same lubricating function as bovine cartilage⁹⁴. Furthermore, the test developed here could be done with artificial meniscus biomaterials for characterization and development efforts. The benefits of this work would be two-fold: it would test the ability of an artificial meniscus to lubricate similarly to a normal, healthy meniscus, as well as assess the lubricating ability of rhPRG4 ± HA at a biointerface that will become increasingly common and relevant in the OA patient cohort.

Surface adsorption can also be further explored to both investigate PRG4+HA synergism as well as quantify the previously observed results. To gain insight into the synergistic interaction of PRG4 and HA at the surface of an articulating surface, rhPRG4 and HA could be imaged alone and in combination. While some antibodies bind to both PRG4 and HA, making it impossible to distinguish between them, recently available fluorescein isothiocyanate (FITC)-labelled HA and rhodamine-labelled rhPRG4 (labelled with a commercially available kit) allow for these fluorescent molecules to be directly imaged. Bovine meniscal discs were depleted of PRG4 by vigorous shaking, as done in Chapter 4, before soaking in the lubricants of interest. Following cryosectioning and fixation, the fluorescent lubricants were mounted with a DAPI mounting medium and imaged directly. Preliminary results from such a test, shown below in Figure 5-1, show that rhPRG4 binds to the surface alone as evidenced by a red immunoreactive layer present at both the articular surface and cut surface. HA also binds to the surface, as well as

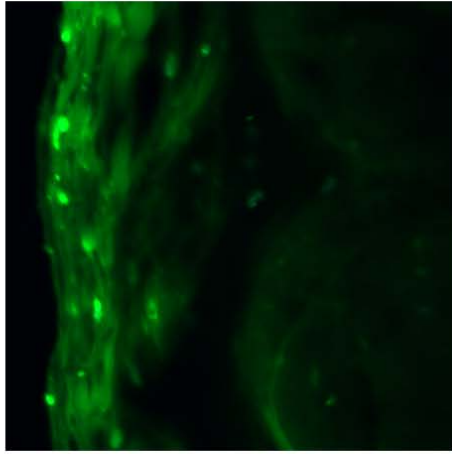
to structures, potentially collagen fibrils, deeper in the tissue, seen as green fluorescence. When combined, however, HA immunoreactivity is localized to the surface where rhPRG4 is found, overlapping to form the surface layer required for boundary lubrication. This overlap is seen as a yellow band where the red and green fluorescence from the individual SF constituents is overlaid. This may support the finding in previous work that HA's MW, while important for HA's lubricating ability alone, does not matter when combined with PRG4 due to PRG4-HA complex that forms⁹⁶.

Articulating
Surface

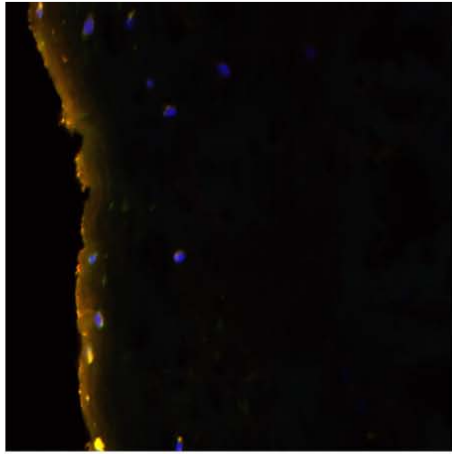
rhPRG4



1.5 MDa HA



rhPRG4 + 1.5 MDa HA



Cut
Surface

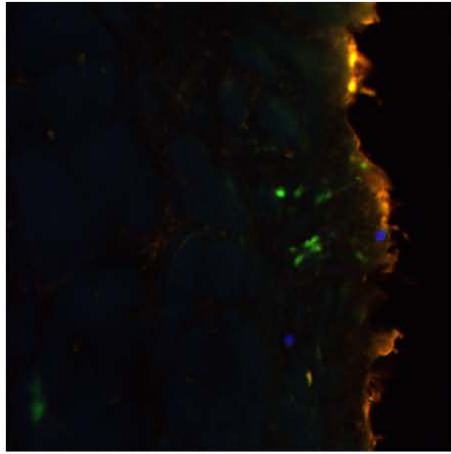
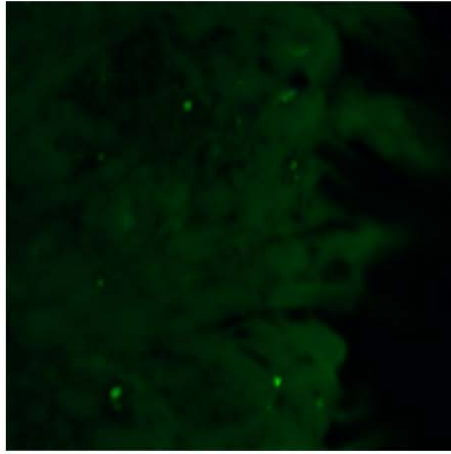
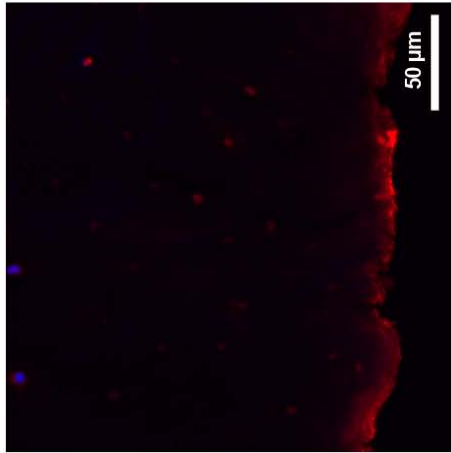


Figure 5-1: Immunolocalization of rhPRG4 and HA at meniscal surface. All samples were shaken overnight in PBS at 4°C, frozen over night at -80°C, shaken again in fresh PBS at 4°C and soaked in solutions of interest overnight at room temperature. Solutions: rhodamine-labelled rhPRG4 at 0.450 mg/mL, FITC-labelled 1.5 MDa HA at 3.33 mg/mL, and a combination of rhPRG4 and HA. Blue shows DAPI staining of chondrocyte cells.

To quantify surface adsorption rhPRG4 can be radio-labelled. After tissue samples are soaked in this radio-labelled rhPRG4, the samples can be placed in an automatic gamma counter that will quantify the amount of rhPRG4 that adsorbs to the surfaces. This would allow for more precise comparisons between different depletion and repletion methods. This methodology has been tested preliminarily on cartilage discs and appears to provide a more accurate comparison between samples that may have been too similar to properly distinguish visually with normal IHC.

rhPRG4 has been shown to reduce friction at cartilage-cartilage and cartilage-meniscus biointerfaces effectively as well as adsorbing to both cartilage and meniscus surfaces. This provides justification for development of an OA therapeutic. Animal models in which OA is induced through surgery and followed by rhPRG4 injections are currently being conducted. The chondroprotective abilities of rhPRG4, if any, in this situation would add credibility to the use of PRG4 as an OA treatment as well as bring the treatment closer to patients. The final step between bench and bedside, of course, would be clinical trials in humans involving a double-blind study protocol. While this is beyond the scope of this thesis, such a treatment of rhPRG4 and HA could improve the lubricating function in patients' knee joints and potentially help alleviate OA related pain and possibly combat the actual pathological tissue degradation.

Bibliography

1. Goldring, M. B. & Goldring, S. R. Osteoarthritis. *J. Cell. Physiol.* **213**, 626–634 (2007).
2. Felson, D. T. Clinical practice. Osteoarthritis of the knee. *N. Engl. J. Med.* **354**, 841–8 (2006).
3. Buckwalter, J. A., Glimcher, M. J., Cooper, R. R. & Recker, R. Bone biology. II: Formation, form, modeling, remodeling, and regulation of cell function. *Instr. Course Lect.* **45**, 387–99 (1996).
4. Gelber, A. C. *et al.* Joint injury in young adults and risk for subsequent knee and hip osteoarthritis. *Ann. Intern. Med.* **133**, 321–8 (2000).
5. Fleming, B. C., Hulstyn, M. J., Oksendahl, H. L. & Fadale, P. D. Ligament Injury, Reconstruction and Osteoarthritis. *Curr. Opin. Orthop.* **16**, 354–362 (2005).
6. Felson, D. T. *et al.* Osteoarthritis: new insights. Part 1: the disease and its risk factors. *Ann. Intern. Med.* **133**, 635–46 (2000).
7. Roos, E. M. Joint injury causes knee osteoarthritis in young adults. *Curr. Opin. Rheumatol.* **17**, 195–200 (2005).
8. Lawrence, R. C. *et al.* Estimates of the prevalence of arthritis and other rheumatic conditions in the United States. Part II. *Arthritis Rheum.* **58**, 26–35 (2008).
9. Murphy, L. *et al.* Lifetime risk of symptomatic knee osteoarthritis. *Arthritis Rheum.* **59**, 1207–13 (2008).
10. Prevalence of doctor-diagnosed arthritis and arthritis-attributable activity limitation --- United States, 2007-2009. *MMWR. Morb. Mortal. Wkly. Rep.* **59**, 1261–5 (2010).
11. Kotlarz, H., Gunnarsson, C. L., Fang, H. & Rizzo, J. A. Insurer and out-of-pocket costs of osteoarthritis in the US: evidence from national survey data. *Arthritis Rheum.* **60**, 3546–53 (2009).
12. Waddell, D. D. Viscosupplementation with hyaluronans for osteoarthritis of the knee: clinical efficacy and economic implications. *Drugs Aging* **24**, 629–42 (2007).
13. Arthritis Alliance of Canada, T. *The Impact of Arthritis in Canada: Today and Over the Next 30 Years.* (2011).
14. Butler-Jones, D. *Life with Arthritis in Canada: A Personal and Public Health Challenge.* (2010).

15. Guccione, A. A. *et al.* The effects of specific medical conditions on the functional limitations of elders in the Framingham Study. *Am. J. Public Health* **84**, 351–8 (1994).
16. White, A. G., Birnbaum, H. G., Janagap, C., Buteau, S. & Schein, J. Direct and indirect costs of pain therapy for osteoarthritis in an insured population in the United States. *J. Occup. Environ. Med.* **50**, 998–1005 (2008).
17. Dibonaventura, M. daCosta, Gupta, S., McDonald, M. & Sadosky, A. Evaluating the health and economic impact of osteoarthritis pain in the workforce: results from the National Health and Wellness Survey. *BMC Musculoskelet. Disord.* **12**, 83 (2011).
18. Messier, S. P., Gutekunst, D. J., Davis, C. & DeVita, P. Weight loss reduces knee-joint loads in overweight and obese older adults with knee osteoarthritis. *Arthritis Rheum.* **52**, 2026–32 (2005).
19. Paxton, E. W. *et al.* A prospective study of 80,000 total joint and 5000 anterior cruciate ligament reconstruction procedures in a community-based registry in the United States. *J. Bone Joint Surg. Am.* **92 Suppl 2**, 117–32 (2010).
20. Callahan, C. M., Drake, B. G., Heck, D. A. & Dittus, R. S. Patient outcomes following tricompartmental total knee replacement. A meta-analysis. *JAMA* **271**, 1349–57 (1994).
21. Mehrotra, C., Remington, P. L., Naimi, T. S., Washington, W. & Miller, R. Trends in total knee replacement surgeries and implications for public health, 1990-2000. *Public Health Rep.* **120**, 278–82 (2005).
22. Jin, Z. M., Dowson, D. & Fisher, J. Analysis of fluid film lubrication in artificial hip joint replacements with surfaces of high elastic modulus. *Proc. Inst. Mech. Eng. H.* **211**, 247–56 (1997).
23. Katz, J. N. *et al.* Association between hospital and surgeon procedure volume and the outcomes of total knee replacement. *J. Bone Joint Surg. Am.* **86-A**, 1909–16 (2004).
24. Bert, J. M. & Waddell, D. D. Viscosupplementation with hylan g-f 20 in patients with osteoarthrosis of the knee. *Ther. Adv. Musculoskelet. Dis.* **2**, 127–32 (2010).
25. Jüni, P. *et al.* Efficacy and safety of intraarticular hylan or hyaluronic acids for osteoarthritis of the knee: a randomized controlled trial. *Arthritis Rheum.* **56**, 3610–9 (2007).
26. McCarty, W. J. *et al.* The biophysical mechanisms of altered hyaluronan concentration in synovial fluid after anterior cruciate ligament transection. *Arthritis Rheum.* **64**, 3993–4003 (2012).

27. Teeple, E. *et al.* Effects of supplemental intra-articular lubricin and hyaluronic acid on the progression of posttraumatic arthritis in the anterior cruciate ligament-deficient rat knee. *Am. J. Sports Med.* **39**, 164–72 (2011).
28. Waller, K. A., Zhang, L. X., Fleming, B. C. & Jay, G. D. Preventing friction-induced chondrocyte apoptosis: comparison of human synovial fluid and hylan G-F 20. *J. Rheumatol.* **39**, 1473–80 (2012).
29. Mow, V. C. & Rosenwasser, M. Articular cartilage: Biomechanics, In Injury and Repair of the Musculoskeletal Soft Tissues. in *The American Academy of Orthopaedic Surgeons: Park Ridge, Illinois* 427–463 (1988).
30. Mow, V., Setton, L., Guilak, F. & Ratcliffe, A. Mechanical factors in articular cartilage and their role in osteoarthritis. in *The American Academy of Orthopaedic Surgeons: Rosemont, Illinois* 147–171 (1995).
31. Buckwalter, J. A. & Mankin, H. J. Instructional Course Lectures, The American Academy of Orthopaedic Surgeons - Articular Cartilage. Part I: Tissue Design and Chondrocyte-Matrix Interactions*†. *J. Bone Jt. Surg.* **79**, 600–11 (1997).
32. Stockwell, R. A. The cell density of human articular and costal cartilage. *J. Anat.* **101**, 753–63 (1967).
33. Aydelotte, M. Chondrocytes from the articular surface and deep zone express different, but stable, phenotype sin alginate gel culture. in *Transactions of the Orthopaedic Research Society* 317 (1996).
34. Buckwalter, J. Articular Cartilage: Composition and structure, In injury and repair of the musculoskeletal soft tissues. in *The American Academy of Orthopaedic Surgeons: Park Ridge, Illinois* 405–425 (1988).
35. Buckwalter, J., Mow, V. & Ratcliffe, A. Restoration of injured or degenerated articular cartilage. *J. Am. Acad. Orthop. Surg.* **2**, 192–201 (1994).
36. Ateshian, G. & Mow, V. in *Basic Orthopaedic Biomechanics and Mechanobiology* 447–494 (Lippincott Williams & Wilkins, 2005).
37. Mow, V. C., Kuei, S. C., Lai, W. M. & Armstrong, C. G. Biphasic creep and stress relaxation of articular cartilage in compression? Theory and experiments. *J. Biomech. Eng.* **102**, 73–84 (1980).
38. Hayes, W. C. & Bodine, A. J. Flow-independent viscoelastic properties of articular cartilage matrix. *J. Biomech.* **11**, 407–19 (1978).
39. Sophia Fox, A. J., Bedi, A. & Rodeo, S. A. The basic science of articular cartilage: structure, composition, and function. *Sports Health* **1**, 461–8 (2009).

40. Hayes, W. C. & Mockros, L. F. Viscoelastic properties of human articular cartilage. *J. Appl. Physiol.* **31**, 562–8 (1971).
41. Buckwalter, J. A. & Mankin, H. J. Instructional Course Lectures, The American Academy of Orthopaedic Surgeons - Articular Cartilage. Part II: Degeneration and Osteoarthritis, Repair, Regeneration, and Transplantation*†. *J. Bone Jt. Surg.* **79**, 612–32 (1997).
42. Mankin, H. J. The reaction of articular cartilage to injury and osteoarthritis (first of two parts). *N. Engl. J. Med.* **291**, 1285–92 (1974).
43. Mankin, H. J. The reaction of articular cartilage to injury and osteoarthritis (second of two parts). *N. Engl. J. Med.* **291**, 1335–40 (1974).
44. Arnoczky, S. & McDevitt, C. in *Orthopaedic Basic Science* 531 (American Academy of Orthopaedic Surgeons, 2000).
45. Evans, B. & Zawadsky, M. *The Knee: Essentials of Orthopedic Surgery*. (Springer Science, 2007).
46. Brindle, T., Nyland, J. & Johnson, D. L. The meniscus: review of basic principles with application to surgery and rehabilitation. *J. Athl. Train.* **36**, 160–9 (2001).
47. Seedhom, B. B. Transmission of the load in the knee joint with special reference to the role of the menisci Part I: anatomy, analysis and apparatus. *Arch. Eng. Med. 1971-1988 (vols 1-17)* **8**, 207–219 (1979).
48. Seedhom, B. B. & Hargreaves, D. J. Transmission of the load in the knee joint with special reference to the role of the menisci Part II: experimental results, discussion and conclusions. *Arch. Eng. Med. 1971-1988 (vols 1-17)* **8**, 220–228 (1979).
49. Fithian, D. C., Kelly, M. A. & Mow, V. C. Material properties and structure-function relationships in the menisci. *Clin. Orthop. Relat. Res.* 19–31 (1990). at <<http://www.ncbi.nlm.nih.gov/pubmed/2406069>>
50. Mow, V. *Structure and function relationships of the meniscus in the knee. Knee Meniscus: Basic and Clinical Foundations* (Raven Press, 1992).
51. Herwig, J., Egner, E. & Buddecke, E. Chemical changes of human knee joint menisci in various stages of degeneration. *Ann. Rheum. Dis.* **43**, 635–40 (1984).
52. Gunja, N. J. & Athanasiou, K. A. Passage and reversal effects on gene expression of bovine meniscal fibrochondrocytes. *Arthritis Res. Ther.* **9**, R93 (2007).
53. Levy, I. M., Torzilli, P. A., Gould, J. D. & Warren, R. F. The effect of lateral meniscectomy on motion of the knee. *J. Bone Joint Surg. Am.* **71**, 401–6 (1989).

54. Levy, I. M., Torzilli, P. A. & Warren, R. F. The effect of medial meniscectomy on anterior-posterior motion of the knee. *J. Bone Joint Surg. Am.* **64**, 883–8 (1982).
55. Walker, P. S. *et al.* Function of the medial meniscus in force transmission and stability. *J. Biomech.* (2015). doi:10.1016/j.jbiomech.2015.02.055
56. Shapeero, L. G. *et al.* Functional dynamics of the knee joint by ultrafast, cine-CT. *Invest. Radiol.* **23**, 118–23 (1988).
57. Andrews, S., Shrive, N. & Ronsky, J. The shocking truth about meniscus. *J. Biomech.* **44**, 2737–40 (2011).
58. Mak, A. F. The apparent viscoelastic behavior of articular cartilage--the contributions from the intrinsic matrix viscoelasticity and interstitial fluid flows. *J. Biomech. Eng.* **108**, 123–30 (1986).
59. Kurosawa, H., Fukubayashi, T. & Nakajima, H. Load-bearing mode of the knee joint: physical behavior of the knee joint with or without menisci. *Clin. Orthop. Relat. Res.* 283–90 (1980). at <<http://www.ncbi.nlm.nih.gov/pubmed/7408313>>
60. Englund, M., Guermazi, A. & Lohmander, L. S. The meniscus in knee osteoarthritis. *Rheum. Dis. Clin. North Am.* **35**, 579–90 (2009).
61. Englund, M., Roemer, F. W., Hayashi, D., Crema, M. D. & Guermazi, A. Meniscus pathology, osteoarthritis and the treatment controversy. *Nat. Rev. Rheumatol.* **8**, 412–9 (2012).
62. Englund, M. *et al.* Incidental meniscal findings on knee MRI in middle-aged and elderly persons. *N. Engl. J. Med.* **359**, 1108–15 (2008).
63. Bhattacharyya, T. *et al.* The clinical importance of meniscal tears demonstrated by magnetic resonance imaging in osteoarthritis of the knee. *J. Bone Joint Surg. Am.* **85-A**, 4–9 (2003).
64. Chang, A. *et al.* Subregional effects of meniscal tears on cartilage loss over 2 years in knee osteoarthritis. *Ann. Rheum. Dis.* **70**, 74–9 (2011).
65. Schmidt, T. A. & Sah, R. L. Effect of synovial fluid on boundary lubrication of articular cartilage. *Osteoarthritis Cartilage* **15**, 35–47 (2007).
66. Coles, J. M., Chang, D. P. & Zauscher, S. Molecular mechanisms of aqueous boundary lubrication by mucinous glycoproteins. *Curr. Opin. Colloid Interface Sci.* **15**, 406–16 (2010).
67. Dunn, A. C., Sawyer, W. G. & Angelini, T. E. Gemini interfaces in aqueous lubrication with hydrogels. *Tribol. Lett.* 1–8 (2014). doi:10.1007/s11249-014-0308-1

68. Shekhawat, V. K., Laurent, M. P., Muehleman, C. & Wimmer, M. A. Surface topography of viable articular cartilage measured with scanning white light interferometry. *Osteoarthritis Cartilage* **17**, 1197–203 (2009).
69. Caligaris, M. & Ateshian, G. A. Effects of sustained interstitial fluid pressurization under migrating contact area, and boundary lubrication by synovial fluid, on cartilage friction. *Osteoarthritis Cartilage* **16**, 1220–7 (2008).
70. Ateshian, G. A. The role of interstitial fluid pressurization in articular cartilage lubrication. *J. Biomech.* **42**, 1163–76 (2009).
71. Jay, G. D. *et al.* Association between friction and wear in diarthrodial joints lacking lubricin. *Arthritis Rheum.* **56**, 3662–9 (2007).
72. Morrell, K. C., Hodge, W. A., Krebs, D. E. & Mann, R. W. Corroboration of in vivo cartilage pressures with implications for synovial joint tribology and osteoarthritis causation. *Proc. Natl. Acad. Sci. U. S. A.* **102**, 14819–24 (2005).
73. Gleghorn, J. P., Jones, A. R. C., Flannery, C. R. & Bonassar, L. J. Boundary mode frictional properties of engineered cartilaginous tissues. *Eur. Cell. Mater.* **14**, 20–8; discussion 28–9 (2007).
74. Jay, G. D. Lubricin and surfacing of articular joints. *Curr. Opin. Orthop.* **15**, 355–359 (2004).
75. Marcelino, J. *et al.* CACP, encoding a secreted proteoglycan, is mutated in camptodactyly-arthropathy-coxa vara-pericarditis syndrome. *Nat. Genet.* **23**, 319–22 (1999).
76. Schumacher, B. L., Block, J. A., Schmid, T. A., Aydelotte, M. B. & Kuettner, K. E. A novel proteoglycan synthesized and secreted by chondrocytes of the superficial zone of articular cartilage. *Arch. Biochem. Biophys.* **311**, 144–52 (1994).
77. Schumacher, B. L., Schmidt, T. A., Voegtline, M. S., Chen, A. C. & Sah, R. L. Proteoglycan 4 (PRG4) synthesis and immunolocalization in bovine meniscus. *J. Orthop. Res.* **23**, 562–8 (2005).
78. Schmidt, T. A. *et al.* Transcription, translation, and function of lubricin, a boundary lubricant, at the ocular surface. *JAMA Ophthalmol.* **131**, 766–76 (2013).
79. Sun, Y. *et al.* Expression and mapping of lubricin in canine flexor tendon. *J. Orthop. Res.* **24**, 1861–8 (2006).
80. Teeple, E. *et al.* Lubricin deficiency in the murine lumbar intervertebral disc results in elevated torsional apparent modulus. *J. Biomech.* (2015). doi:10.1016/j.jbiomech.2015.03.029

81. Rhee, D. K. *et al.* Consequences of disease-causing mutations on lubricin protein synthesis, secretion, and post-translational processing. *J. Biol. Chem.* **280**, 31325–32 (2005).
82. Perez-Vilar, J. & Mabolo, R. Gel-forming mucins. Notions from in vitro studies. *Histol. Histopathol.* **22**, 455–64 (2007).
83. Schmidt, T. A., Plaas, A. H. K. & Sandy, J. D. Disulfide-bonded multimers of proteoglycan 4 PRG4 are present in normal synovial fluids. *Biochim. Biophys. Acta* **1790**, 375–84 (2009).
84. Schmidt, T. A., Gastelum, N. S., Nguyen, Q. T., Schumacher, B. L. & Sah, R. L. Boundary lubrication of articular cartilage: role of synovial fluid constituents. *Arthritis Rheum.* **56**, 882–91 (2007).
85. Waller, K. A. *et al.* Role of lubricin and boundary lubrication in the prevention of chondrocyte apoptosis. *Proc. Natl. Acad. Sci. U. S. A.* **110**, 5852–7 (2013).
86. Seror, J., Zhu, L., Goldberg, R., Day, A. J. & Klein, J. Supramolecular synergy in the boundary lubrication of synovial joints. *Nat. Commun.* **6**, 6497 (2015).
87. Greene, G. W. *et al.* Lubricin: A versatile, biological anti-adhesive with properties comparable to polyethylene glycol. *Biomaterials* **53**, 127–136 (2015).
88. Chan, S. M. T., Neu, C. P., DuRaine, G., Komvopoulos, K. & Reddi, A. H. Tribological altruism: A sacrificial layer mechanism of synovial joint lubrication in articular cartilage. *J. Biomech.* **45**, 2426–31 (2012).
89. Zappone, B., Ruths, M., Greene, G. W., Jay, G. D. & Israelachvili, J. N. Adsorption, lubrication, and wear of lubricin on model surfaces: polymer brush-like behavior of a glycoprotein. *Biophys. J.* **92**, 1693–708 (2007).
90. Pult, H. *et al.* Spontaneous blinking from a tribological viewpoint. *Ocul. Surf.* 1–14 (2015). doi:10.1016/j.jtos.2014.12.004
91. Teeple, E. *et al.* Coefficients of friction, lubricin, and cartilage damage in the anterior cruciate ligament-deficient guinea pig knee. *J. Orthop. Res.* **26**, 231–7 (2008).
92. Elsaid, K. A. *et al.* Decreased lubricin concentrations and markers of joint inflammation in the synovial fluid of patients with anterior cruciate ligament injury. *Arthritis Rheum.* **58**, 1707–15 (2008).
93. Atarod, M., Ludwig, T. E., Frank, C. B., Schmidt, T. A. & Shrive, N. G. Cartilage boundary lubrication of ovine synovial fluid following anterior cruciate ligament transection: a longitudinal study. *Osteoarthritis Cartilage* **23**, 640–7 (2015).

94. Ludwig, T. E., McAllister, J. R., Lun, V., Wiley, J. P. & Schmidt, T. A. Diminished cartilage-lubricating ability of human osteoarthritic synovial fluid deficient in proteoglycan 4: Restoration through proteoglycan 4 supplementation. *Arthritis Rheum.* **64**, 3963–71 (2012).
95. Watterson, J. R. & Esdaile, J. M. Viscosupplementation: therapeutic mechanisms and clinical potential in osteoarthritis of the knee. *J. Am. Acad. Orthop. Surg.* **8**, 277–84 (2000).
96. Kwiecinski, J. J. *et al.* The effect of molecular weight on hyaluronan's cartilage boundary lubricating ability--alone and in combination with proteoglycan 4. *Osteoarthritis Cartilage* **19**, 1356–62 (2011).
97. Laurent, T. C., Laurent, U. B. & Fraser, J. R. The structure and function of hyaluronan: An overview. *Immunol. Cell Biol.* **74**, A1–7 (1996).
98. Jay, G. D., Lane, B. P. & Sokoloff, L. Characterization of a bovine synovial fluid lubricating factor. III. The interaction with hyaluronic acid. *Connect. Tissue Res.* **28**, 245–55 (1992).
99. Das, S. *et al.* Synergistic interactions between grafted hyaluronic acid and lubricin provide enhanced wear protection and lubrication. *Biomacromolecules* **14**, 1669–77 (2013).
100. Pelletier, J.-P., Martel-Pelletier, J. & Raynauld, J.-P. Most recent developments in strategies to reduce the progression of structural changes in osteoarthritis: today and tomorrow. *Arthritis Res. Ther.* **8**, 206 (2006).
101. Schmidt, T. A. *et al.* Differential regulation of proteoglycan 4 metabolism in cartilage by IL-1 α , IGF-I, and TGF- β 1. *Osteoarthritis Cartilage* **16**, 90–7 (2008).
102. Schmidt, T. A., Schumacher, B. L., Klein, T. J., Voegtline, M. S. & Sah, R. L. Synthesis of proteoglycan 4 by chondrocyte subpopulations in cartilage explants, monolayer cultures, and resurfaced cartilage cultures. *Arthritis Rheum.* **50**, 2849–57 (2004).
103. Nugent-Derfus, G. E., Chan, A. H., Schumacher, B. L. & Sah, R. L. PRG4 exchange between the articular cartilage surface and synovial fluid. *J. Orthop. Res.* **25**, 1269–76 (2007).
104. Eckstein, F. *et al.* In vivo cartilage deformation after different types of activity and its dependence on physical training status. *Ann. Rheum. Dis.* **64**, 291–5 (2005).
105. Greene, G. W. *et al.* Adaptive mechanically controlled lubrication mechanism found in articular joints. *Proc. Natl. Acad. Sci. U. S. A.* **108**, 5255–9 (2011).
106. McCutchen, C. W. Joints are not lubricated in the way Greene *et al.* say they are. *Proc. Natl. Acad. Sci. U. S. A.* **108**, E461; author reply E462 (2011).

107. Buckwalter, J. A., Mankin, H. J., Collections, S. & Surgery, J. Instructional Course Lectures , The American Academy of Orthopaedic Surgeons - Articular Cartilage . Part I : Tissue Design and Chondrocyte-Matrix Interactions*. *Instr. Course Lect.* (2007).
108. Flannery, C. R. *et al.* Prevention of cartilage degeneration in a rat model of osteoarthritis by intraarticular treatment with recombinant lubricin. *Arthritis Rheum.* **60**, 840–7 (2009).
109. Jones, A. R. C. *et al.* Binding and localization of recombinant lubricin to articular cartilage surfaces. *J. Orthop. Res.* **25**, 283–92 (2007).
110. Samsom, M. L. *et al.* Characterization of full-length recombinant human Proteoglycan 4 as an ocular surface boundary lubricant. *Exp. Eye Res.* **127**, 14–19 (2014).
111. Abubacker, S. *et al.* Cartilage Boundary Lubricating Ability of Full-Length Recombinant Human Proteoglycan 4 +/- Hyaluronan. *Revis.*
112. Abubacker, S., Ham, H. O., Messersmith, P. B. & Schmidt, T. A. Cartilage boundary lubricating ability of aldehyde modified proteoglycan 4 (PRG4-CHO). *Osteoarthritis Cartilage* **21**, 186–9 (2013).
113. Lu, X. L. & Mow, V. C. Biomechanics of articular cartilage and determination of material properties. *Med. Sci. Sports Exerc.* **40**, 193–199 (2008).
114. Ludwig, T. E., Cowman, M. K., Jay, G. D. & Schmidt, T. A. Effects of concentration and structure on proteoglycan 4 rheology and interaction with hyaluronan. *Biorheology* **51**, 409–22 (2014).
115. Chawla, K., Ham, H. O., Nguyen, T. & Messersmith, P. B. Molecular resurfacing of cartilage with proteoglycan 4. *Acta Biomater.* **6**, 3388–94 (2010).
116. Jay, G. D. *et al.* Prevention of cartilage degeneration and gait asymmetry by lubricin tribosupplementation in the rat following anterior cruciate ligament transection. *Arthritis Rheum.* **64**, 1162–71 (2012).
117. Nugent, G. E. *et al.* Dynamic shear stimulation of bovine cartilage biosynthesis of proteoglycan 4. *Arthritis Rheum.* **54**, 1888–96 (2006).
118. Jay, G. D. *et al.* Prevention of cartilage degeneration and restoration of chondroprotection by lubricin tribosupplementation in the rat following anterior cruciate ligament transection. *Arthritis Rheum.* **62**, 2382–91 (2010).
119. Cregger, M., Berger, A. J. & Rimm, D. L. Immunohistochemistry and quantitative analysis of protein expression. *Arch. Pathol. Lab. Med.* **130**, 1026–30 (2006).

120. McCann, L., Ingham, E., Jin, Z. & Fisher, J. Influence of the meniscus on friction and degradation of cartilage in the natural knee joint. *Osteoarthritis Cartilage* **17**, 995–1000 (2009).
121. Petersen, W. & Tillmann, B. Collagenous fibril texture of the human knee joint menisci. *Anat. Embryol. (Berl)*. **197**, 317–24 (1998).
122. Lodish, H. *et al.* in *Molecular Cell Biology* (W. H. Freeman, 2000).
123. Lai, J. H. & Levenston, M. E. Meniscus and cartilage exhibit distinct intra-tissue strain distributions under unconfined compression. *Osteoarthritis Cartilage* **18**, 1291–9 (2010).
124. Abubacker, S. *et al.* Effect of disulfide bonding and multimerisation on Proteoglycan 4's cartilage boundary lubricating ability and adsorption. *Connect. Tissue Res.*
125. Abubacker, S. *et al.* Effect of counterface on cartilage boundary lubricating ability by hyaluronan and proteoglycan 4: cartilage-cartilage vs cartilage-glass. *In Preparation*.

Appendix

A.1 Torque and Load Profiles

The custom articular cartilage-meniscus boundary lubrication test that was described in Chapter 2 collected torque and load data from which to calculate coefficients of friction, as described in section 2.3.4. The resulting friction coefficients were displayed in Chapters 2 and 3, however the raw torque and load profiles were not. Below in Figure A-1, representative torque and load profiles are displayed for the three v_{eff} of interest, 0.01, 0.3, and 10 mm/s for the positive and negative controls, SF and PBS respectively.

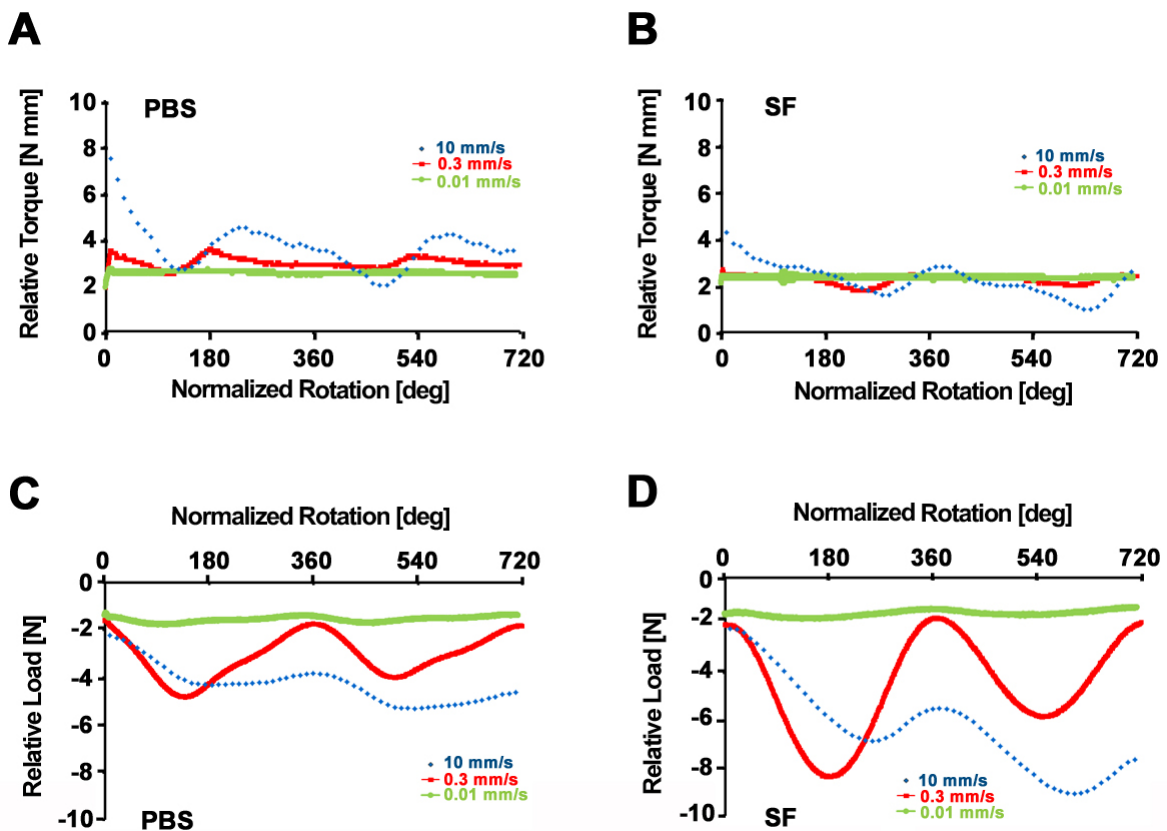


Figure A-1: Friction data acquired on articular cartilage-meniscus biointerfaces. Torque (τ)

profiles obtained during two rotations at three velocities (0.01, 0.3 and 10 mm/s) on PBS (A) and SF (B). Instantaneous axial load (N) profiles acquired simultaneously for PBS (C) and SF (D).

The characteristics of the measured torque and axial load were similar at this biointerface as it was at the cartilage-cartilage biointerface¹²⁵. Measured τ data reached a steady state during the 2nd revolution for both configurations, shown for 0.01, 0.3, and 10 mm/s in PBS and SF (Figure A-1 A, B). The axial load varied at both biointerfaces, with the variance increasing with velocity and demonstrating cyclical behavior during revolutions (Figure A-1 C, D).